



AMERICAN UNIVERSITY OF BEIRUT

DECIPHERING MRNA-CIRCULAR RNA-MICRORNA AXES  
AND MICRORNA REGULATORS IN EARLY BREAST CANCER  
USING A BREAST EPITHELIAL RISK-PROGRESSION 3D  
CULTURE MODEL

by

NATALY MAJDI NASER AL DEEN

A dissertation  
submitted in partial fulfillment of the requirements  
for the degree of Doctor of Philosophy  
to the Department of Biology  
of the Faculty of Arts and Sciences  
at the American University of Beirut

Beirut, Lebanon  
June 2020

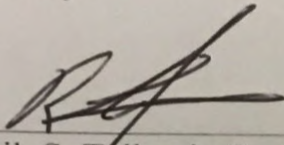
# AMERICAN UNIVERSITY OF BEIRUT

## DECIPHERING MRNA-CIRCULAR RNA-MICRORNA AXES AND MICRORNA REGULATORS IN EARLY BREAST CANCER USING A BREAST EPITHELIAL RISK-PROGRESSION 3D CULTURE MODEL

by

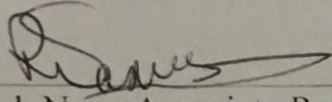
NATALY MAJDI NASER AL DEEN

Approved by:



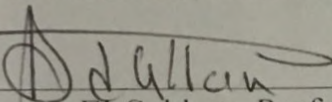
Dr. Rabih S. Talhouk, Professor  
Biology Department  
Faculty of Arts and Sciences, American University of Beirut

Advisor



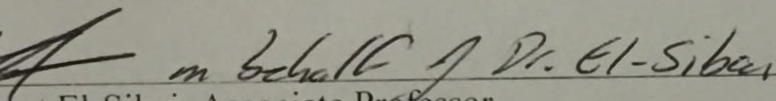
Dr. Rihab Nasr, Associate Professor  
Anatomy, Cell Biology, and Physiological Sciences Department  
Faculty of Medicine, American University of Beirut

Co-Advisor



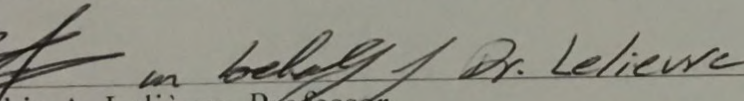
Dr. Marwan El-Sabban, Professor  
Anatomy, Cell Biology, and Physiological Sciences Department  
Faculty of Medicine, American University of Beirut

Chair of Committee



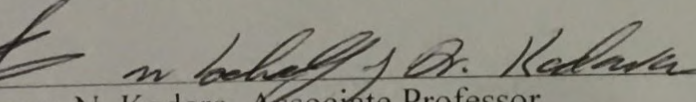
Dr. Mirvat El-Sibai, Associate Professor  
Department of Natural Sciences  
School of Arts and Sciences, Lebanese American University

Member of Committee



Dr. Sophie A. Lelièvre, Professor  
Department of Basic Medical Sciences  
College of Veterinary Medicine, Purdue University

Member of Committee



Dr. Humam N. Kadara, Associate Professor  
Department of Translational Molecular Pathology  
MD Anderson Cancer Center

Member of Committee

Date of thesis/dissertation defense: June 19, 2020

AMERICAN UNIVERSITY OF BEIRUT

THESIS, DISSERTATION, PROJECT RELEASE FORM

Student Name:

Naser Al Deen

Last

Nataly

First

Majdi

Middle

Master's Thesis

Master's Project

Doctoral Dissertation

I authorize the American University of Beirut to: (a) reproduce hard or electronic copies of my thesis, dissertation, or project; (b) include such copies in the archives and digital repositories of the University; and (c) make freely available such copies to third parties for research or educational purposes.

I authorize the American University of Beirut, to: (a) reproduce hard or electronic copies of it; (b) include such copies in the archives and digital repositories of the University; and (c) make freely available such copies to third parties for research or educational purposes after:

- X One ---- year from the date of submission of my thesis, dissertation, or project.**
- Two ---- years from the date of submission of my thesis, dissertation, or project.**
- Three ---- years from the date of submission of my thesis, dissertation, or project.**



June 23, 2020

Signature

Date

This form is signed when submitting the thesis, dissertation, or project to the University Libraries

## ACKNOWLEDGMENTS

I thank my advisor Dr. Rabih Talhouk for his tremendous encouragement, support and dedication over the years. I look up to you and I am forever grateful to you for shaping me into a young researcher. You have elevated my curiosity and passion for science, and most importantly, you taught me how to be an independent researcher with an open eye and heart for collaborations. I cannot thank you enough for always encouraging me to pursue my ambitions and aspirations, be it nationally or internationally. I am so lucky to have had the honor to be trained by such a highly ethical, brilliant and supportive advisor, and I look forward to fruitful future collaborations.

I also thank my co-advisor Dr. Rihab Nasr for her continuous support and scientific guidance, and for inspiring me to become a successful scientist and humanitarian, like the role model she is. I thank our collaborator, Dr. Sophie Lelièvre, for her continuous high-level scientific advice and guidance. Thank you for hosting me at Purdue University and for shaping my scientific thinking. I thank Dr. Shirisha Chittiboyina for her support, guidance and friendship.

I would like to thank my thesis committee members Dr. Marwan El-Sabban, Dr. Mirvat El-Sibai and Dr. Humam Kadara for their valuable time, guidance, insight and support. I also thank deeply Dr. Mounir AbouHaidar for introducing me to my newly found passion for circularRNAs and for being an incredible educator, collaborator and role model. I sincerely thank Dr. Nadia Lanman for being the most responsive, amazing and professional collaborator I could ever ask for. I thank Dr. Heinrich Zu Dohna for his guidance and assistance with bioinformatics analysis. I am grateful for the Biology Department at AUB and all its incredible staff and for all the amazing RST lab members, Ms. Zeina Habli, Ms. Rita Kalot, Ms. Angela Mermerian and Dr. Sabreen Fostok.

I am especially grateful to our President, Dr. Fadlo Khuri, for his tremendous support and belief in my potential, and for selecting and supporting me as the World Economic Forum Precision Medicine Council Academic Fellow. I would like to thank our Dean, Dr. Nadia El Cheikh, for supporting my participation at the 68th Lindau Nobel Laureate Meeting and other international conferences. I am especially grateful for Dr. Pierre Karam's moral and scientific support throughout the years.

This work was supported by the Lebanese National Council for Scientific Research, the University Research Board, the Central Research Science Laboratory, the International Breast Cancer and Nutrition project, the Indiana Clinical and Translational Sciences Institute and Indiana University Center for Global Health, the Commitment Fund Center Research Grant University of Toronto, AUB-CNRS-L Scholarship and the Fulbright Alumni Development Travel Fellowship.

Special gratitude and love go to my family: Mom and Dad, I could not have made it without your encouragement and unconditional love. Mom, you will always be my role model and source of inspiration and I hope to live up to your expectations. Nadine, Nancy (my twin), Khawla and Norma, thank you for being my biggest support system and cheerleaders throughout my life. Nancy, I look forward to turn science into art with you! I thank my loving Pink Steps Family for the wonderful impact we made together. And to my partner and better half, Dr. Rami Srouji, your love, encouragement and dedication are unmeasurable. I look forward to growing together scientifically and professionally!

To my family, Rami, nieces and my late Teta, Jeddo and Majd, I dedicate this work.

# AN ABSTRACT OF THE DISSERTATION OF

Nataly Majdi Naser Al Deen

for

Doctor of Philosophy

Major: Cell and Molecular Biology

Title: Deciphering mRNA-circRNA-miRNA axes and miRNA regulators in early breast cancer using a breast epithelial risk-progression 3D culture model

Breast Cancer accounts for the highest cancer incidence and mortality rate in women worldwide [1]. In Lebanon, breast cancer is the most common malignancy, with the highest incidence in the world for women below 40 and a mean age at diagnosis 10 years younger than in developed countries [2]. These women have low prevalence of deleterious *BRCA* mutations and present with poor prognosis and aggressive phenotypes due to the lack of diagnostic methods at such an early age [3]. Early-onset breast cancer is increasing drastically worldwide [2, 4, 5], which called for identifying potential noninvasive biomarkers and active players for risk-assessment of breast cancer initiation and early detection actions. We therefore focused our study on the post-transcriptional gene regulators, microRNAs (miRNAs), and their “sponges”, circularRNAs (circRNAs), which have been shown to mediate cancerous phenotypes [6, 7]. CircRNAs are a class of endogenous RNAs that originate from RNA splicing and back ligation. miRNAs are small endogenous non-coding RNAs that repress translation. CircRNAs can sponge miRNAs by exhibiting endogenous competing binding sites (one to several) for each specific target miRNA. They covalently bind the mature miRNA, downregulating its expression, hence preventing it from binding its own target mRNAs and repressing translation [7, 8]. miRNAs and circRNAs exhibit unique dysregulation signatures in cancers, are stable and abundant in body fluids and act as attractive novel noninvasive cancer biomarkers. While, mRNA-circRNA-miRNAs axes have been characterized in breast cancer [9-15], axes involved in premalignant transitions that might explain and contribute to heightened risk of breast cancer initiation have not been reported.

The mammary gland development, differentiation and tumorigenesis is dependent on gap junction organization and proper communication, which is mediated by connexins (Cxs) [16-19]. Cx43, the focus of our previous and current research studies [7, 20, 21] plays essential roles during mammary gland development [22, 23] and differentiation [24] and acts as a tumor suppressor [20, 21, 25]. Its loss and mislocalization influence breast cancer initiation [26], progression [27] and is associated with markers of poor prognosis[25]. The nontumorigenic luminal human breast epithelial HMT-3522 S1 (S1) cell line, cultured under three-dimensional (3D) conditions, form a fully polarized epithelium with a central lumen and apicolateral

localization of Cx43. S1 cells recapitulate normal human breast tissue architecture [26]. Silencing Cx43 expression in these nontumorigenic S1 cells via shRNA (Cx43-KO-S1) resulted in cell cycle entry, perturbed apical polarity, mitotic spindle misorientation and loss of lumen, causing cell multilayering and priming cells for enhanced motility and invasion [26, 27]. These features represent architectural and phenotypical premalignant mammary lesions, as seen *in vivo* [28], and increase the risk of breast cancer initiation, thus marking Cx43-KO-S1 as a pretumorigenic culture model. Therefore, this 3D risk-progression culture model was used to capture key pretumorigenic changes and cancer initiation phenotypes that might be triggered by miRNAs and circRNAs into heightening the risk of breast cancer development.

In order to understand post-transcriptional mechanisms that underlie heightened risk of breast cancer initiation, preliminary results from the Lebanese population that are notoriously at the highest risk of this early malignancy were essential for such investigations. Nassar et al. [29] previously identified 74 dysregulated miRNAs in microarrays from 45 invasive ductal carcinoma (IDC) versus 17 normal adjacent breast tissues from the Lebanese population. Forty-two percent of the patients were below the age of 40 and were categorized into early-stage breast cancers. Through a comprehensive literature review, fifteen tumor-associated miRNAs were uncovered here among these patient miRNAs to be involved in early events of breast tumorigenesis that contribute to loss of acinar morphogenesis. Next, circRNA microarrays and miRNA-sequencing from 3D acini of the pretumorigenic Cx43-KO-S1 cells compared to the nontumorigenic S1 counterparts were performed. The results revealed 121 circRNAs and 65 miRNAs that were significantly dysregulated in response to Cx43 silencing in the cultured epithelia. Focusing on the possible sponging activity of the validated circRNAs to their target miRNAs, cross-comparison was done to the actual miRNA datasets from the cultured epithelia and the patient validation cohort. The results revealed **Cx43/hsa\_circ\_0077755/miR-182** as a biomarker signature axis for heightened-risk of breast cancer initiation. Moreover, its differential dysregulation patterns might predict prognosis along breast cancer initiation and progression.

We next aimed to study whether dysregulated miRNAs from the young patient cohort may increase the risk of breast cancer initiation by disrupting breast epithelial polarity, transitioning cells from phenotypically normal epithelium to premalignant phenotype. Thus, a comparative analysis between 65 miRNAs that were significantly dysregulated in response to Cx43 silencing in cultured epithelia and the 15 tumor-associated patient miRNAs involved in epithelial polarity was performed. The first chosen miRNA was miR-183, which was commonly up-regulated among the tumor-associated patient miRNAs involved in epithelia polarity pathways and was downstream of Cx43 loss. Moreover, miR-183 was the most up-regulated miRNA in early-stage Lebanese breast cancer patient cohort (and matched US patients) [29] and its up-regulation conferred with the increased risk of cancer progression in the 3D culture model. The second miRNA, miR-492, was chosen from the panel of up-regulated tumor-associated patient miRNAs that were involved in epithelia polarity pathways but were not downstream of Cx43 loss. Ectopic over-expression of both miR-183 and miR-492 in the non-neoplastic S1 cells (through pLenti-

III-miR-GFP tagged vectors) resulted in the formation of larger acini in 3D cultures, devoid of lumen assembly, with disrupted epithelial polarity observed through mislocalization of  $\beta$ -catenin and Scrib's apico-lateral distribution and Cx43's apical distribution. It also triggered enhanced proliferation and invasion capacity, hence recapitulating tumor-initiation phenotypes seen upon Cx43 loss [26, 27]. Tumor-initiation phenotypes attributed to miR-183 over-expression seem to be due to complete loss of Scrib in miR-183-S1 cells and mis-localization of the distribution of  $\beta$ -catenin and Cx43 in the cultured epithelia. While loss of Scrib in miR-183-S1 cells seems to drive tumor-initiation phenotypes, its mis-localization was also reported to be sufficient in promoting tumorigenesis [30]. Therefore, tumor-initiation phenotypes attributed to miR-492 over-expression seem to be due to mislocalization of Scrib,  $\beta$ -catenin and Cx43 in the cultured epithelia. Moreover, while miR-183 was found up-regulated in response to Cx43 loss, adding a direct link between Cx43 down-regulation and miR-183 up-regulation, Cx43 total mRNA levels were unchanged upon the over-expression of both miRNAs. Therefore, miR-183 and miR-492 over-expression might in part be affecting polarity disruption in a gap junctional dependent manner, through the mislocalization of Cx43 from apical membrane domains in aggregates formed in 3D culture, but not through directly down-regulating Cx43 expression. Although each miRNA is predicted to affect different downstream targets and pathways along breast cancer initiation, both miR-183 and miR-492 ectopic over-expression triggers enhanced proliferation and invasion and loss of apical polarity through Scrib's loss/mis-localization and through altering the distribution of Cx43 and  $\beta$ -catenin in the cultured epithelia.



# CONTENTS

ACKNOWLEDGEMENTS .....	V
ABSTRACT .....	VI
LIST OF ILLUSTRATIONS .....	XIV
LIST OF TABLES .....	XVI
LIST OF ABBREVIATIONS .....	XVII

## Chapter

I. INTRODUCTION .....	1
A. Cross-roads to drug resistance and metastasis in breast cancer: miRNA regulatory function and biomarker capability .....	1
1. Overview on breast cancer and its metastasis .....	2
2. miRNAs biogenesis .....	5
3. Circulating miRNAs origin and function .....	9
4. miRNAs as diagnostic, prognostic and therapy predictive biomarkers in breast cancer .....	10
5. miRNAs and drug resistance in breast cancer.....	14
a. Mechanisms of drug resistance in breast cancer .....	14
b. Role of miRNAs in chemotherapy and in multidrug resistance ...	16
c. Role of miRNAs in hormonal therapy response/resistance .....	19
d. Role of miRNAs in targeted- and immune-therapy response/resistance .....	21
e. Role of miRNAs in radioresistance .....	22
6. miRNAs and metastasis in breast cancer .....	25
a. Circulating miRNAs as biomarkers for metastasis in BC.....	25
b. miRNAs as active players/regulators of breast cancer along the metastatic cascade .....	27
c. Examples of miRNAs implicated in common sites of breast metastases .....	30

7.	miRNAs role in the interplay between drug resistance and metastasis in breast cancer .....	34
B.	Connexin43 as a tumor suppressor: proposed connexin43 mRNA-CircularRNA-miRNA axis towards prevention and early detection in breast cancer .....	41
1.	Cx43 in Normal Mammary Gland Development and Differentiation..	44
2.	Perturbations in Cx43: Cx43 as Tumor Suppressor/Biomarker in BC.	44
3.	Interactions Between Connexins and microRNAs .....	46
4.	CircularRNAs biogenesis, functions and biomarker roles in BC .....	48
5.	Cx43 mRNA-circRNAs-miRNAs Axis .....	51
II.	AIMS .....	58
III.	BREAST EPITHELIAL RISK-PROGRESSION 3D CULTURE MODEL REVEALS CX43/HSA_CIRC_0077755/MIR- 182 AS A BIOMARKER AXIS FOR HEIGHTENED-RISK OF BREAST CANCER INITIATION	
A.	Abstract .....	61
B.	Introduction .....	62
C.	Results .....	66
1.	Three-dimensional (3D) breast cancer risk-progression cell culture model characteristics .....	66
2.	Microarray profiling of Cx43-KO-S1 (pretumorigenic) versus S1 (nontumorigenic) breast epithelial cells in 3D culture revealed 121 significantly dysregulated circRNAs, of which 18 were chosen for validation .....	68
3.	RT-qPCR validation of the 18 selected circRNAs revealed two significantly up-regulated and seven significantly down-regulated circRNAs associated with the loss of Cx43 .....	71
4.	miRNA sequencing revealed 65 differentially expressed miRNAs in Cx43-KO-S1 versus S1 acini specific to Cx43 loss .....	75
5.	Fifteen tumor-associated miRNAs from microarrays of a validation cohort of early-stage young breast cancer patients exhibited reported involvement in epithelial polarity and cancer-related pathways .....	78
6.	Three mRNA-circRNA-miRNAs axes proposed, and one axis validated with potential for risk-assessment of breast cancer initiation.. .....	80

7. Gene co-expression networks associated with Cx43/hsa_circ_0077755/miR-182 axis correspond to cancer-related pathways .....	85
8. Functional analysis for hsa_circ_0077755 is enriched for cancer-related pathways .....	86

D. Discussion

1. Gap junctions are involved in post-transcriptional regulatory pathways in breast cancer initiation .....	88
2. Three mRNA-circRNA-miRNAs axes might act as potential biomarker signatures for heightened-risk of breast cancer initiation .....	90
3. Cx43/hsa_circ_0077755/miR-182 axis might associate with poor prognosis in a differential manner along breast cancer initiation and progression .....	92

E. Conclusion .....

94

F. Limitations and future directions .....

94

G. Materials and Methods

1. Three-dimensional cell culture .....	95
2. Total RNA isolation and quality control (QC) .....	96
3. Sample Preparation and hybridization for circRNAs microarrays.	96
4. Data Processing and Analysis for circRNAs microarrays .....	97
5. Annotation for circRNA/miRNA Interaction .....	97
6. miRNA Library Preparation and Sequencing .....	98
7. Heatmap of miRNAs from the breast epithelia that are in common with the MREs sponged by the significant circRNAs .....	98
8. Functional enrichment of mRNAs associated with circRNA binding miRNAs .....	99
9. RT-qPCR validation of chosen circRNAs (and selection of candidate circRNAs) and divergent primer design .....	99
10. Cytoscape analysis.....	101

IV. MIR-183 AND MIR-492 OVEREXPRESSION TRIGGER INVASION, PROLIFERATION AND LOSS OF POLARITY IN NON-NEOPLASTIC

## BREAST EPITHELIUM AND IS REPORTED IN EARLY BREAST CANCER PATIENTS

A. Abstract.....	102
B. Introduction .....	103
C. Results .....	107
1. Comparative analysis from miRNomes of a breast epithelial 3D risk-progression culture model and a young early-stage patient cohort lead to the selection of miR-183 and miR-492 for investigation in the nontumorigenic S1 cells .....	107
2. Functional and gene-set enrichment analyses for the differentially expressed miRNAs in (pretumorigenic) Cx43-KO-S1 compared to (nontumorigenic) S1 cells were enriched in cancer-related pathways .....	111
3. miR-183 and miR-492 were stably over-expressed in nontumorigenic S1 cells using pLenti-III-miR-GFP tagged vectors .....	113
4. Over-expression of miR-183-S1 and miR-492-S1 in S1 cells disrupts epithelial polarity, causes loss in lumen assembly and increase in acinar sizes and alters the localization of junctional and polarity proteins.....	115
5. Over-expressing miR-183 and miR-492 in nontumorigenic S1 cells resulted in significant enhanced proliferation and invasion potential .....	118
6. Potential downstream targets of miR-183 and miR-492 that might drive the pretumorigenic phenotypes observed .....	120
D. Discussion	
1. miR-183 over-expression promotes cell proliferation, invasion and loss of epithelial polarity in nonneoplastic breast epithelial cells .....	125
2. miR-492 over-expression promotes cell proliferation, invasion and loss of epithelial polarity in nonneoplastic breast epithelial cells .....	127
3. miR-183 and miR-492 over-expression might drive pre-tumorigenic phenotypes through possible involvement with gap junction proteins .....	129

E. Conclusion .....	130
F. Materials and Methods	
1. Three-dimensional cell culture .....	131
2. Total RNA isolation and quality control (QC) .....	131
3. miRNA Library Preparation and Sequencing .....	132
4. Heatmap of miRNAs from the breast epithelia that are in common with the MREs sponged by the significant circRNAs .....	132
5. Functional enrichment of mRNAs associated with circRNA binding miRNAs .....	133
6. miRNA Expression by Quantitative Real Time-Polymerase Chain Reaction .....	133
7. Lentiviral Infection for Delivery of mature miRNAs.....	134
8. Immunofluorescence .....	136
9. Diameter measurements, lumen assembly and apico-lateral polarity markers scoring .....	137
10. Trypan Blue Exclusion Method .....	137
11. Transwell Cell Invasion Assay .....	138
V. CONCLUSION .....	139
BIBLIOGRAPHY .....	145

## ILLUSTRATIONS

Figure	Page
1. Canonical miRNA biogenesis .....	8
2. Gap junction (GJ) complex dis-assembly in breast cancer initiation .....	54
3. Axes parallel to and downstream of Cx43 loss in breast cancer initiation .....	55
4. HMT-3522 S1 nontumorigenic and Cx43-KO-S1 pretumorigenic cells in 3D culture as a breast cancer risk-progression model .....	67
5. Microarrays revealed 121 differentially expressed circRNAs in response to Cx43 silencing in Cx43-KO-S1 cells versus S1 breast epithelial cells in 3D.....	71
6. RT-qPCR validated nine significant differentially expressed circRNAs in the cultured epithelia .....	73
7. Sequencing revealed 121 significantly dysregulated mature miRNAs in Cx43-KO-S1 cells as compared to S1 cells in response to Cx43 silencing in cultured epithelia.....	77
8. Selection of one validated mRNA-circRNA-miRNA breast cancer initiation risk-assessment axis .....	84
9. Gene co-expression networks shows the involvement of the validated Cx43/has_circ_0077755/miR-182 axis in cancer-related pathways.....	86
10. The chosen and validated hsa_circ_0077755 is functionally enriched in cancer-related pathways .....	87
11. Comparative analysis from miRNomes of a breast cancer risk-progression 3D culture model and a young early-stage patient cohort and validation of candidate miRNAs .....	110
12. Functional and gene-set enrichment analyses for differentially expressed miRNAs in Cx43-KO-S1 compared to S1 cells .....	112

13. Stable over-expression of miR-183 and miR-492 in nontumorigenic S1 cells using pLenti-III-miR-GFP tagged vectors .....	114
14. Immunofluorescence (IF) staining characterizing the (nontumorigenic) S1 cells upon miR-183 and miR-492 over-expression .....	117
15. Proliferation and invasion potential assessment upon over-expressing miR-183 and miR-492 in nontumorigenic S1 cells .....	119
16. Potential downstream targets of miR-183 and miR-492 that might be driving pretumorigenic phenotypes .....	121
17. Comparative summary of major players driving proliferation, invasion and epithelial polarity loss upon loss of Cx43, over-expression of miR-183 and over-expression of miR-492, respectively .....	143
18. A graphical abstract summarizing the methodology used to select Cx43/has_circ_0077755/miR-182 as the only validated risk-assessment axis for breast cancer initiation .....	144

## TABLES

Table 1: Summary of miRNAs that exhibit biomarker role in BC .....	14
Table 2: Summary of miRNAs implicated in drug resistance in BC .....	24
Table 3: Summary of miRNAs implicated in metastasis in BC .....	34
Table 4: Summary of miRNAs implicated in both drug resistance and metastasis in BC .....	38
Supplementary Table 1: The “initiation” circRNA isoforms that originate from the linear transcript of Cx43 (or GJA1) and their predicted sponged miRNAs .....	56
Table 5. Selection of eighteen circRNAs involved in cancer-related and/or epithelial polarity pathways for RT-qPCR validation .....	74
Table 6. Literature search of tumor-associated miRNAs from microarrays of early-stage Lebanese breast cancer patients [29] uncovered fifteen miRNAs involved in epithelial polarity and cancer pathways .....	80
Table 7. Expression and detection of selected circRNAs (cells microarray) and their target miRNAs (cells sequencing and patients microarray [29]) identified three potential risk-assessment axes for breast cancer initiation .....	83
Table 8. Comparative analysis of targets dysregulated downstream of Cx43 loss as reported by Fostok et al. (2019) that contribute to pretumorigenic phenotypes in Cx43-KO-S1 cells as compared to targets downstream of miR-183-5p and miR-492 .....	123



## ABBREVIATIONS

2D	Two-dimensional
3D	Three-dimensional
BC	Breast cancer
CTCs	Circulating tumor cells
DCIS	Ductal carcinoma in situ
IDC	Invasive ductal carcinoma
DFS	Disease-free survival
ER	Estrogen receptor
PR	Progesterone Receptor
mBC	Metastatic breast cancer
MDR	Multidrug resistance
miRNAs or miRs	microRNAs
OS	Overall survival
PFS	Progression-free survival
TNBC	Triple negative breast cancer
TDLUs	Terminal duct lobular units
ECM	Extracellular matrix
Cxs	Connexins
GJIC	Gap junction intercellular communication
GJ	Gap Junction
UTR	Untranslated region
siRNA	Short interfering RNA
RBP	RNA-binding proteins
FOXO3	Forkhead Box O3
FOXO1	Forkhead Box O1
ZEB1	Zinc Finger E-Box Binding Homeobox 1
ZEB2	Zinc Finger E-Box Binding Homeobox 2
TNBC	Triple-negative BC
SOCS3	Suppressor of cytokine signaling 3
HER2	Human epidermal growth factor receptor 2
PUMA	p53 upregulated modulator of apoptosis
PRDM16	PR domain containing 16
USP7	Ubiquitin-specific-processing protease 7
GJA1	Gap Junction Protein Alpha 1

MSO	Mitotic-spindle orientation
DCIS	Ductal Carcinoma in Situ
EMT	Epithelial to mesenchymal transition
CEA	carcinoembryonic antigen
SLNB	ymph node biopsy
DGCR8	DiGeorge syndrome chromosomal region 8
XPO5	exportin-5
TIF	tumor interstitial fluid
DOX	Doxorubicin
GSTP1	Glutathione S-transferase P1
PDCD4	Programmed cell death 4
PTEN	Phosphatase and tensin homolog
AKT	Protein kinase B
PI3K	Phosphoinositide 3-kinases
FFPE	Formalin-fixed, paraffin-embedded tissues
CDK2	Cyclin dependent kinase 2
IRES	Internal ribosome entry site
SPRED2	Sprouty-related, EVH1 domain-containing protein 2
FBXO24	F-Box Protein 24
EIF6	Eukaryotic translation initiation factor 6
MTUS1	Microtubule Associated Scaffold Protein 1
PRKD1	Protein Kinase D1
MRE	MiRNA response element
IPA	Ingenuity Pathway Analysis
SCRIB	Scribbled
BRCA	BReast CAncer gene
ERK	Extra cellular signal-related kinase
MAPK	Mitogen-activated protein kinase
GFP	Green fluorescent protein
RhoA	Ras Homolog Family Member A
Rac1	Ras-related C3 botulinum toxin substrate 1
RT-qPCR	Real time quantitative polymerase chain reaction
SOX7	SRY-Box Transcription Factor 7
LATS2	Large Tumor Suppressor Kinase 2

# CHAPTER I

## INTRODUCTION

### **A. Cross-roads to drug resistance and metastasis in breast cancer: miRNAs regulatory function and biomarker capability**

Authors: Nataly Naser AL Deen <sup>a</sup>, Farah Nassar <sup>b</sup>, Rihab Nasr <sup>c,\*</sup>, Rabih Talhouk <sup>a,\*</sup>  
Published Book Chapter: *Springer Nature* (Naser Al Deen et al. 2019)

Breast cancer and specifically metastatic breast cancer (mBC) constitutes a major health burden worldwide with the highest number of cancer-related mortality among women across the globe. Despite having similar subtypes, breast cancer patients present with a spectrum of aggressiveness and responsiveness to therapy due to cancer heterogeneity. Drug resistance and metastasis contribute to therapy failure and cancer recurrence. Research in the past two decades has focused on microRNAs (miRNAs), small endogenous non-coding RNAs, as active players in tumorigenesis, therapy resistance and metastasis and as novel non-invasive cancer biomarkers. This is due to their unique dysregulated signatures throughout tumor progression and their tumor suppressive/oncogenic roles. Identifying miRNAs signatures capable of predicting therapy response and metastatic onset in breast cancer patients might improve prognosis and offer prolonged median and relapse-free survival rate. Despite the growing reports on miRNAs as novel non-invasive biomarkers in breast cancer and as regulators of breast cancer drug resistance

or metastasis, the quest on whether some miRNAs are capable of regulating both simultaneously is inevitable, yet understudied. This chapter will review the role of miRNAs as biomarkers and as active players in inducing/reversing anti-cancer drug resistance, driving/blocking metastasis or regulating both simultaneously in breast cancer.

### ***1. Overview on breast cancer and its metastasis***

Breast cancer is a global public health burden, constituting the highest cancer incidence in females and the second most common cancer diagnosed worldwide, with around 1.7 million new cases each year. In the U.S., almost 1 in 8 females fall victims of invasive breast cancer throughout their lifetime [112]. Recent statistics by the American Cancer Society reported breast cancer to be amongst the three most commonly diagnosed female cancers, along with lung and bronchus cancer and colorectal cancer, all of which comprise 50% of all female cancer cases and contribute to most cancer deaths in women [112]. Breast cancer is a heterogeneous disease with various subtypes, conventionally classified according to histology (most common types are ductal carcinoma in situ, invasive ductal carcinoma and invasive lobular carcinoma), immunopathology (estrogen receptor, progesterone receptor and human epidermal growth factor receptor 2 (HER2) status) and molecular signature (luminal A, luminal B, triple-negative/basal-like, HER2-enriched or normal-like) [113-115]. Despite having similar subtypes, breast cancer patients present with a spectrum of aggressiveness and responsiveness to therapy [116]. This questioned the efficacy of the mentioned conventional classification methods and the available

prognostic and diagnostic tests for breast cancer. Hence, recent studies are focusing on complementing the conventional breast cancer classification tools using patients' distinct signature of microRNAs (miRNAs), small non-coding single-stranded nucleotides [6]. For instance, Bhattacharyya et al. [117] used 5-fold cross-validation techniques in an attempt to subclassify breast cancer using miRNA signatures compared to pre-existing clinical records. Their results not only validated that miRNA can corroborate the conventional molecular subtype classification, but also proposed the existence of further subtypes through using hierarchical clustering.

Metastatic breast cancer (mBC) is the most aggressive form of breast cancer, which affects 10–15% of patients within 3 years from diagnosis and is characterized by increased tumor burden and its spread to distal regions [118]. The metastatic cascade begins with tumor dissemination, denoted by local invasion of neighboring tissues, intravasation into the blood or lymph, persistence of the escaped cells in the circulation and subsequent extravasation. It is then followed by colonization, where the escaped cells adjust to the new microenvironment [119]. Epithelial to mesenchymal transition (EMT), an inherent developmental process, necessary for the proper morphogenesis of tissues, is one key step in driving invasion and metastasis. Epithelial cancer cells devise EMT to provoke motility, migration and invasion, switch to a mesenchymal phenotype to lose epithelial polarity and cellular interactions [120]. Developing better diagnostic and therapeutic interventions for mBC is fundamental. miRNAs play key regulatory roles along all stages of the metastatic cascade whereby McGuire et al. [121]

summarized the different miRNAs in mBC implicated in invasion (miR-199a, miR-214, miR-200a/b/c, miR-141 and miR-429), dissemination (miR-31), extravasation (miR-10b, miR-373, miR-20a, miR-214 and miR-31) and proliferation (miR-10b, miR-34a, miR-155, miR-200a/b/c, miR-141 and miR-429).

Drug resistance and metastasis continue to pose a challenge in breast cancer and mBC treatment due, in part, to the limitations that entail the available prognostic and diagnostic tests, which range from having low sensitivity, to being highly invasive, to yielding high false positive rates and over-diagnosis [122]. For instance, first, the use of serum carbohydrate antigens such as carcinoembryonic antigen (CEA) and cancer antigen 153 (CA153) as biomarkers is limited by its low sensitivity [68]. Second, there exists few available multi-gene expression DNA microarrays based testing, like Oncotype DX, MammaPrint, Veridex 76-gene and MapQuant Dx. Oncotype DX test, which estimates the recurrence likelihood through assessing 16 cancer-related genes, 5 reference genes and whether patients are eligible for chemotherapy [123], MammaPrint, a prognostic test that analyzes 70 genes and identifies patients with stage 1 or 2, node negative, invasive breast cancer <5 cm in size. Veridex 76-gene signature, a diagnostic test that predicts distant metastasis in ER-positive (ER+) patients within 5 years of diagnosis through a signature of 60 genes for ER+ patients and 16 for ER-negative (ER-) patients [124]. MapQuant Dx, which further classifies grade II tumors into grade I-like (low chance of distant relapses) and grade III-like (clinically similar to grade III) and predicts chemotherapeutic benefit, but can only be used as prognostic tool for ER+ tumors [124]. However, all these tests necessitate patient tissue

samples, and thus are highly invasive. Third, mammograms not only exhibit high false positive rates and are incapable of detecting mBC and cause over-diagnosis, but patients below the age of 40 are not recommended to undergo mammography screening because of their dense breast tissue architecture [125, 126]. Additionally, the conventional diagnostic tool for mBC, sentinel lymph node biopsy (SLNB), only detects local but not distal metastasis [121]. Thus, the limitations of the conventional classification tools along with the unavailability of non-invasive, highly sensitive and highly specific mBC diagnostic, prognostic and therapy predictive tests called for the investigation of miRNAs; to better understand their regulatory role in drug resistance and distant metastasis and their biomarker potential.

## **2. *miRNAs biogenesis***

miRNAs are small (16-29 nucleotides) endogenous, non-coding, single-stranded RNAs that negatively regulate gene expression at the post-transcriptional level [6]. Around half of miRNAs exist in clusters with other miRNAs and are transcribed as polycistronic precursor miRNAs, while others reside within exons and the 3'-untranslated region (UTR) of mRNAs [127]. Various miRNAs promoters transcribe their own miRNAs in intergenic sites, whereas, the majority of miRNAs are transcribed by their host gene promoters when they reside in the introns of protein coding or non-coding host genes. miRNAs biogenesis undertakes a sequence of processes, where RNA polymerase II/III first transcribes miRNAs into primary transcripts (pri-miRNAs) which are several kilobases long. pri-miRNAs in the nucleus are then cleaved by

RNase III endonuclease Drosha and DGCR8 protein into intermediate (60-70 nucleotide-long stem loop) precursor miRNAs (pre-miRNAs). The latter are exported to the cytoplasm via exportin-5 (XPO5) complexed with Ran-GTP, and undergo cleavage into mature length by Dicer, another RNase III endonuclease together with the double-stranded RNA-binding protein TRBP [128]. At this stage, the mature miRNA strand unwinds from its complementary strand (passenger strand), and is normally targeted for degradation. The mature strand gets presented onto the RNA-induced silencing complex (RISC), a ribonucleoprotein complex comprised of the mature miRNAs and Argonaute (AGO2) proteins [128, 129]. However, recent studies have shown that the passenger strand can also be loaded onto RISC and therefore can have regulatory function [130]. The RISC complex preferentially binds the seed-matching sequence of the 3'-UTR of target protein-coding mRNA genes, whereby perfect complementarity leads to mRNA degradation by AGO2 via the induction of RNA-mediated interference (RNAi) pathway. Imperfect complementarity leads to translational repression of the target mRNA or mRNA degradation as a result of deadenylation by the CAF1-CCR4-NOT1 de-adenylase complex and subsequent de-capping of the target mRNA [131, 132] (Figure 1). Although miRNAs are known to silence their target mRNA, studies shed light on few miRNAs that promote the expression of their target mRNA, a mechanism termed "RNA activation" (RNAa), majorly attributed to epigenetic regulation of AGO2 [133]. A single miRNA can regulate many genes, which normally exhibit cellular regulatory roles including proliferation, metabolism, differentiation,



cell death or aging [134]. Various miRNAs exhibit oncogenic or tumor suppressive roles during cancer pathogenesis, and hence, play part in cancer progression, drug resistance or metastasis.

However, deciphering miRNAs that concurrently control drug resistance and metastasis is fundamental, yet understudied [135]. Due to their dysregulation along the different stages of tumorigenesis and their presence and stability in bodily fluids, miRNAs have gained much attention in the past decade. Several studies reported miRNAs diagnostic, prognostic and therapy predictive biomarker potential in breast cancer and others discuss their role as active players in drug resistance and metastasis, all of which will be discussed thereof.

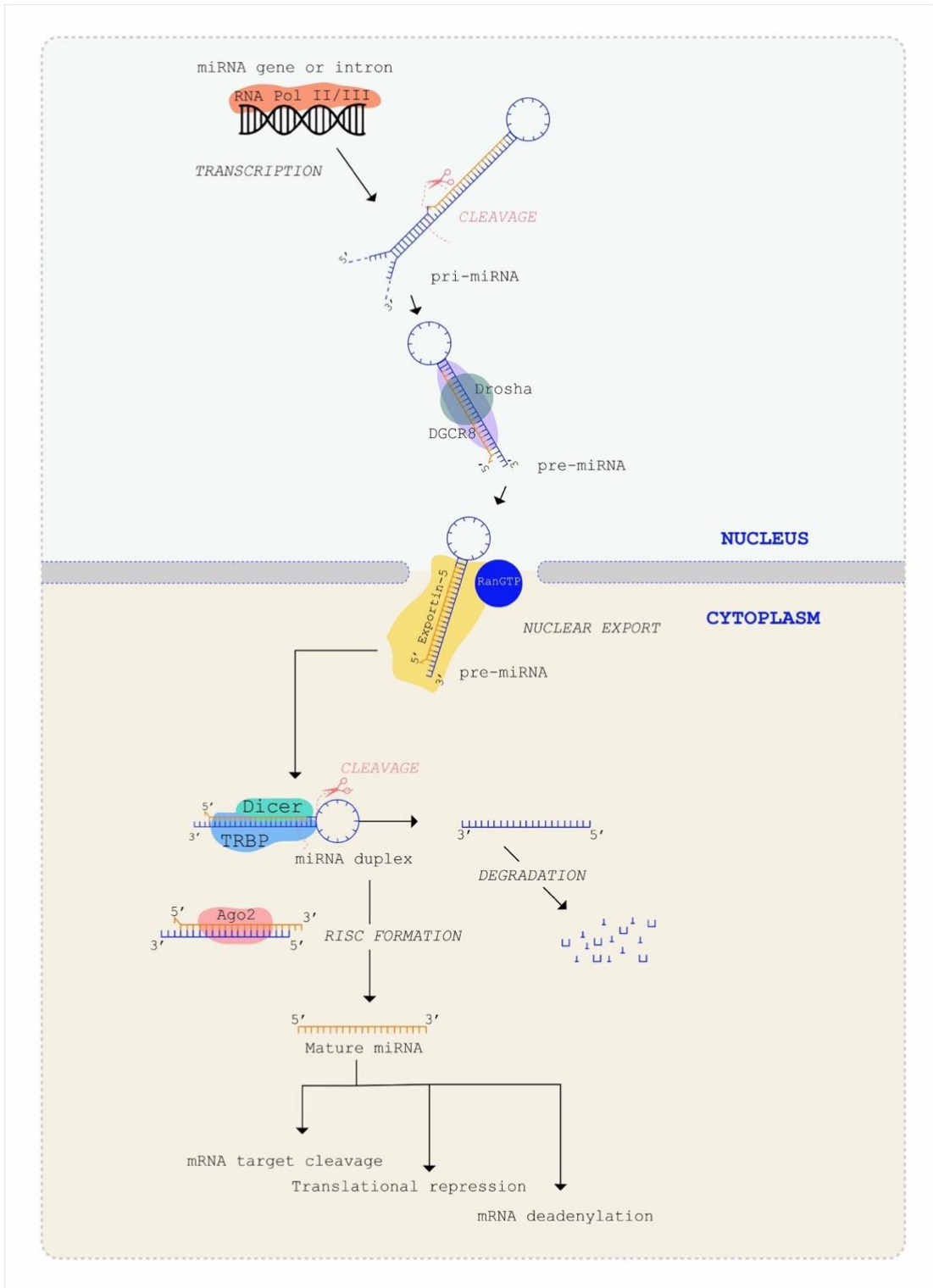


**Figure 1: Canonical miRNA biogenesis.** Canonical miRNA biogenesis starts by RNA polymerase II/III transcribing miRNAs into primary transcripts (pri-miRNAs) in the nucleus, which are then cleaved by Drosha and DGCR8 protein into intermediate precursor miRNAs (pre-miRNAs). Pre-miRNAs are exported to the cytoplasm via exportin-5 (XPO5) complexed with Ran-GTP, and undergo cleavage into mature length by Dicer complexed with TRBP. The mature miRNA strand is unwound from its complementary strand (passenger strand), which gets degraded, while the mature strand is presented onto the RNA-induced silencing complex (RISC), comprised of the mature miRNAs and AGO2 proteins. The RISC complex preferentially binds the seed-matching sequence of the 3'-UTR of target protein-coding mRNA genes and perfect complementarity leads to mRNA degradation while imperfect complementarity leads to translational repression or deadenylation, which results in degradation of the target mRNA (*modified from: Winter et al., 2009, Nature cell biology, 11(3), 228-234*)[128] .

### **3. Circulating miRNAs origin and function**

miRNAs were first detected in bodily fluids by Chim et al. [136] who discovered circulating placental miRNA in pregnant women plasma. Soon after, Lawrie et al. [137] identified the first miRNA signature in patients with diffuse large B-cell lymphoma with elevated serum miR-155, miR-210 and miR-21. Circulating miRNAs were then found in blood and plasma, colostrum and breast milk, tears, bronchial lavage and in amniotic, peritoneal, seminal, pleural and cerebrospinal fluids [138]. Previous studies by Lima et al. [139] related the stability of miRNAs in the circulation to their encapsulation in microvesicles or in exosomes. Turchinovich et al. [140] showed that some circulating miRNAs are generated from dead cells, while Merkerova et al. [141] attributed a portion of circulating miRNAs to have originated from blood or immune cells. Recent studies mainly attribute the origin of circulating miRNAs to their passive out-flow from dead cells or active secretion in exosome by tumor and other cell types. Wu et al. [142] characterized exosome-derived miR-19a as a key player in breast cancer

metastasis to the bones through facilitating breast cancer and osteoclast cellular communication. Zhong et al. [143] argued that drug resistance can be transmitted from resistant to sensitive breast cancer cells through exosomal miRNA discharge. Similarly, Le et al. [144] showed that transferring cells expressing miR-200 and extracellular vesicles from tumors into murine and human cancer xenografts resulted in acquisition of metastatic potential in weakly metastatic cells, both locally and distally.

Circulating miRNAs harbor a plethora of non-invasive biomarkers and warrant more extensive investigation due to their ease of accessibility in bodily fluids, stability, resistance to RNase digestion and extreme conditions and withstanding long storage [142, 145]. Many studies bid the urge of using miRNAs as novel non-invasive biomarkers for prognosis, diagnosis and therapy prediction in breast cancer and mBC [122, 142] while others discuss the role miRNAs play in controlling metastasis [146-150] inducing and/or reversing breast cancer drug resistance [135, 151, 152], setting new patient selection criteria for clinical trials [153], characterizing new breast cancer subtypes [117] and identifying miRNAs that have both therapy-sensitizing and metastasis blocking roles in breast cancer [135]; most of which will be discussed hereafter. This chapter will highlight the biomarker roles of miRNAs in breast cancer and mBC and will review the regulatory role of miRNAs in causing or reversing drug resistance, metastasis, or both simultaneously.

#### ***4. miRNAs as diagnostic, prognostic and therapy predictive biomarkers in breast cancer***

McGuire et al. [121] reviewed the essential role circulating miRNAs play as mBC diagnostic or prognostic biomarkers in discriminating non-metastatic from metastatic tumors to guide mBC early diagnosis and monitor disease progression. For instance, circulating miR-10b, miR-34a and miR-155 were elevated in mBC patients [154] and circulating miR-10b and miR-373 [155] as well as miR-20a and miR-214 [156] were upregulated in patients with lymph node positive breast cancer as opposed to patients with no lymph node involvement. Moreover, miR-10b has been reported as a potential mBC biomarker to the brain and bones [157, 158] while miR-141, miR-200a, miR-200b, miR-200c, miR-203, miR-210, miR-375 and miR-801 were significantly upregulated in plasma of mBC patients with circulating tumor cells, CTC [159]. Upregulation in miR-105 predicted metastasis in early onset breast cancer [160], while elevation in miR-17 and miR-155 discriminated metastatic from non-metastatic breast cancers [161]. Moreover, metastasis as a result of primary breast tumors correlated with over-expression of miR-34a and miR-155 in the serum, while upregulated miR-34a predicted increased aggressiveness [162].

Nassar et al. [122] shed light in their review on prognostic miRNAs in breast cancer in terms of predicting the overall survival (OS), disease outcome and recurrence in patients. Out of the prognostic biomarkers, miR-106b, found in serum and tissues, predicted risk of high recurrence and shorter OS [163], while miR-122, which was over-expressed in serum of relapsed patients, served as metastasis predictive miRNA. Sahlberg et al. [164] reported that miR-18b, miR-103, miR-107 and miR-652 predicted recurrence and decreased OS in triple negative breast

cancer (TNBC) patients. Recent study by Halvorsen et al. [165] was the first to characterize miRNAs profiled from tumor interstitial fluid (TIF) as prognostic and diagnostic biomarkers and as potential bridges between tumor cells and their micro-environment. The authors profiled TIF, normal interstitial fluid, tumor tissues and serum samples from breast cancer patients and a corresponding validation cohort. The results identified upregulation of 266 miRNAs in TIF, of which 61 were present in more than three quarters of the serum samples. Seven miRNAs of the latter predicted poor survival rate and 23 miRNAs were linked to immune cells and adipocyte existence in the serum. Furthermore, Lániczky et al. [166] devised an integrated platform that can search for all documented miRNAs through GEO, EGA, TCGA and PubMed database to arrive at survival analysis capable of predicting the efficiency of miRNAs acting as prognostic biomarkers. Importantly, via this platform, miR-210, miR-328, miR-484 and miR-874 were shown to be capable of predicting prognosis or risk of recurrence [121].

Dysregulation of miRNAs could also predict the therapy outcome and patient's sensitivity or resistance to a specific treatment, which is the leading cause of recurrence and poor prognosis in breast cancer patients [167]. Chen et al. [168] showed in breast cancer formalin-fixed paraffin-embedded (FFPE) tissues that miR-222, miR-29a, miR-34a, miR-423, miR-140, miR-3178, miR-574, miR-6780b and miR-744 were significantly associated with drug resistance and that miR-222, miR-29a, miR-140, miR-574, miR-6780b, miR-7107 and miR-744 were correlated with poor prognosis. Moreover, some miRNAs were associated with radioresistance, like the over-expression of miR-21, miR-144 and miR-27a and the down-regulation of miR-205,

miR-200c and miR-302 [122]. Gasparri et al. [162] reviewed urinary miRNAs in breast tumors, wherein miR-125b predicted resistance to chemotherapy while miR-21, miR-34a, miR-125b, miR-155, miR-195, miR-200b, miR-200c, miR-375 and miR-451 were specific to breast cancer patients and were capable of predicting therapy outcome [169]. Other miRNAs offer potential therapeutic roles in addition to their therapy predictive roles, like the case with miR-200 family, which inhibits angiogenesis through targeting EMT [170]. However, drug resistance remains the leading cause of therapy failure, cancer recurrence and metastasis in breast cancer patients, and thus, understanding its underlying mechanisms along with miRNAs regulatory function holds major promises.

Role	miRNA	sample source (cell line vs patient samples)	breast cancer type	Function	Ref.
Biomarker miRNAs	miR-10b, miR-34a, miR-155, miR-17, miR-122	patient samples	mBC	distinguishes mBC from non-mBC patients	45,52
	miR-10b, miR-373, miR-20a, miR-214	patient samples	lymph node+ BC	upregulated in patients with lymph node positive breast cancer	46-47
	miR-10b	patient samples	mBC	mBC biomarker to the brain and bones	48,49
	miR-141, miR-200a, miR-200b, miR-200c, miR-203, miR-210, miR-375, miR-801	patient samples	BC	significantly elevated in patients with circulating tumor cells	50
	miR-105	patient samples	early onset BC	predicted metastasis in early onset BC	51
	miR-34a, miR-155	patient samples (serum)	mBC	metastasis as a result of primary BC	48
	miR-17-5p	TNBC tissues	TNBC	opposing patterns between miR-17-5p levels and overall survival (OS)	37
	266 miRs in TIF	TIF and serum from BC patients	BC	prognostic and diagnostic biomarkers	56
	miR-222, miR-29a, miR-140,	FFPE tissues	BC	correlated with poor prognosis	59
	miR-210, miR-328, miR-484, miR-874	patient samples	BC	predicting prognosis or risk of recurrence	11
	miR-106b	serum and tissues	BC	predicted high recurrence & shorter OS	54
	miR-18b, miR-103, miR-107, miR-652	patient samples	TNBC	predicted recurrence and decreased OS in TNBC	55

**Table 1:** Summary of miRNAs that exhibit biomarker role in BC and their dysregulation pattern versus their target protein/pathway, sample source, breast cancer type and function. Within each cluster, upregulated miRNAs are highlighted in yellow, downregulated miRNAs in dark blue and dysregulated miRNAs (meaning miRNAs with conflicting dysregulation patterns between studies or dysregulation patterns not indicated in the study) in purple. (Abbreviations: ND = Not Determined, BC= Breast Cancer, mBC= Metastatic Breast Cancer, OS= overall survival, DFS= disease-free survival, PFS= progression-free survival, TNBC= triple negative breast cancer, DCIS= ductal carcinoma in situ, CTCs= circulating tumor cells).

## 5. miRNAs and drug resistance in breast cancer

### a. Mechanisms of drug resistance in breast cancer

The conventional treatment regimens for breast cancer, and mBC, include a combination of surgery with chemotherapeutic agents [mostly anthracyclines (doxorubicin and epirubicin), taxanes (paclitaxel and docetaxel), fluorouracil (5-FU) and cyclophosphamide], hormonal



therapies [estrogen antagonists: tamoxifen, toremifene and fulvestrant that compete with estrogen to bind and block its receptor or aromatase inhibitors (AIs): letrozole, anastrozole, exemestane, which stop estrogen production], targeted therapy (trastuzumab against HER2+) or a combination thereof. Despite the available treatment regimens, breast cancer drug resistance is amongst the leading causes of therapy futility, cancer recurrence and distant metastasis worldwide [121, 135, 151, 171]. One in two breast cancer patients are expected to present with therapy failure or acquire chemotherapy resistance with aggressive malignancy [172, 173]. Anti-cancer therapy resistance can be classified into intrinsic and acquired, wherein pre-existing resistance mechanisms render the patient unresponsive or resistant to cancer therapy (intrinsic resistance), while acquired selection pressure along the course of treatment might tilt the balance from initially-responsive to resistant variants (acquired resistance) [174]. Various mechanisms contribute to cancer drug resistance including reduction in the intracellular drug concentrations brought by aberrant drug transport and metabolism (less drug reaching the cells or higher drug efflux), deregulation in cell cycle, apoptosis and/or DNA repair machineries, overexpression of oncogenic signaling pathways responsible for tumor transformation, dysregulation in DNA methylation and histone modifications and changes in drug target expression and/or availability [129, 174]. All of which have been implicated in breast cancer and have been shown to be regulated in part by miRNAs. In this regard, miRNAs have been studied as potential biomarkers, to predict treatment response and as master regulators in chemotherapy, hormonal, targeted and radiotherapy resistance.

b. Role of miRNA in chemotherapy and in multidrug resistance

Breast cancer drug resistance poses a threat through therapy failure, cancer recurrence and distant metastasis. One major hurdle in chemotherapeutic response is cancer cells acquisition of multidrug resistance (MDR), a phenomenon cancer cells develop upon exposure to one chemotherapeutic agent that renders them unresponsive and resistant to various drugs, subjecting breast cancer patients to treatment futility, poor prognosis and cancer-related deaths [175]. MDR is classified into non-classical and transport-based classical MDR phenotypes. Changes in enzymatic activity of glutathione S-transferase and topoisomerase or alteration in apoptotic proteins are responsible for the non-classical phenotype, while reduced uptake of the drug by cancer cells or increased drug efflux out of the cell represent classical MDR.

The major players in classical MDR are comprised of one or more ATP binding cassette (ABC) transporters, which are ABCB1 (MDR-1/P-gp), multidrug resistance-associated protein ABCC1 (MRP-1) and breast cancer-resistant protein ABCG2 (BCRP), all of which possess hydrophobic elements that compete with drug transport across the cellular membrane [175]. For instance, an upregulation of miR-130 and consequent downregulation of PTEN was detected in tumor tissues as compared to normal adjacent tissues as well as in MCF-7 breast cancer cells resistant to adriamycin (MCF-7/ADR) as compared to sensitive MCF-7 and MCF-10A cells, a non-malignant breast epithelial cell line [152]. Increased drug resistance and proliferation and decreased apoptotic levels were observed upon over-expression of miR-130b in MCF-7/ADR

cells, while downregulation of miR-130b showed opposite patterns. The authors also noted along with the downregulation of PTEN an induction of MDR through activation of the PI3K/Akt pathway and linked it to the upregulation of miR-130b, which in turn induced proliferation and apoptosis. Another example of MDR was reported in doxorubicin-resistant (MCF-7/DOX) breast cancer cells that exhibited low levels of miR-451 compared to DOX-sensitive cells and resulted in increased MDR1 levels, hence increased DOX resistance [176]. By rescuing the levels of miR-451, DOX sensitivity increased through bypassing MDR. Furthermore, MRP-1-mediated MDR can be regulated by miR-326, particularly, in VP-16 (Etoposide)-resistant MDR cell line (MCF-7/VP), where MRP-1 was the only over-expressed ABC transporter protein [175]. A downregulation of miR-326 and up-regulation of MRP-1 were reported in MCF-7/VP cells as well as in different tissues of advanced breast cancer, while a decrease in MRP-1 expression and an increase in VP-16 and DOX sensitivity were identified upon transfection with miR-326 mimics [176].

In non-classical MDR, Glutathione S-transferase P1 (GSTP1) was studied in tissue samples and exosomes from sera of patients with advanced breast cancer pre-and-post anthracycline/taxane-based neoadjuvant chemotherapy to reduce the tumor burden and block metastasis [177]. GSTP1, a member of the phase II metabolic enzymes, can drive chemoresistance through conjugating various anti-cancer drugs with glutathione, resulting in their detoxification. After therapy, levels of GSTP1 were elevated in advanced patients compared to responsive patients with partial re-localization of cellular GSTP1 to the cytoplasm, both in

tissue and exosomal samples. The same pattern was seen in the exosomal marker, tumor susceptibility gene 101 protein (TSG101). This proposed the use of GSTP1-containing exosomes in predicting/transferring chemo-resistance. Therefore, future studies could develop exosomal miRNA biomarkers for MDR prediction, to prevent chemoresistance beforehand, and anti-cancer treatments could govern a merge between the already available therapies and ones that take into consideration preventing/reversing MDR, including exosomal miRNAs [178].

As for the role of miRNAs in chemoresistance, miRNAs are shown either to exhibit a confirmed involvement in chemoresistance, thus increasing the value of  $IC_{50}$  *in vitro* or drug resistance *in vivo* or to serve as a biomarker of chemoresistance [174]. For instance *in vitro* analysis showed that miR-451 was downregulated in MCF-7/DOX-resistant breast cancer cells and was involved in DOX-resistance through targeting P-glycoprotein (MDR1 gene) [176], while the up-regulation of miR-221-222 served as biomarkers for Tamoxifen resistance via targeting p27(Kip1) in MCF-7 and T47D cells [179]. The same pattern was seen with miR-449a/b upregulation in Tamoxifen resistance in frozen breast cancer tissues. In addition, an increase in miR-449a/b levels was shown in tamoxifen-sensitive ZR75 cells while decreased levels of miR-449a/b conferred chemo-resistance in tamoxifen-resistant AK47 cells and other resistant cell lines, which is possibly a consequence of repression of miR-449a/b through DNA methylation [180].

Moreover, aggressive TNBC cells exhibited higher survival and metastatic potential as a

result of miR-181a upregulation upon Dox treatment, which is in line with the poor disease free survival and overall survival noticed in TNBC patients that have high levels of miR-181a upon DOX treatment [151]. Hong et al. [181] discussed one of the most studied miRNAs in breast cancer, oncomiR miR-21. miR-21 upregulation infers chemoresistance, possibly through either enhancing proliferation and suppressing tumor suppressor programmed cell death 4 (PDCD4), thus inhibiting apoptosis, or through repressing PTEN, therefore boosting growth and invasion [182, 183]. A combination therapy of miR-21 inhibitors with paclitaxel was shown to be more efficacious than paclitaxel alone [184]. Zhou et al. [185] characterized a crucial role upregulation of miR-125b plays in paclitaxel-resistant breast cancer cells, by directly downregulating pro-apoptotic Bcl-2 antagonist killer 1 (Bak1), which in turn is partially responsible for paclitaxel cellular uptake. Rescuing the sensitivity of breast cancer cells to paclitaxel was attained through re-expressing Bak1, or inhibiting miR-125b.

c. Role of miRNAs in hormonal therapy response/resistance

miRNAs also play important regulatory roles in hormonal and targeted therapy resistance that might also be breast cancer sub-type specific. As for ER+ breast tumors, treatment regimens typically rely on decreasing (both endogenous or circulating) estrogen levels or on blocking ER using tamoxifen. Although tamoxifen is widely used, ER- breast cancer patients, which comprise 20-30% of breast cancer cases, cannot benefit from this endocrine therapy, neither do a large number of ER+ patients that display intrinsic resistance to endocrine therapy. Unfortunately,

most of the patients who primarily respond to endocrine therapy acquire resistance along the way due to the evasion of cancer cells to endocrine regulatory effect by means of estrogen-independent ER constitutive activation, estrogen/ER-independent growth pathway activation, EMT or miRNAs aberrant expression. While remission is documented in post-menopausal women who receive aromatase inhibitors or other post-tamoxifen therapies, the majority fall victims to relapse and metastasis. This reflects one of the limitations in the conventional staging tools that are incapable of stratifying patients with more stringent differential prognosis and predicting their likelihood to respond to endocrine therapy. Thus, the latter is now accompanied by further cancer subtype classification methods such as the Oncotype DX and MapQuant Dx, which should also be coupled by characterizing the patient's miRNAs signature for enhanced therapy response prediction [186].

miRNAs regulatory role was studied in three tamoxifen-resistant breast cancer cell lines (TamRs) and their tamoxifen-sensitive counterparts in a pursuit to interpret the molecular machineries behind tamoxifen resistance [187]. Out of the 131 dysregulated miRNAs in TamRs, 22 miRNAs showed comparative expression levels among all TamRs, and were shown to affect common underlying pathways, despite regulating different target genes. Of the regulated gene targets *ESR1*, *PGR1*, *FOXMI* and *14-3-3* family genes were noted. Integrational and functional analysis revealed two significantly upregulated target genes, *SNAI2* (a member of the Snail superfamily which can repress E-cadherin, plays a role in EMT and has an anti-apoptotic activity) and *FYN* (a proto-oncogene tyrosine-protein kinase and a member of the Src family of

kinases) in all TamRs, with the downregulation of their regulatory miRNAs and a growth regulatory effect on TamRs. To corroborate the results, combination of miR-190b and miR-516a-5p expression (out of the 131 dysregulated miRNAs in TamRs) exhibited a therapy predictive role in ER+ breast cancer patient cohort who underwent adjuvant tamoxifen treatment.

Moreover, transfection of miR-101 in tamoxifen sensitive MCF-7 cells rendered them resistant to tamoxifen and enhanced their growth, independent of estrogen, via AKT activation and Magi-2 suppression [188].

d. Role of miRNAs in targeted- and immune-therapy response/resistance

Trastuzumab (HER2 monoclonal antibody) resistance is correlated with poor prognosis in HER2+ breast cancer patients [189]. Downregulation of tumor suppressor PTEN, a key regulator of apoptosis and cell invasion, is related to the up-regulation of miR-21. Treatment of breast cancer cells that are resistant to Trastuzumab therapy with antisense oligonucleotides against miR-21 re-sensitized cells through prompting cell death and arresting cell cycle [190]. Moreover, overexpression of miR-125a and miR-125b in SKBR3 cell lines, which overexpress HER2 (ErbB2), efficiently decreased mRNA and protein levels of ErbB2 and ErbB3. It also suppressed anchorage-dependent growth, migration and invasion, subsequently, suppressing MAPK and PI3K/Akt pathways [191]. This is of importance since many studies have been working on the inhibition of PI3K/Akt/mTOR pathway in an effort to target ErbB2 overexpression for the treatment of HER2+ tumors [192]. Studies have also characterized the

miRNAs profile specific to HER2 status in breast tumors represented by miR-520d, miR-181c, miR-302c, miR-376b, miR-30e as well as let-7f, let-7g, miR-107, mir-10b, miR-126, miR-154 and miR-195 [193, 194].

Interestingly, not only do miRNAs take part in drug resistance of different breast cancer types, but they can also help cancer cells escape immunosurveillance and acquire therapy resistance in aggressive breast tumors via regulating apoptosis and immune detection. Elevated levels of miR-519a-3p in breast cancer is correlated to poor survival and breast cancer resistance through regulating TRAIL-R2, FasL and granzyme B/perforin and enhancing apoptosis. By directly repressing TRAIL-R2 and caspase-8 and indirectly repressing caspase-7, miR-519a-3p increases breast cancer cell resistance to therapy and hinders their responsiveness to apoptotic stimuli. As for its role in evading immunosurveillance, miR-519a-3p impairs the recognition of tumor cells by natural killer (NK) cells by means of decreasing the expression of NKG2D ligands ULBP2 and MICA present on tumor cell surface, necessary for cancer cell recognition [195].

e. Role of miRNAs in radioresistance

miRNAs also play part in breast cancer radioresistance. For instance, miR-21 over-expression plays a major role in radioresistance in breast cancer cells through inducing DNA damage-G2 checkpoint upon irradiation, subsequently, aiding tumor cell survival [196]. A transient upregulation of miR-21 in radioresistant T47D breast cancer cells was reported upon 5



Gy irradiation compared to a downregulation in radiosensitive MDA-MB-361 cells. Inhibiting miR-21 pre-irradiation resulted in DNA damage-G2 checkpoint decrease and increase in apoptosis both in T47D cells (7% to 27%) and in MDA-MB-361 cells (18% to 30%). In a validation cohort of 86 invasive breast cancer patient samples and their normal adjacent tissues, miR-21 was overexpressed in the cancerous tissues and associated with decreased metastases-free survival. This proposed the potential of combining anti-miR-21 with radiotherapy to avoid radioresistance. Moreover, downregulation of miR-302 correlated with radioresistance, because rescuing of its expression in breast cancer cells increased their radiosensitivity. miR-302 acts as a key player in sensitizing radioresistant breast cancer cells to radiotherapy through downregulating key regulators in radioresistance, AKT1 and RAD52, both *in vitro* and *in vivo* [197].

Thus, studying the miRNome of breast cancer patients will help discover predictive biomarkers to circumvent unnecessary toxic treatments, and using miRNAs in combination with conventional therapy may reverse subsequent drug resistance. Deciphering the roles miRNAs play in drug (chemo/hormonal/targeted/radio therapy) resistance across different breast cancer types is of great importance.

Role	miRNA	target protein/pathway	validated targets from IPA	sample source (cell line vs patient samples)	breast cancer type	Function	Ref.
miRNAs implicated in drug resistance	miR-21	ND	ND	ND	BC	associated with radio resistance	12
	miR-144		ND				
	miR-27a		FADD, FOXO1, GRB2, IGF1, MMP13, NOTCH1, PDPK1, PXN, SMAD3, SMAD4				
	miR-130	PTEN, MDR, PI3K/Akt pathway	NOTCH, SMAD3, SMAD4, SMAD5	tumor tissues and MCF-7/ADR	BC	Increased drug resistance and proliferation and decreased apoptotic levels	43
	miR-21	PTEN	ND	HER2+ BC patient samples	HER2+ BC	predicted Trastuzumab resistance and poor prognosis	73,74
	miR-101	AKT, Magi-2	ND	MCF-7 cells	benign BC	resistance to tamoxifen and increased ER-independent growth	79
	miR-125b	Bak1	TP53	paclitaxel-resistant BC cells	BC	increased paclitaxel resistance	76
	miR-519a-3p	TRAIL, FasL, granzyme B/perforin	ND	BC cells	aggressive BC	poor survival and resistance to apoptosis and therapy	86
	miR-519a-3p	NKG2D, ULBP2, MICA	ND	BC cells	aggressive BC	escaping immunosurveillance and recognition by NK cells	73
	miR-21	PDCD4, PTEN	ND	Trastuzumab-resistant (BC cells and in vivo xenografts models)	Trastuzumab-resistant BC	chemoresistance	73,74
	miR-21	G2 checkpoint	ND	radioresistant T47D cells, radiosensitive MDA-MB-361 cells, BC patients	radioresistant and invasive breast cancer	increase in DNA damage-G2 checkpoint and increased cell survival	87
	miR-221	p27(Kip1)	FOXO3, PIK3R1, PTEN	in vitro	BC	biomarkers for Tamoxifen resistance	70
	miR-222		FOXO3, PIK3R1, PTEN				
	miR-449a/b		ND				
	miR-449a	ND	ND	frozen BC tissues	BC	inverse correlation with BC grade and tamoxifen resistance	71
	miR-449b		ND				
	miR-451	ND	ABCB1	doxorubicin-resistant (MCF-7/DOX) BC cells	BC	increased MDR1 levels and doxorubicin resistance	67
	miR-326	MRP-1	SMO	VP-16-resistant MDR (MCF-7/VP) & advanced BC tissues	advanced BC	preventative and MDR-reversing role of miR-326 in MRP-1 mediated MDR BC	67
	miR-302	AKT1 and RAD52	ND	<i>in vitro</i> and <i>in vivo</i>	radioresistant breast cancer cells	downregulation causes radioresistance, and re-expression radiosensitivity	88
	miR-205	ND	PTEN	ND	BC	associated with radio resistance	12
	miR-200c, miR-302		ND				
	miR-222	ND	FOXO3, PIK3R1, PTEN	FFPE tissues	BC	associated with drug resistances	59
	miR-29a		PIK3R1, PTEN				
	miR-34a		MAP2K1, TP53				
	miR-140		HDAC4, SMAD3, VEGFA				
	miR-3178, miR-574, miR-6780b, miR-744, miR-423		ND				
miR-21, miR-155	ND	ND	urinary miRNAs	breast and ovarian cancer	distinguishing patients with BC and miR-125b predicted resistance to chemotherapy	60	
miR-125b		TP53					
miR-451		ABCB1					
miR-190b, miR-516a-5p	ND	ND	patient cohort	ER+ BC patients with adjuvant tamoxifen treatment	therapy predictive role	79	

**Table 2:** Summary of miRNAs implicated in drug resistance in BC and their dysregulation pattern, their target protein/pathway, validated targets from IPA, sample source, breast cancer type and function. Within each cluster, upregulated miRNAs are highlighted in yellow, downregulated miRNAs in dark blue and dysregulated miRNAs (meaning miRNAs with conflicting dysregulation patterns between studies or dysregulation patterns not indicated in the study) in purple. The validated pathways selected in IPA only included cancer and drug resistance pathways. (Abbreviations: ND = Not Determined, BC= Breast Cancer, mBC= Metastatic Breast Cancer, OS= overall survival, DFS= disease-free survival, PFS= progression-free survival, TNBC= triple negative breast cancer, DCIS= ductal carcinoma in situ, CTCs= circulating tumor cells).

## **6. *miRNAs and metastasis in breast cancer***

### **a. Circulating miRNAs as biomarkers for metastasis in breast cancer**

Breast cancer morbidity and mortality is generally consequent to distant metastasis rather than the primary tumor per se, constituting 90% of mortality in solid tumors [198, 199]. mBC usually manifests in the lungs, liver, brain or bones. Almost half of mBC patients suffer from distal metastasis to the bones, the most common site, followed by lungs, liver and brain, respectively. Moreover, breast cancer relapse as a result of therapy failure results in metastasis, whereby around 22 % of relapsed patients present with various metastatic sites. Different breast cancer molecular subtypes metastasize into distinct sites. For instance, luminal A, B and HER2+ breast cancers metastasize mostly to the bones while basal breast cancers metastasize mainly to the lungs. While luminal tumors rarely metastasize to the brain, HER2+ cancers do [121].

Despite the significant drop in deaths from breast cancer in the last 2 decades, the majority of female cancer mortality is attributed to breast cancer, specifically mBC. The continuous follow-up on patient's prognosis, through predicting progression-free survival (PFS) and OS tailored to a patient's unique profile is key for personalized medicine, which can increase patient's overall quality of life. CTC are FDA-approved mBC prognostic markers. To date, clinicopathological characteristics including patient's age at diagnosis, size of the tumor, number and types of metastatic sites, receptor status, distant disease-free survival (DDFS), among others are used for metastasis and patient survival prediction. Circulating miRNAs are promising biomarkers for mBC. For instance, elevated levels of miR-141, miR-200a, miR-200b, miR-200c,

miR-203, miR-375, miR-210 and miR-801 not only predicted mBC onset, but also correlated with CTC status and predicted PFS, OS and metastasis 2 years prior to onset [148]. Markou et al. [149] studied the expression level of a panel of miRNAs (miR-21, miR-146a, miR-200c and miR-210) in primary breast tumors from formalin-fixed, paraffin-embedded tissues (89 FFPE samples) compared to normal breast tissues (30 samples) and in CTCs as well as in the plasma of mBC patients (55 donors) compared to healthy subjects (20 donors). CTCs, plasma and primary tumor tissues were studied concurrently from more than half (30) of the metastatic patients under study. Results revealed a differential expression in all metastatic miRNAs between the normal and mBC tissues and an upregulation of all metastatic miRNAs in CTC and matching plasma samples (especially miR-21 in CTCs). More so, overexpression of miR-21 and miR-146a and down-regulation in miR-200c and miR-210 were noted in tumor tissues, while miR-21, miR-146a, and miR-210 were exclusively dysregulated in plasma of breast cancer patients, but not healthy subjects. Another study characterized the miRNome of 40 mBC patients, confirmed it in another patient cohort and found a panel of 16 prognostic miRNAs that correlated with overall survival, of which 11 related to progression-free survival [148]. Importantly, 6 miRNAs (miR-200a, miR-200b, miR-200c, miR-210, miR-215 and miR-486-5p) were identified as early detection markers for metastasis, up to 2 years before its clinical manifestation. Thus, identifying miRNAs signature capable of predicting metastatic onset might offer prolonged median and relapse-free survival rates and might enhance prognosis in breast cancer and mBC patients.

b. miRNAs as active players/regulators of breast cancer along the metastatic cascade

miRNAs, through regulating genes involved in breast tumorigenesis, have been reported to play crucial roles in the genetic and epigenetic alterations along the metastatic cascade.

miRNAs can play a dichotomous role as metastasis promoters, like the scenario with miR-373, miR-151, miR-520, miR-143 or miR-10b or as metastasis suppressors, as with miR-9, miR-139, miR-335, miR-125 or miR-206 [198]. Ma et al. [200] correlated the increase in migration and invasion in mBC cells to the upregulation of miR-10b, which is transcriptionally controlled by TWIST, basic helix–loop–helix protein. Recent studies showed that restoration of tumor-suppressor miR-340 in metastatic MDA-MB-231 cells drastically suppressed migration, invasion and metastasis through targeting the Wnt signaling pathway [147].

miRNAs contribute to metastasis first by priming cells to adopt an EMT phenotype, thus rendering them more motile and invasive. EMT regulatory miRNAs are miR-7, miR-124, miR-145, miR-200 family, miR-205, miR-375 and miR-448 [201]. EMT is characterized by the loss of cells to their epithelial features like apical-basal polarity and tight cell-cell adhesion and the subsequent acquisition of mesenchymal ones via development of extensions, loosened cell-cell adhesion and actin cytoskeletal reorientation. Key players in EMT are Snail (SNAI1), Slug, ZEB (ZEB1 and ZEB2/SIP1) and TWIST1 and E47, all of which act towards the suppression of E-cadherin. miRNAs not only control the initial step of metastasis, EMT, but they also contribute to intravasation of cancer cells into the circulation and the successive extravasation and survival in the metastatic sites. For instance, in SUM149 breast cancer cells, miR-9 was shown to regulate

E-cadherin coding gene, CDH1, thus increased EMT, cell motility and invasiveness [202]. In ER- breast cancer cells, miR-520/373 family repressed invasion and intravasation *in vitro* and *in vivo*, respectively. Moreover, in patients with ER- breast tumors, miR-520c suppression was indicative of lymph node metastasis. After cancer cells undergo EMT, intravasation, extravasation and manage to survive and disseminate to the appropriate distal organ, the final step towards metastasis is the cells' proper colonization at the metastatic site. This is defined as the well-known seed-and-soil hypothesis, implying that cancer cells or "seed" grow in fertile or appropriate tumor microenvironment, the "soil" [119]. For instance, miR-200 through directly regulating the metastasis suppressor Sec23a contributes to breast tumor cells colonization [203].

McGuire et al. [121] summarized different miRNAs implicated in invasion (miR-199a, miR-214, miR-200a/b/c, miR-141, miR-429), dissemination (miR-31), extravasation (miR-10b, miR-373, miR-20a, miR-214, miR-31) and proliferation (miR-10b, miR-34a, miR-155, miR-200a/b/c, miR-141, miR-429). Moreover, antagonistic effects of miRNAs were studied for miR-214 and miR-148b that act as pro-metastatic and anti-metastatic miRNAs in mBC dissemination through dictating the interactions between tumor and endothelial cells. Metastatic dissemination was blocked through dual alteration; downregulating miR-214 and upregulating miR-148b, resulted in downregulation of cell adhesion genes ITGA5 and ALCAM, subsequently blocked tumor escape through blood endothelial vessels *in vitro*, *in vivo* and in primary breast cancer patient samples [204].

miR-22/SIRT1 (Sirtuin1) axis was linked to breast cancer growth and metastatic suppression and proposed it as a potential therapeutic target against mBC [205]. Notably, miR-22 directly suppresses SIRT1 in MCF-7 breast cancer cells. The suppression of miR-22 and significant upregulation of SIRT1 was revealed in breast cancer tissues as compared to normal tissues and in stage III-IV breast tumors as compared to stage I-II breast tumors. Thus, miR-22 downregulation was indicative of poor differentiation, metastasis and progressive breast cancer stages. On the contrary, overexpression of miR-22 attenuated proliferation, migration and invasion in MCF-7 cells, while overexpressing SIRT1 reversed the tumor-suppressive and metastasis-suppressive role of up-regulated miR-22 in the cells. Moreover, Li et al. [206] related breast cancer metastatic initiation to the downregulation of miR-452 and the resulting upregulation in RAB11A, both in breast cancer tissues and cell lines. miR-452 acts a tumor suppressor through downregulating RAB11A and is responsible for suppressing migration and invasion in breast cancer. In addition, by upregulating the pro-metastatic gene RhoA, miR-155 promoted EMT, cell migration and invasion [207], while miR-31 blocked metastasis by inhibiting RhoA and disabling cancer cells from exiting the primary tumor site, disseminating and/or surviving in distal sites [208, 209]. miR-31 targets also include Frizzled3 (Fzd3), integrin  $\alpha$ -5 (ITGA5), myosin phosphatase-Rho interacting protein (M-RIP), matrix metalloproteinase 16 (MMP16), radixin (RDX), as well as PKC $\epsilon$ , which deregulates NF- $\kappa$ B signaling pathway, increase apoptosis and enhances MCF-10A and MDA-MB-231 cells radiosensitivity [210, 211]. In MCF-7 cells, upregulation of miR-17-5P increased invasiveness and migration via targeting

HBP1/ $\beta$ -catenin pathway [212]. In addition, miR-145, through regulating c-Myc and mucin and downregulating c-Myc downstream targets like cyclin D1 and eIF4E plays a role in cancer cell motility and cell cycle progression [188].

Moreover, miRNAs not only control metastasis, but they also regulate angiogenesis. Lu et al. [213] investigated the role of the tumor suppressive miR-140-5p in breast cancer in regulating invasion and angiogenesis. Their results showed that miR-140-5p regulates the vascular endothelial growth factor VEGF-A *in vitro* and *in vivo*. Similarly, miR-378 and miR-27a have been shown to enhance angiogenesis and tumor cell survival in breast cancer [214, 215]. Moreover, downregulation of miR-140-5p was observed in breast cancer and mBC tissues as compared to their normal counterparts, and thus, might serve as a novel anti-metastatic and anti-angiogenic agent in breast cancer.

c. Examples of miRNAs implicated in common sites of breast metastases

miRNAs can play a role in breast cancer metastasis to distal regions such as brain, bone and lung. LI et al. [146] discussed the importance of deciphering the role miRNAs play in diagnosing and, possibly, treating breast cancers with brain metastasis. This is since (10-30%) of patients with advanced breast cancer suffer from brain metastasis with poor prognosis. The universal gene expression signatures of patients with primary *in situ* breast carcinoma and patients with brain metastasis were investigated in a pursuit to identify the differential expression patterns in miRNAs, their corresponding mRNA targets and the underlying signaling pathways that might



serve as early detection markers for brain metastasis. Results showed a strong correlation between miR-17-5p and miR-16-5p and BCL2, SMAD3 and SOCS1 and subsequent oncogenic pathways like ones concerned with EMT, cell cycle control, adherence junctions and extracellular matrix-receptor communication. A comparison of patient samples to matched breast cancer patients from The Cancer Genome Atlas (TCGA) revealed similar expression levels in 11 miRNAs, wherein miR-17-5p was upregulated in TNBC tissues extracted from the database, with opposing patterns between miR-17-5p levels and overall survival and PTEN and BCL2 levels. Thus, devising a systems-gene expression patterns can better guide clinicians into predicting optimal treatment options specific for patients with breast cancer brain metastasis.

Soria-Valles et al. [216] linked downregulation of miR-21 to matrix metalloproteinase, collagenase-2 (MMP-8), which exhibited a tumor suppressive role and lung metastasis blockage in MDA-MB-231 breast cancer cells. The authors validated the results *in vitro* and *in vivo* and related the protective role of MMP-8 to decorin cleavage and inhibition in TGF- $\beta$  signaling, which in turn downregulates miR-21. This eventually induces tumor suppressors such as programmed cell death 4. An example of miRNAs effect on bone metastasis was discussed in a study on the stimulatory role of TWIST1 on breast cancer intravasation and dissemination to the bones using human osteotropic MDA-MB-231/B02 breast cancer cells and immunodeficient mice [217]. TWIST1 stable transfection *in vitro* showed enhancement in tumor cell invasion, but not tumor growth, and resulted in upregulation in the pro-invasive miR-10b level. *In vivo*, TWIST1 transfection caused higher osteolytic lesions, reduced bone volume and caused

doubling of the tumor burden. Upon treatment with DOX, TWIST1 was suppressed, and hence, bone metastasis was blocked *in vivo*. Blocking miR-10b in the mice caused drastic reduction in TWIST1-expressing breast cancer cells found in the bone marrow. Therefore, miR-10b takes part in regulating TWIST1-induced breast cancer bone metastasis.

Bishopric et al. [218] inoculated MDA-MB-231 and MDA-MB-436 breast cancer xenografts into immunodeficient mice mammary fat pads to produce primary tumors and corresponding lymph node, liver, lung and diaphragm metastases. By comparing the miRNAs profiles of the primary and the metastatic tumors, the authors found miR-203 levels, which acts as a tumor suppressor, to be significantly associated with the size of the primary tumor at all metastatic sites. miR-203 acted by directly targeting TWF1 and APBB2. Although miR-203 was shown to be necessary for metastasis growth, its over-expression inhibited metastasis, thus

implicating opposing function and a dynamic, context-dependent function of miR-203 along the

miRNA	target protein/pathway from the literature	validated targets from IPA	sample source (cell line vs patient samples)	breast cancer type	Function	Ref.
miR-141	ND	CTNNB1, MAP2K4, PTPRD, STAT5B, TGFB2, ZEB1, ZEB2	Circulating miRNA	Breast Cancer	predicted MBC onset, correlated with CTC status and predicted PFS and OS	39
miR-200a/b/c		PLCG1, PTEN, PTPN12, PTPN13, PTPRD, ZEB1, ZEB2				
miR-203		ABL1, SOCS3				
miR-375, miR-210, miR-801		ND				
miR-10b	TWIST	ND	mBC cells	mBC	increase in migration and invasion	38,89
miR-17-5P	HBP1/β-catenin	BCL2, BMPR2, CCND1, CDKN1A, CREB1, JAK1, MAP3K12, MMP3, PTEN, STAT3, TGFB2, TNF, VEGFA, VIM	MCF-7 cells	BC	increased invasiveness and migration	37
miR-203	TWF1, APBB2	ABL1, SOCS3	MDA-MB-231 and MDA-MB-436 breast cancer xenografts	lymph node, liver, lung and diaphragm metastases	opposing function and a dynamic, context-dependent function of miR-203 in metastasis (enhancer and suppressor)	
miR-181a	STAT3,NF-κB, IL-6	BCL2, CDKN1B, KRAS, MMP14, NOTCH4, TIMP3	TNBC patients with Dox treatment	TNBC	higher metastatic potential, and poor DFS & OS	115
miR-340	Wnt pathway	ND	metastatic MDA-MB-231 cells	invasive BC	migration, invasion & metastasis suppression	38
miR-17-5p	BCL2, SMAD3, SOCS1, EMT	BCL2, BMPR2, CCND1, CDKN1A, CREB1, JAK1, MAP3K12, MMP3, PTEN, STAT3, TGFB2, TNF, VEGFA, VIM	patient samples and TCGA database	patients with DCIS or brain metastasis	devising a systems-gene expression patterns to predict cancer metastasis	37
miR-16-5p		ANLN, BCL2, CCND1, CDC14B, CDC25A, CFL2, EGFR, EIF4E, FGF2, FGF7, FGFR1, GRB2, H3F3A/H3F3B, HSP90B1, IGF1, IGF1R, IGF2R, ITGA2, JUN, MAP2K1, MAP2K4, MAPK3, MCL1, PHKB, PPP2R5C, PTGS2, RAF1, RECK, RHOT1, VEGFA, WIPF1, WNT3A, ZYX				
miR-452	RAB11A	ND	BC tissues and cell lines	BC	MBC initiation (when upregulated, acts as tumor suppressor)	97
miR-520c	ND	ARHGEF3, CCND1, CDKN1A, CFL2, PRKACB, RECK, RELA, VEGFA	ER-ve BC patients	ER-ve BC	indicative of lymph node metastasis	94
miR-155	RhoA	ARFIP2, CCND1, CEBPB, CTNNB1, ETS1, FADD, FGF7, GNA13, IKBKE, INPP5D, MET, MYD88, PDE3A, PRKCI, PTPRJ, RAB5C, RHEB, RHOA, RIPK1, SMAD2, TAB2, TCF7L2	ND	BC	promoted EMT, cell migration and invasion	98
miR-21	MMP-8, decorin, PCD4, TGF-β	ND	MDA-MB-231	BC	tumor suppressor and lung metastasis blockage	107
miR-146a	ND	CD40, CDKN3, CHUK, FADD, IL1R1, IL36B, IL36G, IRAK1, MMP16, STAT1, TLR10, TLR4, TLR9, TRAF6	ND	ND	ND	
miR-200c, miR-210, miR-21		ND				
miR-373, miR-151, miR-10b	ND	ND	ND	BC	metastasis promoters	89
miR-520		ARHGEF3, CCND1, CDKN1A, CFL2, PRKACB, RECK, RELA, VEGFA				
miR-143		BCL2, KRAS, MAPK12, MDM2				
miR-9		ND				
miR-139	ND	FOXO1, IGF1R, SHC1	ND	BC	metastasis suppressors	89
miR-335		PTPN11, PXN				
miR-125		BMPR1B, CDC25A, ELAVL1, H3F3A/H3F3B, ID2, IL1RN, IL1RN, MAP2K7, MYD88, SMO, TP53				
miR-206		ARF3, ARF4, ARHGEF18, BCL2, EGFR, H3F3A/H3F3B, IGF1, INPP5F, ITGB4, LRP1, MET, NOTCH3, NRP1, PTPRF, TIMP3, TSPAN4, YWHAQ				

metastatic cascade.

miR- +B27:H36520/373 family	ND	ARHGEF3, CCND1, CDKN1A, CFL2, PRKACB, RECK, RELA, VEGFA	in vitro and in vivo	ER-ve BC cells	repressed invasion and intravasation	94
miR-200	Sec23a	ND	BC cells	BC	contributes to BC colonization	94
miR-22/SIRT1 (Sirtuin1) axis	SIRT1	ND	MCF-7 cells and (stage III- IV) BC tissues	mBC	BC growth and metastatic suppression and a potential therapeutic target against MBC	96
miR-10b	TWIST	ND	mBC cells	mBC	increase in migration and invasion	108
miR-199a	ND	ETS1, HIF1A	ND	mBC	implicated in invasion	11
miR-214, miR-141		ND				
miR-200a/b/c		PLCG1, PTEN, PTPN12, PTPN13, PTPRD, ZEB1, ZEB2				
miR-429		PLCG1, PTEN, PTPN12, PTPN13, PTPRD, ZEB1, ZEB2				
miR-31, miR-10b, miR- 373, miR-214	ND	ND	ND	mBC	implicated in extravasation	11
miR-20a		BCL2, BMP2, CCND1, CDKN1A, CREB1, JAK1, MAP3K12, MMP3, PTEN, STAT3, TGFBR2, TNF, VEGFA, VIM				
miR-10b, miR-34a, miR-155, miR-141	ND	ND	ND	mBC	implicated in proliferation	11
miR-200a/b/c, miR-429		PLCG1, PTEN, PTPN12, PTPN13, PTPRD, ZEB1, ZEB2				
miR-214	ITGA5 and ALCAM	ATF4, FGF16, PTEN	in vitro, in vivo, in primary BC patients	mBC	miR-214 downregulation & miR-148b upregulation blocked dissemination	95
miR-148b		ND				
miR-378	ND	ND	ND	BC	enhance angiogenesis & tumor survival	105,106
miR-27a		FADD, FOXO1, GRB2, IGF1, MMP13, NOTCH1, PDPK1, PXN, SMAD3, SMAD4				
miR-31	RhoA, Fzd3, ITGA5, M- RIP, MMP16, RDX, PKC $\epsilon$ , NF- $\kappa$ B	ND	MCF-10A and MDA-MB- 231	BC	blocked metastasis, increase apoptosis and enhances radiosensitivity	99,100
miR-9	CDH1	ND	SUM149 breast cancer cells	BC	elevated cell motility and invasiveness	93
miR-145	c-Myc and mucin, cyclin-D1, eIF4E	CLINT1, DDR1, EIF4E, IGF1R, IRS1, MDM2, MMP1, PPP3CA, RTKN	ND	BC	regulates cancer cell motility and cell cycle progression	79
miR-140-5p	VEGF-A	SMAD3, VEGFA	in vitro and in vivo	BC and MBC	tumor suppressor, and possible novel anti-metastatic and anti-angiogenic agent	104

**Table 3:** Summary of miRNAs implicated in metastasis in BC and their dysregulation pattern, their target protein/pathway, validated targets from IPA, sample source, breast cancer type and function. Within each cluster, upregulated miRNAs are highlighted in yellow, downregulated miRNAs in dark blue and dysregulated miRNAs (meaning miRNAs with conflicting dysregulation patterns between studies or dysregulation patterns not indicated in the study) in purple. The validated pathways selected in IPA included metastasis, NF- $\kappa$ B signalling, VEGF signalling and VEGF family ligands, inhibition of MMPs, JAK/STAT signalling, PI3K/AKT signalling, Integrin signalling, epithelial adhesion, remodelling of the epithelium and EMT pathways. (Abbreviations: ND = Not Determined, BC= Breast Cancer, mBC= Metastatic Breast Cancer, OS= overall survival, DFS= disease-free survival, PFS= progression-free survival, TNBC= triple negative breast cancer, DCIS= ductal carcinoma in situ, CTCs= circulating tumor cells).

## 7. miRNAs role in the interplay between drug resistance and metastasis in breast cancer

Despite the booming reports on miRNAs that act on drug resistance or metastasis, the quest on whether some miRNAs are capable of regulating both simultaneously is fundamental, yet understudied. The rationale behind this is that the likelihood of recurrence and subsequent

distant metastasis in tumor cells increases due to drug resistance. For instance, miR-644a acts pleiotropically through increasing cell death and inhibiting EMT, thus sensitizing various breast cancer subtypes to both hormonal-and-targeted therapeutic agents (like tamoxifen and gefitinib) and blocking metastasis [135]. EMT inhibition was thus proposed as the common underlying mechanism towards drug sensitization and metastasis blockade. Moreover, miR-644a was shown to directly downregulate transcriptional co-repressor C-Terminal Binding Protein 1 (CTBP1), which in turn upregulates wild type-or mutant-p53. The downregulation of CTBP1 retarded growth, metastasis and drug resistance and was validated in miR-644a CRISPR-Cas9 knockouts. Of note, only patients with mutant-p53 and upregulation in CTBP1 exhibited shorter survival, priming CTBP1 to serve as a prognostic marker for p53-mutant patients. This suggested a therapy-sensitizing and metastasis blocking potential through reactivation of miR-644a/CTBP1/p53 axis in breast cancer along with its potential as progression and therapy predictive biomarker. Another study suggested NSC95397, a small molecule capable of obstructing transcriptional repression brought by CTBP1, as an easier drug target than miR-644a [219].

Other examples of the role miRNAs play in regulating EMT in breast cancer, leading to endocrine (hormone) therapy resistance is how breast cancer cells acquired a mesenchymal phenotype due to the upregulation of miR-9 that resulted in E-cadherin repression and vimentin overexpression [186, 202]. Moreover, miRNAs can initiate drug resistance and metastasis concomitant with cancer stem cell (CSC) characteristics. Although CSCs only constitute part of

the tumor burden, they are known to initiate growth, metastasis and drug resistance in tumors [198]. While some miRNAs have been reported to control the interplay between cancer stemness and drug resistance, others reported how miRNAs control stem cell and metastatic characteristics of cancer cells via EMT regulation. For instance, compared to non-CSCs extracted from advanced mBC cells, CD24<sup>-</sup>/CD44<sup>+</sup>/ESA<sup>+</sup> CSC population was capable of driving metastasis. When these CSC metastasize to the bones and brain, downregulation in miR-7 was noted; however, blockade of brain metastasis was possible through re-expressing miR-7 in breast CSCs, which in turn repressed stemness regulatory gene, KLF4 [220]. In addition, miRNAs can play a role in breast cancer drug resistance and metastasis through epigenetics [221]. Thus, studies are investigating the effect of differentially methylated regions (DMRs) of miRNAs loci in invasive breast cancers. For instance, analysis of DMRs and methylation patterns in miR-31, miR-135b and miR-138-1 were correlated with patterns seen in early and late postpartum breast cancer patients [222]. Moreover, a correlation was shown between aggressiveness and advanced breast cancer disease and the methylation of tumor suppressive and DNMT3b targets which are miR-124a-1, miR-124a-2 and miR-124a-3 [223]. However, while aberrant DNA methylation, in part, controls the expression of miRNAs and subsequent downstream pathways, miRNAs can also control some DNA methylators.

In addition, miRNAs can play a role in chemoresistance in aggressive TNBC, which does not respond to any targeted therapies. Niu et al. [224] showed that TNBC cells exhibited higher survival and metastatic potential as a result of miR-181a upregulation upon genotoxic DOX

treatment. These results were also noticed in TNBC patients with high levels of miR-181a post-DOX treatment who had poor disease-free survival and overall survival. Moreover, chemoresistance was attributed to apoptosis evasion and enhanced invasion in DOX-treated TNBC cells to the direct suppression of BAX by miR-181a. Thus, blocking miR-181a could potentially rescue DOX sensitivity in TNBC cells and alleviate metastasis. A similar pattern was observed in HER2+ breast cancer patients, with noted upregulation in miR-181a, whereby blocking miR-181a re-sensitized breast cancer cells to Trastuzumab and inhibited metastasis. Thus, inhibiting miR-181a could reverse both chemo-and-targeted therapy resistance and block metastasis in TNBC and HER2+ breast tumors, respectively. Moreover, Bai et al. [225] showed increase in EMT and TGF- $\beta$  signaling with a downregulation of miR-200c in highly invasive, tumorigenic, Trastuzumab-resistant HER2+ breast cancer cells. Re-expression of miR-200c targeted both a TGF- $\beta$  transcriptional activator ZNF217 and a key player in the TGF- $\beta$  signaling pathway, ZEB1, thus rescuing Trastuzumab sensitivity and blocking invasion concomitantly. Alternatively, silencing of ZEB1 or ZNF217 or inhibiting TGF- $\beta$  signaling exhibited same response as restoration of miR-200c in resistant cells, suggesting a miR-200c/ZEB1 and miR-200c/ZNF217/TGF- $\beta$ /ZEB1 regulatory circuits in Trastuzumab resistance and distal metastasis.

Therefore, it is vital to focus on miRNAs that act both as therapy sensitizers and metastasis blockers, for an optimal understanding of their regulatory role, and for widening their potential use as biomarkers and therapeutic tools against breast cancer. One successful promising example is oncomiR, miR-21, which is almost upregulated in most breast cancers and has been

reported to drive both drug resistance and metastasis. Mei et al. [184] potentiated the simultaneous delivery of miR-21 inhibitor and paclitaxel through G5-PAMAM dendrimer, in order to impede both tumor growth and invasiveness in breast cancer. Thus, complimenting conventional therapies with miRNAs inhibitors/mimics holds hope in combating drug-resistance and circumventing metastasis in breast cancer [129].

Role	miRNA	target protein/pathway	validated targets from IPA	sample source (cell line vs patient samples)	breast cancer type	Function	Ref.
miRNAs implicated in both drug resistance and metastasis	miR-644a	CTBP1, p53, Noxa	ND	BC cell lines	various BC subtypes	sensitizes cells to targeted/chemotherapy and blocks metastasis	26, 110
	miR-9	E-cadherin, vimentin	ND	BC cell lines	BC	regulates EMT leading to endocrine resistance	77,93
	miR-21	G5-PAMAM	ND	BC cell lines	BC	drive drug resistance and metastasis	75
	miR-7	KLF4	ND	breast CSCs	breast CSCs	CSC metastasize to the bone and brain	111
	miR-7	EMT	ND	BC cell lines	BC	EMT regulatory miRs that might lead to drug resistance	92
	miR-124		ARAF				
	miR-145		CLINT1, DDR1, EIF4E, IGF1R, IRS1, MDM2, MMP1, PPP3CA, RTKN				
	miR-200 family		PLCG1, PTEN, PTPN12, PTPN13, PTPRD, ZEB1, ZEB2				
	miR-205		ERBB3, INPPL1, MED1, PRKCE, PTEN, VEGFA				
	miR-375, miR-448		ND				
	miR-31		ND				
	miR-135b	ND	APC	early/late postpartum BC patients	BC	correlation with differentially methylated regions	113
	miR-138-1		RHOC, ROCK2				
	miR-124a-1/2/3	DNMT3b	ARAF, ARHGEF1, CDK2, CDK4, CDK6, CTGF, CTNND1, DRAM1, DVL2, E2F5, ELF4, ELK3, GNAI3, ITGB1, MAPK14, PRKD1, RARG, RELA, RHOG, SMAD5, SNAI2, SOX9, SP1, TLN1, TRIM29, TUBB6	ND	advanced BC	correlates aggressiveness and advanced BC with methylation patterns	114

**Table 4:** Summary of miRNAs implicated in both drug resistance and metastasis in BC and their dysregulation pattern, their target protein/pathway, validated targets from IPA, sample source, breast cancer type and function. Within each cluster, upregulated miRNAs are highlighted in yellow, downregulated miRNAs in dark blue and dysregulated miRNAs (meaning miRNAs with conflicting dysregulation patterns between studies or dysregulation patterns not indicated in the study) in purple. The validated pathways selected in IPA included cancer, drug resistance, metastasis, NF- $\kappa$ B signalling, VEGF signalling and VEGF family ligands, inhibition of MMPs, JAK/STAT signalling, Pi3K/AKT signalling, Integrin signalling, epithelial adhesion, remodelling of the epithelium and EMT pathways. (Abbreviations: ND = Not Determined, BC= Breast Cancer, mBC= Metastatic Breast Cancer, OS= overall survival, DFS= disease-free survival, PFS= progression-free survival, TNBC= triple negative breast cancer, DCIS= ductal carcinoma in situ, CTCs= circulating tumor cells).



However, a few caveats are common in most of the mentioned studies, and must be addressed. Markou et al. [149] pointed out the pitfalls underlying the lack of reproducibility across studies performed by different groups on similar patients and cancer profiles. For instance, when comparing the databases of 15 studies characterizing circulating miRNAs profiles of breast cancer patients, very little overlap was detected. The authors attributed the lack of reproducibility to variations in sample origins (plasma, serum, whole blood), variability in cohort population and inconsistencies in sample collection protocols/timings and sample processing. As for the discrepancies in miRNAs profiles reported from the same tumor, it might be partly attributed to the lack of an established endogenous miRNA for normalization [226]. Pichler and Calin [227] addressed few solutions, like the importance of designing larger prospective clinical trials that encompass the published work on candidate diagnostic or prognostic miRNAs and comparing them to the gold standard techniques in a blinded fashion. Most of the current findings were done retrospectively, were prone to error-and-selection bias and lacked long-term follow-up. Cortez et al. [153] stressed on the importance of characterizing specific panels of differentially expressed miRNAs rather than single miRNAs as exclusive biomarker panels to a certain type of cancer, stage (early vs advanced), therapy response, patient outcome, recurrence or metastatic output, which will also account for intra-tumoral and intercellular heterogeneity. One major area that requires development in miRNA-based therapies is the establishment of stable and effective delivery systems with minimal off-target and adverse effects. As exosomes house miRNAs, they have proven to be efficient in miRNAs delivery to breast cancer cells

expressing EGFR. Ohno et al. [228] described how engineering protocols were capable of expressing transmembrane domain of platelet-derived growth factor receptor (PDGF) merged to GE11 peptide, a less mitogenic EGFR binding partner, on donor cells. These exosomes were then able to successfully deliver let-7a miRNA, intravenously, in RAG2<sup>-/-</sup> mice breast cancer xenografts that exhibited EGFR. Some successful nucleic acid therapies made it to human clinical trials, the first of which was miraversen ([www.clinicaltrials.gov](http://www.clinicaltrials.gov), study no. NCT01200420), which was designed to capture miR-122 to inhibit the replication of hepatitis C virus, after it was proven effective in chimpanzees [174]. More than dozens of clinical trials are underway, testing the prognostic, metastatic and therapy predictive potential possessed by some candidate miRNAs, or alternatively, players in the biogenesis pathway of miRNAs ([www.clinicaltrials.gov](http://www.clinicaltrials.gov)). Adams et al. [118] predicted the potential of using miR-34a for treatment of TNBC based on clinical studies investigating MRX34, an amphoteric liposome coupled with a synthetic miR-34a mimic, for its efficacy against hepatocellular carcinoma in phase I clinical trial. The rationale behind their prediction is that miR-34a was capable of sensitizing TNBC to dasatinib treatment by targeting c-SRC, and thus, administering miR-34a and dasatinib might be worth investigating in aggressive TNBC.

Recent studies are focusing on circRNAs and their roles in “sponging” microRNAs. circRNAs are a large class of endogenous RNAs that originate from cellular splicing and play regulatory roles in mammalian cells. Sequencing analysis has also shown circRNAs to be dysregulated in cancers (cell lines, patient tissues, plasma and serum) and are characterized by their stability,

conserved sequences and presence in the circulation. Thus, sequencing circRNAs along with their downstream miRNAs targets will add one more layer to better understand the drivers of cancer initiation, progression, drug resistance and metastasis and will bring us a step closer towards devising better breast cancer biomarkers [229]. Moreover, the commonly used integrative analysis approach for predicting miRNAs gene and protein targets and networks, known as the systems biology approach, is continuously being updated and developed to accommodate for better prediction of efficacy and activity of candidate miRNAs on a universal scale [198]. Improving the already available breast cancer miRNAs databases to elucidate details on sample sources, miRNAs expression profiles, extraction protocols, their diagnostic, prognostic, therapy predictive, therapeutic and metastatic potential, would lay grounds for better, more reproducible and more tumor-specific miRNAs studies [122]. This, of course, calls for a more integrative understanding of the miRNA–gene and miRNA-protein interaction networks through the development of multi-disciplinary systems biology approaches assimilating genomics, genetics, proteomics and bioinformatics, to better understand and combat cancer initiation, development, progression and recurrence.

## **B. Connexin43 as a tumor suppressor: proposed connexin43 mRNA-CircularRNA-miRNA axis towards prevention and early detection in breast cancer**

Authors: Nataly Naser Al Deen <sup>1</sup>, Mounir AbouHaidar <sup>2</sup>, Rabih Talhouk <sup>1\*</sup>  
Published Manuscript: *Frontiers in Medicine* (Naser Al Deen et al. 2019)

BC registers the highest incidence and mortality rates in females and is the second most commonly diagnosed cancer (after lung cancer) [31]. Incidence of early-onset BC in young women is alarming and has increased drastically [5, 32, 33]. It is crucial to focus on non-invasive biomarkers and active players in BC early initiation processes, towards prevention and early detection [6]. The mammary gland undergoes extensive remodeling during development, from prenatal to post lactation stages [22, 23]. Lobules, milk ducts, connective tissues and adipose tissues constitute the mature human female breast. Functional centers that link a lobule to its terminal duct and to the ductal system are terminal duct lobular units (TDLUs). Each lobule contains group of alveoli, responsible for milk secretion during lactation. Both ducts and alveoli are lined by luminal epithelial cells, forming ductal and lobular epithelium, respectively, which in turn are lined by discontinuous layer of myoepithelial cells and are separated by a supporting basement membrane. The latter is underlain by the stroma, an extracellular matrix (ECM) and stromal cells, including fibroblasts, adipocytes, endothelial cells and immune cells [20, 34, 35].

Mammary gland development requires well-orchestrated cell-cell and cell-ECM communication by gap junctions and systemic signals. Connexins (Cxs) are a family of transmembrane proteins. They are responsible for establishing gap junction intercellular communication (GJIC), capable of linking cytoplasm of two neighboring cells, allowing intercellular exchange of ions, second messengers and metabolites [18, 36, 37]. Each GJ channel is made up of two docked connexons, spanning the two membrane bilayers of adjacent cells,

whereby each connexon forms by oligomerization of hexagonally arrayed connexins [19]. GJs mediate channel-dependent and channel-independent functions. Any perturbations in Cxs expression/localization may alter the function of the gland and lead to tumorigenesis. Cxs act as tumor-suppressors, in a context-dependent manner, like Cx43, the focus of this review [20, 34] **(Figure 1)**.

Recently, we revealed an apicolateral distribution/localization of Cx43 in luminal human breast epithelium, and that loss of Cx43 expression contributes to breast tumorigenesis by disrupting apical polarity and promoting cell multi-layering, a hallmark of tumor initiation [27]. Furthermore, populations at higher risk of BC (like obese patients) exhibit loss of Cx43 apical distribution and cell multi-layering in an inflammatory microenvironment [38, 39]. Studies from our group have characterized pathways and phenotypes downstream of Cx43 loss/mis-localization in 3D human breast epithelial HMT-3522 S1 cells [26, 27, 40-42]. Hence, an axis that parallels Cx43 mRNA loss will be proposed. miRNAs are small non-coding RNAs that repress translation, and circRNAs originate from RNA splicing and act as miRNA “sponges” [29, 43]. circRNAs and miRNAs unique dysregulation signatures in cancers (in tissue- and development stage-specific manner), their tumor suppressive/oncogenic roles and stability and abundance in body fluids make them attractive non-invasive biomarkers in liquid biopsies [6, 43]. Here, an axis by Cx43-derived circRNAs and their sponged miRNAs is proposed during BC

initiation stages, which might act as promising biomarker signature towards BC early-onset detection and prevention, especially in patients at increased risk.

### ***1. Cx43 in Normal Mammary Gland Development and Differentiation***

GJs play major role in establishing communication between adjacent cells [44-47] and studying mice made it possible to infer Cxs spatio-temporal expression patterns across mammary gland development [48]. The mammary gland expresses Cx43 in myoepithelial and epithelial cells junction [40], whereby Cx43 mRNA levels drop half-way through gestation and lactation, while its active phosphorylated form is evident during lactation [34]. Autosomal dominant Cx43 mutant mice (Cx43<sup>I130T/+</sup>) exhibited delay in ductal elongation and atrophied glands pre-puberty [49]. Myoepithelial contractility was inhibited upon Cx43 knockdown or GJIC blockage in primary mammary organoids of wild-type mice [50]. Substituting Cx43 levels with Cx32 retarded growth and survival of (Cx43<sup>Cx32/+</sup>) heterozygous knock-in pups, due to perturbation in milk ejection [51]. These studies confirm Cx43 pivotal role along mammary gland development. We also demonstrated crucial roles for Cx43 in mammary epithelial differentiation, which relied on proper GJ complex assembly composed of Cx43,  $\alpha$ -catenin,  $\beta$ -catenin and ZO-2 [24]. Thus, studying Cx43 perturbation is important in understanding early events in breast cellular transformation.

### ***2. Perturbations in Cx43: Cx43 as Tumor Suppressor/Biomarker in BC***

Since the mammary gland development is sensitive to perturbations in Cx43 expression, localization and function, Cx43 plays a tumor-suppressive role and contributes to breast tumorigenesis, in a context- and stage-dependent manner [52-56]. Overexpression of Cx43 in MCF-7 and MDA-MB- 231 BC cells significantly decreased cells proliferation and nuclear levels of  $\beta$ -catenin in 3D cultures, which was mediated by membranous Cx43 recruitment of  $\alpha$ -catenin,  $\beta$ -catenin and ZO-2 [41]. McLachlan et al., [57] linked an impedance of tumor growth to upregulation of Cx43 *in vivo*, by favoring a mesenchymal to epithelial transition. Recently, we showed for the first time an apicolateral distribution and localization of Cx43 in luminal breast epithelium. Further, we showed that silencing Cx43 expression contributes to breast tumorigenesis by enhancing proliferation and cell cycle progression and inducing mis-localization of membranous  $\beta$ -catenin, resulting in loss of apical polarity, misorientation of mitotic spindle, cell multi-layering and loss of lumen (hallmarks of tumor initiation). Silencing Cx43 activates signaling pathways that promote invasion in non-tumorigenic breast epithelium [26, 27]. Similarly, Lesko et al., [58] showed that disruption of epithelial polarity was a marker of epithelial-derived tumor initiation.

Teleki et al., [59, 60] conducted a meta-analysis on Cx isotype expression data in breast tissue microarray from patients from all tumor grades. Their results showed, both in normal and breast tissues, the expression of Cx43, Cx46, Cx26, Cx30 and Cx32. Of the detected Cxs, only Cx43 correlated with improved disease prognosis and served as better prognostic marker than vascular invasion or necrosis. High levels of Cx43 in grade 2 tumors marked them as good

relapse free survival subgroups. Other microarray results from tissue samples of invasive breast carcinoma patients showed that Cx43 levels positively correlated with progesterone and estrogen receptor status, but negatively correlated with Ki67 (proliferation marker) expression [61]. In contrast, high levels of Cx43 was detected in BC patient biopsies at later tumor stages, suggesting its potential role in inducing tumor progression [62, 63]. This is since during invasion, the tumor epithelial cells may reactivate GJIC with endothelial cells to facilitate intravasation/extravasation [44]. Thus, Cx43 acts as a tumor suppressor in normal breast tissues, its loss/mis-localization contributes to BC initiation, its high levels in the primary tumor serves as a good prognostic marker while its re-expression at later tumor-stages facilitates invasion and metastasis [44].

### ***3. Interactions Between Connexins and microRNAs***

Recent studies reported two possible modes of interaction/regulation between miRNAs and Cxs. The first through direct binding of miRNAs to 3'-UTR of mRNAs coding for Cxs and other junctional proteins, and the second via direct transfer of candidate miRNAs through gap junctions between neighboring cells. Lin et al., [64] correlated BC distant metastasis to opposite expression levels of miR-206 and Cx43 in triple-negative MDA-MB-231 cells via miR-206 direct binding to Cx43-3'UTR. Inhibition of miR-206 caused an increase in Cx43 levels with significant upregulation in cell proliferation, migration and invasion. Chang et al., [65] showed that low expression levels of miR-30a increased BC invasion and metastasis, while rescuing



miR-30a levels caused cancer cells to switch from mesenchymal to epithelial etiology, by inhibiting interactions between Slug and claudin promoter (tight junction proteins).

Oligonucleotides (size of siRNAs) passed only through Cx43/Cx43 GJ channels [66] and transfer of miR-5096 between tumor and endothelial cells was mediated by GJs in co-cultures of glioblastoma (U87) and microvascular endothelial (HMEC) cells [67].

Cxs-miRNAs interactions are important not only for their regulatory roles, but also for their biomarker potential. Current available BC prognostic and diagnostic tests exhibit limitations [29]. Serum antigens like carcinoembryonic antigen (CEA) and cancer antigen 153 (CA153) exhibit low sensitivity [68]. Other tests require patient tissue biopsies, like Oncotype DX test, which estimates recurrence likelihood, MammaPrint, a prognostic test, and Veridex 76-gene signature, a diagnostic test that predicts distant metastasis in ER+ patients [69].

Furthermore, mammograms usually display high false positive rates and do not detect cancers in young patients [70, 71]. Amongst the BC diagnostic miRNAs, onco-miR-21 was significantly upregulated in plasma/serum and in frozen/ Formalin-Fixed, Paraffin-Embedded BC tissues compared to their normal counterparts in various ethnic cohorts [72]. miR-155 and miR-18a were upregulated in sera and tissues of different ethnic cohorts and in sera of ER+ BC patients, respectively [29]. Among the prognostic biomarkers, miR-106b predicted risk of high recurrence and shorter overall survival, while miR-122 was over-expressed in sera of relapsed patients and predicted metastasis [73]. miR-18b, miR-103, miR-107 and miR-652 predicted recurrence and

decreased overall survival in triple-negative BC patients [74]. Therefore, Cxs and miRNAs serve as promising biomarkers for BC initiation and progression.

#### ***4. CircularRNAs biogenesis, functions and biomarker roles in BC***

CircRNAs are known to regulate miRNAs function and biogenesis and dysregulated mRNA-circRNAs-miRNAs axes may act as signatures in cancers [75-78]. CircRNAs are generated from RNA splicing (conserved sequences AG GT) by back ligation. CircRNAs are covalently closed continuous loops without 5' cap or 3' polyadenylated tail and are resistant to exonucleases (e.g. RNase R), which degrade linear RNA. They are structurally stable, and their isolation and purification is easy. CircRNAs are expressed in tissue- and- developmental stage-specific manner and primarily localize to the cytoplasm and function as miRNA sponges (sequestering miRNAs and enhancing mRNAs stability and translation) [79-81]. Known functions of circRNAs are sponging miRNAs and RNA-binding proteins (RBP)s, regulating cell cycle (e.g. FOXO3 circRNA in BC) [82], translation of few exonic circRNAs with an open reading frame [83], acting as scaffolds in protein complexes assembly [83], protein sequestration from subcellular localization [84], modulating parental gene expression [85] and regulating alternative splicing [86, 87]. CircRNAs are primarily located in the cytoplasm and are up to 10 times more abundant than their linear counterparts [88], are released from cell lines via exosomes and microvesicles [89], are differentially expressed in exosomes from mice with tumors compared to healthy controls [76] and hundreds of circRNAs are significantly

upregulated in human blood compared to their linear counterparts [90].

Several studies have reported a role for circRNAs in the initiation and progression of BC through acting as competing endogenous miRNA sponges. Xie et al., [91] identified differentially expressed circRNAs in BC tissues, and described circ\_0004771/miR-653/ZEB2 as potential regulatory feedback axis for treatment of BC. Knockdown of hsa\_circ\_0004771 and ZEB2 exhibited similar functions as using miR-653 mimics to promote growth inhibition and apoptosis in BC cells. Tang et al., [9] revealed that hsa\_circ\_0001982 was significantly overexpressed in tissues and cell lines, whereby circ\_0001982 knockdown suppressed BC cell proliferation and invasion and induced apoptosis by targeting miR-143. Xu et al., [92] detected circTADA2A-E5 and circTADA2A-E6, among five most differentially expressed circRNAs in large cohort of triple-negative BC (TNBC) patients, whose downregulation associated with poor survival. Through sponging miR-203a-3p, and therefore restoring the expression of its target *SOCS3*, circTADA2A-E6 suppressed proliferation, migration, and invasion *in vitro* and possessed tumor-suppressive capability. Thus, circTADA2A-E6/miR-203a-3p/*SOCS3* might act as a promising prognostic biomarker in TNBC.

In a validation BC patient cohort, circ\_103110, circ\_104689 and circ\_104821 levels were elevated and were predicted to sponge oncogenic miR-339-5p, miR-143-5p, miR-409-3p, miR-153-3p and miR-145-5p. Moreover, circ\_006054, circ\_100219 and circ\_406697 were downregulated and were predicted to sponge miR-298, miR-485-3p, and miR-100 (miRNAs involved in pathways in BC). Thus, these circRNAs are important promoters of carcinogenesis

and may be useful biomarkers for BC [93]. Nair et al., [94] identified 256, 288 and 411 tumor-specific circRNAs in triple negative, estrogen receptor positive and HER2-positive BC subtypes, respectively, from 885 samples from The Cancer Genome Atlas. The tumor suppressor, circ-Foxo3, significantly downregulated in BC patients and cell lines [95], likely contributes to BC progression [88] and its levels significantly increase when cancer cells undergo apoptosis. Upon knockdown of endogenous circ-Foxo3, cell viability was enhanced, while its ectopic expression inhibited xenografts tumor growth and prompted stress-induced apoptosis by upregulating PUMA and downregulating p53 [95]. Moreover, circ-ABCB10 was upregulated in BC and its knockdown *in vitro* suppressed proliferation and enhanced apoptosis through sponging miR-1271 [96, 97]. The upregulation of circ-Amotl1 in cancer patients and cell lines exhibited tumorigenic capacity through interacting with proto-oncogene, c-myc [98].

Although there exists a correlation between obesity and loss of Cx43 apical distribution and cell multi-layering in breast epithelial tissues in an inflammatory micro-environment [38, 39], no studies have linked so far the involvement of adipocytes in regulating Cx43-derived circRNAs or their sponged miRNAs. However, few studies have reported the exchange of circRNAs between adipocytes and tumor cells in other cancers [99, 100]. Through activating PRDM16 and suppressing miR-133, exosomes from gastric cancer cells shuttle ciRS-133 into pre-adipocytes, thus stimulating differentiation into brown-like cells [99]. CircRNAs in exosomes secreted from adipocytes stimulated growth of hepatocellular carcinoma and decreased

DNA damage by suppressing miR-34a and activating USP7/Cyclin A2 signaling pathway [100]. CircRNAs thus serve as an attractive new class of cancer biomarker axes [101].

### **5. *Cx43 mRNA-circRNAs-miRNAs Axis***

Cx43 acts as a tumor suppressor, its loss/mis-localization is an important player in breast tumor initiation [26], plays role in BC progression [27] and places some individuals (obese women) at increased risk of BC [38, 39]. Follow-up on differential expression levels of Cx43 mRNA in breast tissues requires tissue biopsies. We thus predict that circulating Cx43-derived circRNAs and their sponged miRNAs could be indicative of Cx43 mRNA levels in tissues [102], and might serve as non-invasive biomarker signatures for breast cancer initiation and prevention.

To predict human circRNA isoforms that originate from linear Cx43 (GJA1) transcript, CircularRNA Interactome was used and three Cx43-derived circRNA isoforms (circ\_0077753, circ\_0077754 and circ\_0077755) along with their sponged miRNAs were identified [83] (**Supplementary Table1**). We propose that a drop in circulating Cx43-derived circRNAs levels might reflect downregulation of Cx43 expression in breast epithelial tissue. Most of the sponged miRNAs by all three Cx43-derived circRNAs isoforms are involved in cancer-related signaling pathways, as predicted by miRSystem database [103]. These circRNAs associate with early events of breast tumorigenesis and are referred to hereafter as “initiation circRNAs”. Thus, when Cx43-derived circRNAs levels drop, their sponged miRNAs are expected to be relieved, and might be free to induce downstream cancer-initiating pathways. Indeed, upregulation of

predicted sponged miRNAs by the three “initiation circRNAs” is involved in oncogenic initiation pathways, cellular multi-layering and loss in organization in BC [104, 105]. For instance, of the predicted sponged miRNAs, miR-182, miR-375 and miR-203 were found up-regulated during lobular neoplasia progression and miR-375 associated with loss of breast cellular organization and development of hyperplastic phenotypes. These miRNAs were indicative of a transition from lobular carcinoma in situ (LCIS), a benign precursor lesion, to invasive breast lobular carcinoma (ILC) [104, 105]. Overexpression of oncomiRs, miR-21, miR-155, miR-10b, miR-373 and miR-520 was observed in many breast tumors [105], of which oncomiRs, miR-520g and miR-520h are potentially sponged by two “initiation circRNAs”. Therefore, the axis parallel to Cx43 mRNA loss, denoted by “initiation” Cx43-derived circRNAs and their sponged miRNAs seems to recapitulate phenotypes along BC initiation.

However, circRNAs and miRNAs present with few caveats that should be addressed. Interestingly, the proposed Cx43-derived circRNAs may circumvent them. First, miRNAs and circRNAs are highly expressed in circulating blood cells and their increased levels in blood might be due to high number of blood cells. Future studies thus should focus on defining actual abundance of circRNAs in different sub-populations of blood cells, characterize their mode of transportation in serum and plasma and devise markers that predict their origin [106]. Cx43, however, is abundant in endothelial cells of large arteries (at aortic and coronary arteries branch points) but not in circulating blood cells [107]. Thus, Cx43-derived circRNAs in plasma and sera

are expected to surpass this caveat. Secondly, some circRNAs are differentially expressed in cancer tissues compared to normal adjacent tissues, but not in plasma or sera of patients compared to healthy controls [43]. Thus, Cx43-derived circRNAs can overcome this caveat through future studies that compare Cx43-derived circRNAs levels in plasma to Cx43 mRNA levels in tissues of patients at risk, patients with early-stages of the disease and those with more aggressive etiologies. Therefore, it is worth further investigating the proposed “initiation” Cx43-derived circRNAs and their sponged miRNAs signatures towards BC early-onset detection and prevention.

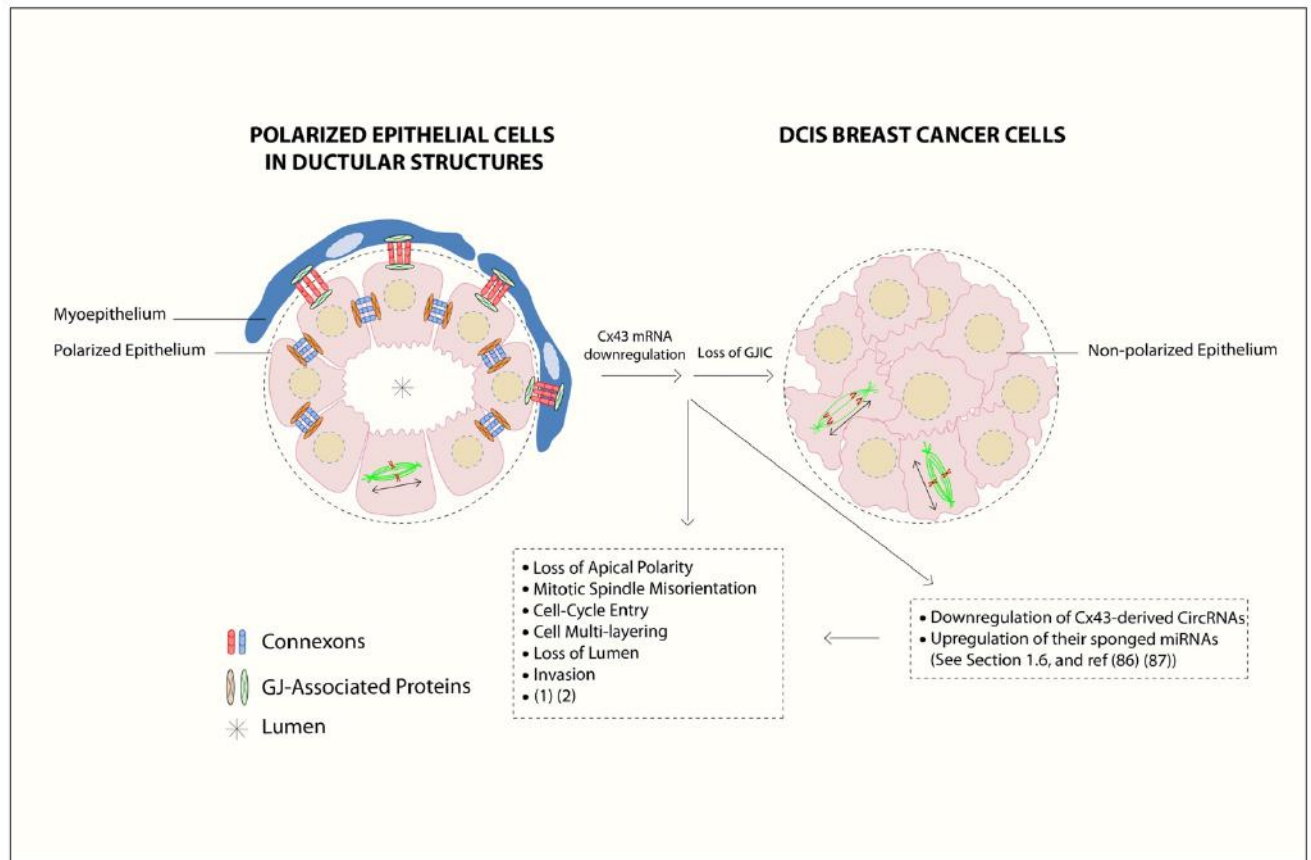


**Figure 2: Gap junction (GJ) complex dis-assembly in breast cancer initiation.** In normal differentiated mammary epithelium, the cells polarize with apical and basolateral domains and assemble membranous GJs between epithelial cells and between epithelial and myoepithelial cells. Mammary Cxs ( ), including Cx43, form a complex assembly with GJ-Associated Proteins ( ) such as ZO-2,  $\alpha$ - and  $\beta$ -catenins [24] in a differentiated epithelial cell. At the primary tumor site, the downregulation of Cx43 mRNA levels leads to loss of gap junction intercellular communication (GJIC) and dissociation of GJ-associated proteins complexes, which in turn causes loss of communication between neighboring cells, activation of cellular proliferation and alteration in polarity protein distribution. Loss of apical polarity, mitotic spindle misorientation, cell cycle entry, cell multi-layering, loss of lumen (\*) and enhanced invasive capability in Cx43 knock out breast epithelial cells is also reported [26, 27]. Mitotic-spindle orientation (MSO) is depicted based



on the directionality of the  $\alpha$ -tubulin poles, either parallel to the basement membrane [or tangential to the circumference of the growing acini], which is the proper MSO to maintain a monolayered epithelium (in polarized epithelial cells in ductular structures), in contrast to cell multilayering (in DCIS breast cancer cells). Double-headed arrows indicate MSO. Thus, Cx43 contributes to breast epithelial polarity and proper MSO in single layered mammary epithelial cells, whereas its loss contributes to disrupted polarity and MSO and multilayering, which are hallmarks of tumor initiation. In this review, an axis by Cx43-derived circRNAs and their sponged miRNAs is proposed during BC initiation stages, which almost parallels the roles of Cx43 mRNA downregulation and GJIC loss. This is denoted by loss of breast epithelial polarity and development of hyperplastic phenotypes [104, 105]. The axis might act as promising biomarker signature towards BC early-onset detection and prevention, as discussed in section 1.6 (*Figure is modified from [44]*).

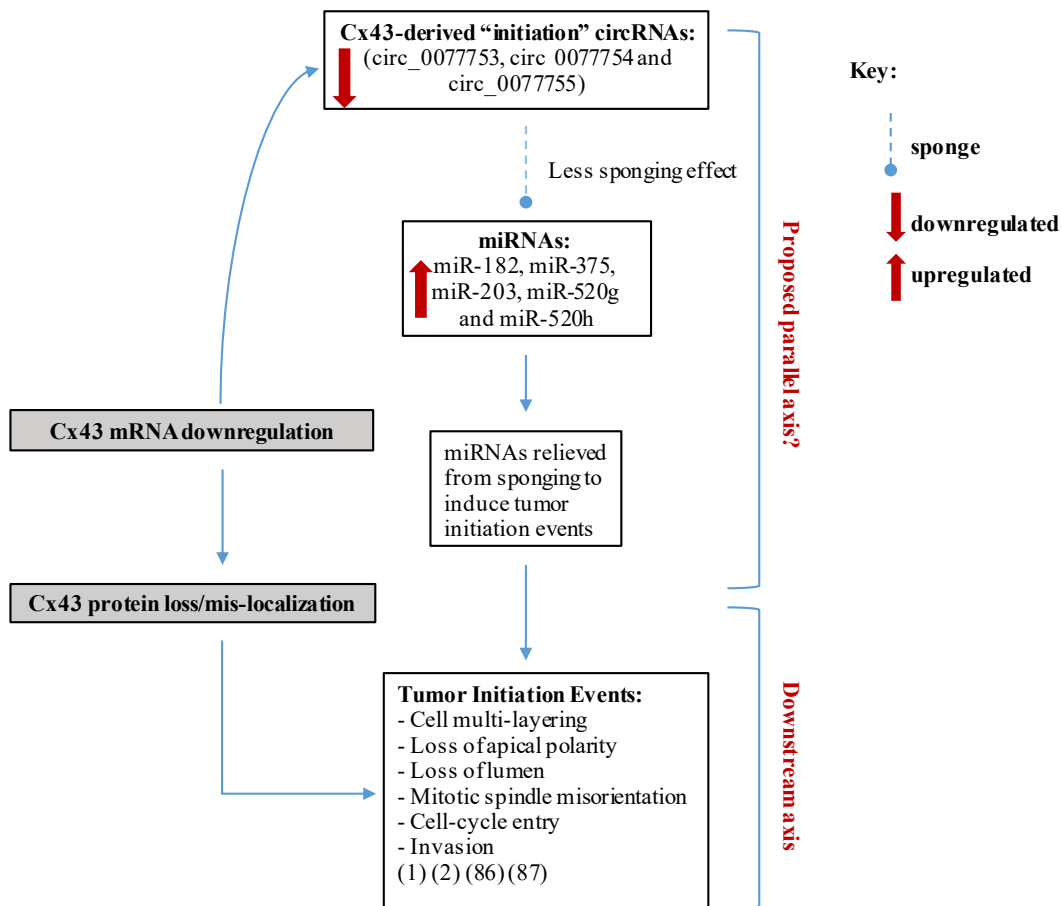


**Figure 3: Axes parallel to and downstream of Cx43 loss in breast cancer initiation.** We recently showed that silencing Cx43 expression contributes to breast tumorigenesis by enhancing proliferation and cell cycle progression and inducing mis-localization of membranous  $\beta$ -catenin, resulting in loss of apical polarity, misorientation of mitotic spindle, cell multi-layering and loss of lumen (hallmarks of tumor initiation) and by activating signaling pathways that promote invasion in non-tumorigenic breast epithelium [26], [27]. We propose a possible parallel signature axis of Cx43 mRNA-circRNAs-miRNAs in BC early-onset for detection and prevention, which recapitulates the roles Cx43 loss plays along breast tumorigenesis. The Cx43 mRNA- “initiation circRNAs”-miRNAs axis is denoted by three “initiation circRNAs” (circ\_0077753, circ\_0077754 and circ\_0077755) [83] and a panel of their sponged miRNAs, miR-182, miR-375, miR-203, miR-520g and miR-520h. When the initiation Cx43-derived circRNAs levels drop, their sponged miRNAs are expected to be relieved, and might be free to induce downstream tumor-initiation pathways [104, 105].

**Supplementary Table 1: The “initiation” circRNA isoforms that originate from the linear transcript of Cx43 (or GJA1) and their predicted sponged miRNAs.** Panels A, B & C represent the three “initiation circRNAs” isoforms (has\_circ\_0077753, has\_circ\_0077754, has\_circ\_0077755) that originate from the linear transcript of Cx4 (GJA1) using the *in silico* tool, CircularRNA Interactome (<https://circinteractome.nia.nih.gov>) [83]. CircInteractome database utilizes 109 datasets of RNA-binding proteins (RBPs) to predict and map circRNAs based on RNA-binding sites [108] and their sponged miRNAs based on TargetsScan [109, 110]. The second column represents the nomenclature of circRNAs ID (as annotated by circBase) followed by the chromosomal location of the circRNAs and the number of total miRNAs sponged by each circRNAs isoform and finally the samples from which these circRNAs were extracted and validated [111]. The third column includes all the miRNAs sponged by its corresponding circRNAs with the number of sponge sites for each miRNA color-coded; miRNAs bolded in red are sponged at 3 sites, bolded in blue at 2 sites while the rest at one site. The miRNAs highlighted in yellow represent the sponged miRNAs that have been reported in the literature to be *involved in oncogenic pathways and are associated with loss of breast cellular organization and development of hyperplastic phenotypes during initiation stages of breast tumorigenesis* [104, 105].

Panel	CircRNAs derived from Cx43 (GJA1) transcript	sponged miRNAs
A	<p><a href="#">hsa_circ_0077753</a></p> <p>chr6:121756744-121770873</p> <p>(101 sponged miRNAs)</p> <p><u>Samples:</u> Huvec, H1hesc, Ag04450, Nhek [111]</p>	<p>miR-1178, -1179, -1183, -1184, -1197, -1205, -1225-5p, -1228, -1231, -1236, -1238, -1243, -1249, -1263, -1264, -127-5p, -1270, <b>-1272</b>, -1278, -1279, -1286, -1303, <b>-1305</b>, -139-5p, -144, -149, <b>-182</b>, <b>-186</b>, -197, -198, <b>-203</b>, -217, -224, -31, -323-3p, -331-5p, <b>-338-3p</b>, -361-3p, <b>-375</b>, -421, <b>-432</b>, <b>-495</b>, <b>-498</b>, -507, -508-3p, -510, -512-5p, -515-5p, -518a-5p, <b>-520g</b>, <b>-520h</b>, -524-3p, -525-3p, -527, -545, <b>-548c-3p</b>, <b>-548g</b>, -548k, -557, <b>-561</b>, -562, -564, -567, -570, -574-5p, -576-3p, <b>-576-5p</b>, <b>-578</b>, <b>-579</b>, -582-3p, -595, -599, <b>-607</b>, -609, -614, -619, -620, -623, -630, -633, -634, -636, -646, -648, -651, -653, -661, -665, -668, -758, <b>-766</b>, -767-3p, -769-5p, -873, -875-5p, -890, -892a, -935, -938, -942 and -944.</p>
B	<p><a href="#">hsa_circ_0077754</a></p> <p>chr6:121767977-121768070</p> <p>(6 sponged miRNAs)</p> <p><u>Samples:</u> H1hesc [111]</p>	<p>miR-1228, -338-3p, -524-3p, -525-3p, -661 and -766.</p>
C	<p><a href="#">hsa_circ_0077755</a></p> <p>chr6:121767977-121770873</p> <p>(94 sponged miRNAs)</p> <p><u>Samples:</u> Huvec, H1hesc, Bj, Ag04450, A549, Nhek, Sknshra [111]</p>	<p>miR-1178, -1179, -1183, -1184, -1197, -1205, -1225-5p, -1228, -1231, -1236, -1243, -1249, -1264, -127-5p, -1270, <b>-1272</b>, -1278, -1279, -1286, -1303, -1305, -139-5p, -144, -149, <b>-182</b>, <b>-186</b>, -197, -198, <b>-203</b>, -217, -31, -323-3p, -331-5p, <b>-338-3p</b>, -361-3p, <b>-375</b>, -421, <b>-495</b>, -498, -507, -508-3p, -510, -512-5p, -515-5p, -518a-5p, <b>-520g</b>, <b>-520h</b>, -524-3p, -525-3p, -527, -545, <b>-548c-3p</b>, <b>-548g</b>, -548k, -557, -562, -564, -567, -570, <b>-574-5p</b>, <b>-576-3p</b>, <b>-576-5p</b>, <b>-578</b>, <b>-579</b>, -582-3p, -595, -599, <b>-607</b>, -609, -614, -619, -620, -623, -630, -633, -634, -636, -646, -648, -651, -653, -661, -665, -668, -758, <b>-766</b>, -767-3p, -769-5p, -873, -892a, -935, -938, -942 and -944.</p>

## CHAPTER II

### AIMS

Breast cancer constitutes one third of all female cancers in Lebanon, with an alarming high percentage diagnosed under the age of 40 (22% of cases compared to 6% in the West) [2]. Previous studies have shown that this early malignancy is not attributed to genetic alterations [2]. Thus we focused on post-transcriptional master regulators, mainly miRNAs, and more recently their circRNA sponges, which act by exhibiting endogenous competing binding sites for miRNAs [7, 8], to help identify regulatory circRNAs axis and miRNA networks and players in the early malignancy. This project has **three main aims. The first** is to characterize key miRNA players from the miRNome of the young Lebanese breast cancer population (42.2% of which are under the age of 40) [29], which might disrupt epithelial polarity. Through a comprehensive literature review, fifteen tumor-associated miRNAs were uncovered be involved in early events of breast tumorigenesis that contribute to loss of acinar morphogenesis. Moreover, Cx43 acts as a tumor suppressor [20, 21, 25] and its loss and mislocalization influence breast cancer initiation [26], progression [27] and is associated with markers of poor prognosis. Nontumorigenic HMT-3522 S1 (S1) cells form fully polarized epithelium while pretumorigenic counterparts silenced for gap junction Cx43 (Cx43-KO-S1) lose epithelial polarity, multilayer and mimic premalignant *in vivo* mammary epithelial morphology [28]. Therefore, this 3D culture model serves as a breast cancer risk-progression culture series. miRNA sequencing was performed on the risk-

progression series and revealed 65 significant differentially expressed miRNAs that were specific to Cx43 loss. Next, a comparative analysis between the Cx43-specific miRNAs and the fifteen tumor-associated patient miRNAs that were involved in epithelial polarity was done. This led to the selection of two candidate miRNAs for further investigation. The first miRNA was **miR-183**, which was downstream of Cx43 loss, was commonly upregulated in patient and cultured epithelia miRNomes and its up-regulation conferred with the increased risk of cancer progression in the 3D culture model. The second miRNA was **miR-492**, which was not attributed to Cx43 loss and was exclusively up-regulated in the Lebanese patients.

**The second aim** was to investigate whether the patient tumor-associated miR-183 and miR-492 over-expression in the non-neoplastic S1 breast epithelial cells might recapitulate phenotypes seen upon the loss of Cx43. Ectopic over-expression of both miR-183 and miR-492 in the non-neoplastic S1 cells carried out using pLenti-III-miR-GFP tagged vectors. The results revealed that over-expression of miR-183 and miR-492 resulted in the formation of larger acini in 3D cultures, devoid of lumen assembly, with disrupted epithelial polarity observed through mislocalization of  $\beta$ -catenin and Scrib's apico-lateral distribution and Cx43's apical distribution. It also triggered enhanced proliferation and invasion capacity, hence recapitulating tumor-initiation phenotypes seen upon Cx43 loss [26, 27].

Next, we opted to characterize for the **third aim** axes parallel to or upstream of Cx43 loss, which are less understood. Thus, mRNA-circRNA-miRNA signature axes in heightened risk of breast cancer initiation using the breast epithelial risk progression culture model and the

Lebanese patients as a validation cohort were investigated. Dysregulated mRNA-circRNA-miRNAs signature axes were identified via circRNAs microarray (Arraystar Human circRNA Array V2) and miRNA sequencing specific to Cx43 loss in pretumorigenic Cx43-KO-S1 cells compared to nontumorigenic S1 counterparts. The results revealed 121 circRNAs and 65 miRNAs specific to Cx43 silencing in the cultured epithelia. Focusing on the possible sponging activity of the validated circRNAs to their target miRNAs, these were compared to the tumor-associated miRNAs patient miRNAs involved in epithelial polarity and the miRNome of the cultured epithelial specific to Cx43 loss. Therefore, **Cx43/hsa\_circ\_0077755/miR-182** was identified as a biomarker signature axis for heightened-risk of breast cancer initiation, and that its dysregulation patterns might predict prognosis along breast cancer initiation and progression.

## CHAPTER III

### BREAST EPITHELIAL RISK-PROGRESSION 3D CULTURE MODEL REVEALS CX43/HSA\_CIRC\_0077755/MIR-182 AS A BIOMARKER AXIS FOR HEIGHTENED-RISK OF BREAST CANCER INITIATION

Authors: Nataly Naser AL Deen<sup>1</sup>, Nadia Atallah Lanman<sup>2,3</sup>, Shirisha Chittiboyina<sup>4</sup>, Sophie Lelièvre<sup>2,4</sup>, Rihab Nasr<sup>5</sup>, Farah Nassar<sup>6</sup>, Heinrich zu Dohna<sup>1</sup>, Mounir AbouHaidar<sup>7\*</sup>, Rabih Talhouk<sup>1\*</sup>

To be submitted to *Scientific Reports* – June 2020

#### A. Abstract

mRNA-circRNA-miRNAs axes have been characterized in breast cancer, but not as risk-assessment axes for tumor initiation in early-onset breast cancer that is increasing drastically worldwide. To address this gap, we performed circular RNA (circRNA) microarrays and microRNA (miRNA) sequencing on acini of HMT-3522 S1 (S1) breast epithelial risk-progression culture model in 3D and chose an early-stage young population miRNome for a validation cohort. Nontumorigenic S1 cells form fully polarized epithelium while pretumorigenic counterparts silenced for gap junction Cx43 (Cx43-KO-S1) lose epithelial polarity, multilayer and mimic premalignant *in vivo* mammary epithelial morphology. Here, 121 circRNAs and 65 miRNAs were significantly dysregulated in response to Cx43 silencing in cultured epithelia and 15 miRNAs from the patient cohort were involved in epithelial polarity disruption. Focusing on the possible sponging activity of the validated circRNAs to their target miRNAs, we found all

miRNAs to be highly enriched in cancer-related pathways and cross-compared their dysregulation to actual miRNA datasets from the cultured epithelia and the patient validation cohort. We present the involvement of gap junction in post-transcriptional axes and reveal **Cx43/hsa\_circ\_0077755/miR-182** as a potential biomarker signature axis for heightened-risk of breast cancer initiation, and that its dysregulation patterns might predict prognosis along breast cancer initiation and progression.

## **B. Introduction**

Breast cancer accounts for the highest cancer incidence (24.2%) and mortality rate (15%) in women globally and is the second most commonly diagnosed cancer (after lung cancer) when both sexes are combined (11.6%) [1]. In Lebanon, breast cancer constitutes one-third of all female cancers, with an alarming high percentage diagnosed under the age of 40 (22% of cases compared to 6% in Western populations) and a mean age at diagnosis 10 years younger than in Western countries [2]. These women have low prevalence of deleterious *BRCA* mutations [3] and present with poor prognosis and aggressive phenotypes due to the lack of diagnostic methods at such an early age [230]. Early-onset breast cancer is increasing drastically worldwide [2, 4, 5], which called for this study to identify potential noninvasive biomarkers and active players [6, 7] for risk-assessment and early detection actions.



Among key players involved in breast cancer onset are gap junction components. Gap junction intercellular communication (GJIC) is mediated by transmembrane proteins, called connexins (Cxs) that allow the intercellular exchange of ions, second messengers and metabolites between adjacent cells [16-19]. Cx43, the focus of our previous and current research studies [7, 20, 21] plays essential roles during mammary gland development [22, 23] and differentiation [24] and acts as a tumor suppressor [20, 21, 25]. Its loss and mislocalization influence breast cancer initiation [26], progression [27], increase risk of breast cancer development in overweight women [231, 232] and is associated with markers of poor prognosis, increased metastasis and poor survival in breast cancer patients [25]. We recently showed that Cx43 functions via PI3 Kinase and noncanonical Wnt signaling pathways in priming the breast epithelium for neoplastic behavior [26, 27]. The nontumorigenic luminal human breast epithelial HMT-3522 S1 (S1) cell line, cultured under three-dimensional (3D) conditions, forms growth-arrested and basoapically polarized acini with a central lumen and apicolateral localization of Cx43. Hence S1 cells recapitulate normal human breast tissue architecture [26]. Silencing Cx43 expression in these nontumorigenic S1 cells via Cx43-shRNA (Cx43-KO-S1) resulted in cell cycle entry, perturbed apical polarity, mitotic spindle misorientation and loss of lumen, causing cell multilayering [26] and priming cells for enhanced motility and invasion [26, 27]. These phenotypic features observed in Cx43-KO-S1 acini represent architectural and phenotypical premalignant mammary lesions, like those observed in ductal hyperplasia in a murine model [28], which increase the risk of breast cancer initiation, thus marking Cx43-KO-S1 as

pretumorigenic culture model. Therefore, this 3D risk-progression culture model was utilized to capture key pretumorigenic signatures that might delineate post-transcriptional profiles seen in the young patients with heightened risk of breast cancer development.

Cancerous phenotypes have been shown to be mediated by circRNAs, a class of endogenous RNAs that originate from RNA splicing and back ligation and act as miRNA “sponges”, and miRNAs, small endogenous non-coding RNAs that repress translation [7, 8]. CircRNAs are covalently closed continuous loops without 5’ cap or 3’ polyadenylated tail and are resistant to degradation by exonucleases (e.g. RNase R) that degrade linear RNA [80, 233, 234]. One of the known functions of circRNAs [86] includes “sponging” mature miRNAs and RNA-binding proteins (RBP)s. Sponging refers to circRNAs exhibiting endogenous competing binding sites (one to several) for each specific target miRNA. They covalently bind the mature target miRNA, downregulating its expression, hence preventing it from binding its own target mRNAs and repressing translation [235]. For instance, ciRS-7 exhibits over 70 conserved binding sites to miR-7 [75] while circ-SRY exhibits 16 binding sites to miR-138 [235, 236] and circ-Foxo3 [82] and circ-MBL (muscleblind) can sponge RBPs [87]. Other functions of circRNAs include i) cell cycle regulation, for example, by interacting with CDK2 and p21, circ-Foxo3 can block cell cycle progression from G1 to S phase [82], ii), translation of exonic circRNAs with open reading frames, for example, through an internal ribosome entry site, IRES, hcirc-ZNF609 is capable of translating proteins in mouse myoblasts [237], iii) control of stability of some mRNAs, for instance, CDR1as circular antisense RNA can stabilize mRNAs through

formation of a duplex structure [80], iv) positive regulation and modulation of their own parental gene expression through association with RNA polymerase II (like ci-ankrd52 and ci-sirt7 [85]) and v) regulation of alternative splicing [86, 87].

While dysregulated mRNA-circRNAs-miRNAs axes have been reported as biomarker signatures in cancers [75-77, 238] and specifically in breast cancers [9-15], axes involved in premalignant epithelial polarity transitions that might explain and contribute to heightened risk of breast cancer initiation have not been reported. We therefore, through utilizing a unique breast cancer risk-progression 3D culture model that mimics normal and premalignant *in vivo* mammary epithelial morphology [26, 239] and profiles of a validation cohort of early-stage Lebanese patients that is notoriously at highest risk for the early malignancy with 42.2% below the age of 40 [2, 29], characterized new potential post-transcriptional risk-assessment axes of breast cancer initiation.

In recent work [7], in an attempt to predict such post-transcriptional axes, we identified *in silico* possible biomarker signatures for early-onset breast cancer risk assessment through Cx43 mRNA-circRNAs-miRNAs. These were denoted by the three Cx43-derived circRNA isoforms (hsa\_circ\_0077753, hsa\_circ\_0077754, and hsa\_circ\_0077755) and a panel of their predicted sponged miRNAs (miR-182, miR-375, miR-203, miR-520g and miR-520h). When dysregulated in breast tissues, these miRNAs recapitulate phenotypes observed upon Cx43 loss; namely disruption of epithelial polarity and cell-multilayering during initiation stages of tumorigenesis and oncogenic pathways [21, 76, 104, 105].

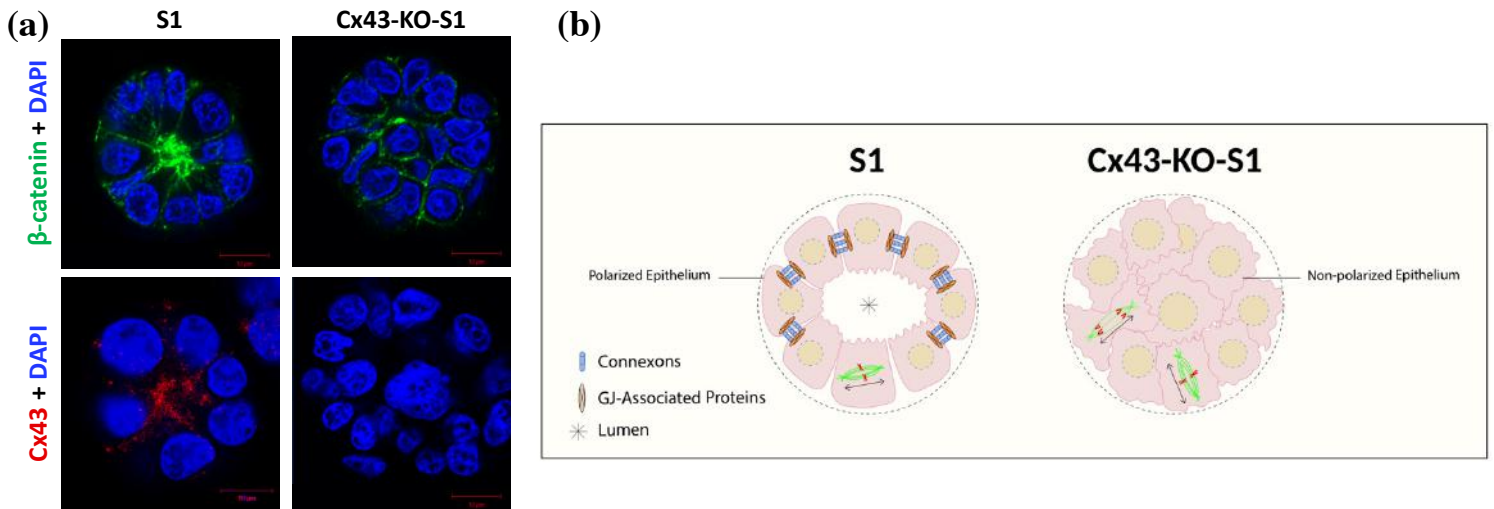
In the present report, dysregulated mRNA-circRNA-miRNAs signature axes were studied using 66circRNAs microarray and miRNA sequencing analysis of nontumorigenic S1 and pretumorigenic Cx43-KO-S1 cells, and microarrays of a validation young patient cohort with early-stage breast cancer [29]. The potential biomarker roles of three validated significantly dysregulated circRNAs were investigated. We focused on their sponging capacity to their target miRNAs in the breast cancer risk progression 3D culture model and looked for matched dysregulation in the patient validation cohort. Only **Cx43/has\_circ\_0077755/miR-182** axis specific to Cx43 loss was validated, which might serve as a biomarker signature axis for heightened-risk of breast cancer initiation and whose dysregulation patterns seem to predict prognosis along breast cancer initiation and progression.

## **C. Results**

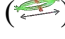
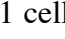
### ***1. Three-dimensional (3D) breast cancer risk-progression cell culture model characteristics***

S1 nontumorigenic cells [239] have been used previously in 3D cell culture, in the presence of extracellular matrix of basement membrane type, as a model of phenotypically normal differentiation of breast luminal epithelium [240, 241]. They form a fully polarized epithelium that displays apicolateral distribution of tight junction proteins ZO-1 and ZO-2 [242, 243]. We have shown in previous studies that Cx43 drives apical polarity *in vivo*, and that it controls the distribution of tight junction proteins and of adherens junction component  $\beta$ -catenin (**Fig. 4a**) [26]. Its loss is associated with cell multilayering and polarity disruption as shown in

the S1 epithelium silenced for Cx43 (pretumorigenic Cx43-KO-S1 cells) (**Fig. 4a & 1b**) and in archival biopsy tissue samples [26]. This *in vitro* 3D risk-progression culture model was used here to study the post-transcriptional signature axes (namely miRNAs and circRNAs) that are dysregulated as a result of Cx43 loss in the breast epithelium, a feature commonly associated with heightened risk of breast cancer initiation [25, 232].



**Figure 4: HMT-3522 S1 nontumorigenic and Cx43-KO-S1 pretumorigenic cells in 3D culture as a breast cancer risk-progression model.** (a) Upper panel of immunofluorescence images shows the localization of  $\beta$ -catenin (green) on day 11 in 3D cultures of S1 cells (left panel showing typical apicolateral  $\beta$ -catenin distribution) and in Cx43-KO-S1 cells (right panel showing  $\beta$ -catenin mis-localization upon knockdown of Cx43). Lower panel of immunofluorescence images shows the localization of Cx43 (red) on day 11 in 3D cultures of S1 cells (left panel showing typical apical Cx43 distribution) and in Cx43-KO-S1 cells (right panel showing loss of Cx43 upon knockdown of Cx43). Nuclei were counterstained with DAPI (blue). (b) A diagram depicting S1 cells that form phenotypically normal differentiated mammary epithelium (left panel), where the cells assemble around a lumen (\*), polarize with apical and basolateral domains and assemble membranous connexons (blue) with GJ-associated proteins (brown) in GJs between epithelial cells. The down-regulation of Cx43 mRNA levels by knocking-down Cx43 leads to loss of GJ intercellular communication (GJIC), causing loss of communication between neighboring cells, activation of

cellular proliferation, disruption of mitotic spindle orientation (MSO), multi-layering, loss of polarity and alteration in polarity protein distribution [26, 27]. MSO (indicated by the double-headed arrows) is depicted based on the directionality of the  $\alpha$ -tubulin poles. Proper MSO is shown tangential to the circumference of the growing acinus () to maintain a monolayered epithelium, in contrast to cell multilayering () in Cx43-KO-S1 cells (*modified from Naser Al Deen et al., 2019 [7]*).

## 2. *Microarray profiling of Cx43-KO-S1) versus S1 breast epithelial cells in 3D culture*

*revealed 121 significantly dysregulated circRNAs, of which 18 were chosen for validation*

To identify circRNA expression profile specific to the loss of Cx43, microarrays for circRNAs (Arraystar Human circRNA Array V2) were performed. Triplicates of Cx43-KO-S1 cells and S1 counterparts in 3D drip culture were prepared for the microarray in the presence of Matrigel™ over 11 days to induce the formation of acinus-like structures. CircRNA expression levels were processed and analyzed upon sample quantile normalization (**Fig. 5a**). Differential expression levels of circRNAs showed that hsa\_circ\_0001568 (originating from *DUSP22* gene), hsa\_circ\_405443 (originating from *NDE1* gene) and hsa\_circ\_0039238 (originating from *NETO2* gene) were the most significantly up-regulated in Cx43-KO-S1 cells with fold changes of 5, 4 and 3.6, respectively. Hsa\_circ\_0001072 (originating from *GTDC1* gene) and hsa\_circ\_0084765 (originating from *EYAI* gene) were most significantly down-regulated in Cx43-KO-S1 cells with a fold change of 4 (**Fig. 5b**). Most circRNAs were transcribed from chr1, chr2, chr7, chr11, chr12, chr15, chr16 and chr17, but rarely from chr18 and chrX (**Fig. 5c**). Hierarchical clustering of the 121 significantly dysregulated circRNAs resulted in separate clustering of pretumorigenic and nontumorigenic cells (Fold Change > 2 and adjusted p-value < 0.05). Of these circRNAs, 75

were up-regulated (62%) and 46 down-regulated (38%) (**Fig. 5d**). Moreover, eighteen significantly dysregulated circRNAs (ten up-regulated and eight down-regulated) were selected for validation (**Table 5a**) based on whether the genes from which they originate were involved in cancer-related and/or epithelial polarity pathways. Furthermore, since all detected circRNAs were differentially expressed due to the loss of Cx43 in the cultured epithelia, all three circRNA isoforms originating from the Cx43 (*GJA1*), were additionally chosen for validation (**Table 5b**).

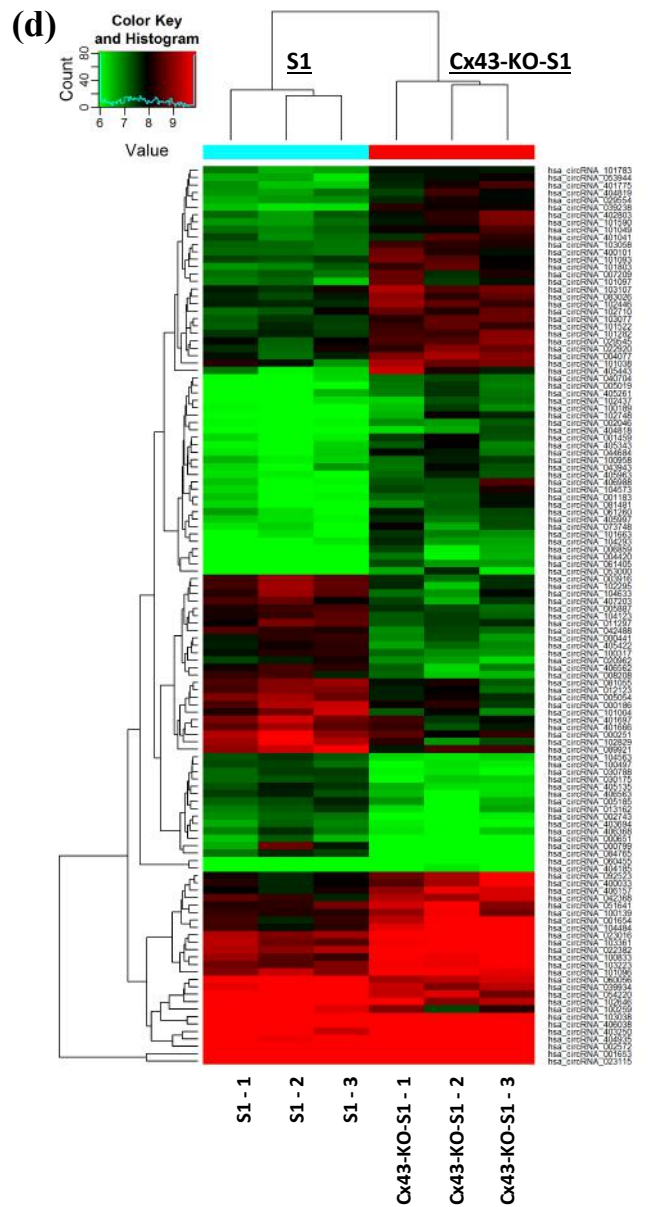
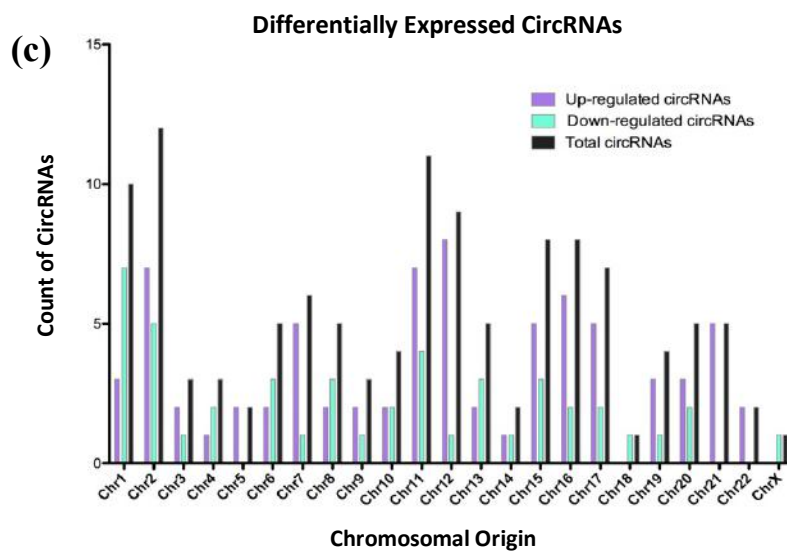
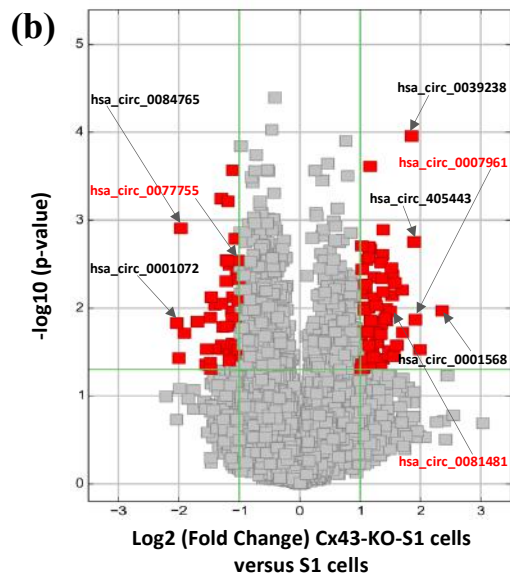
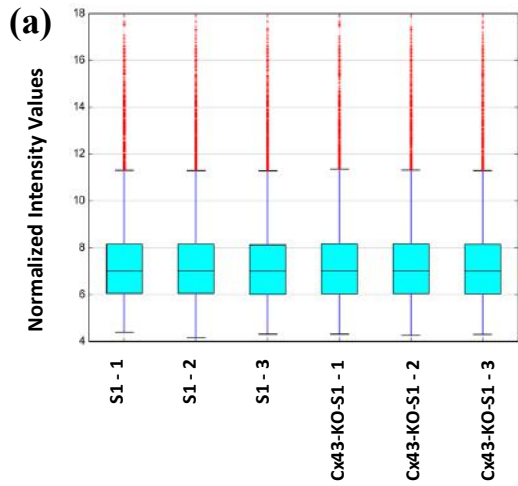




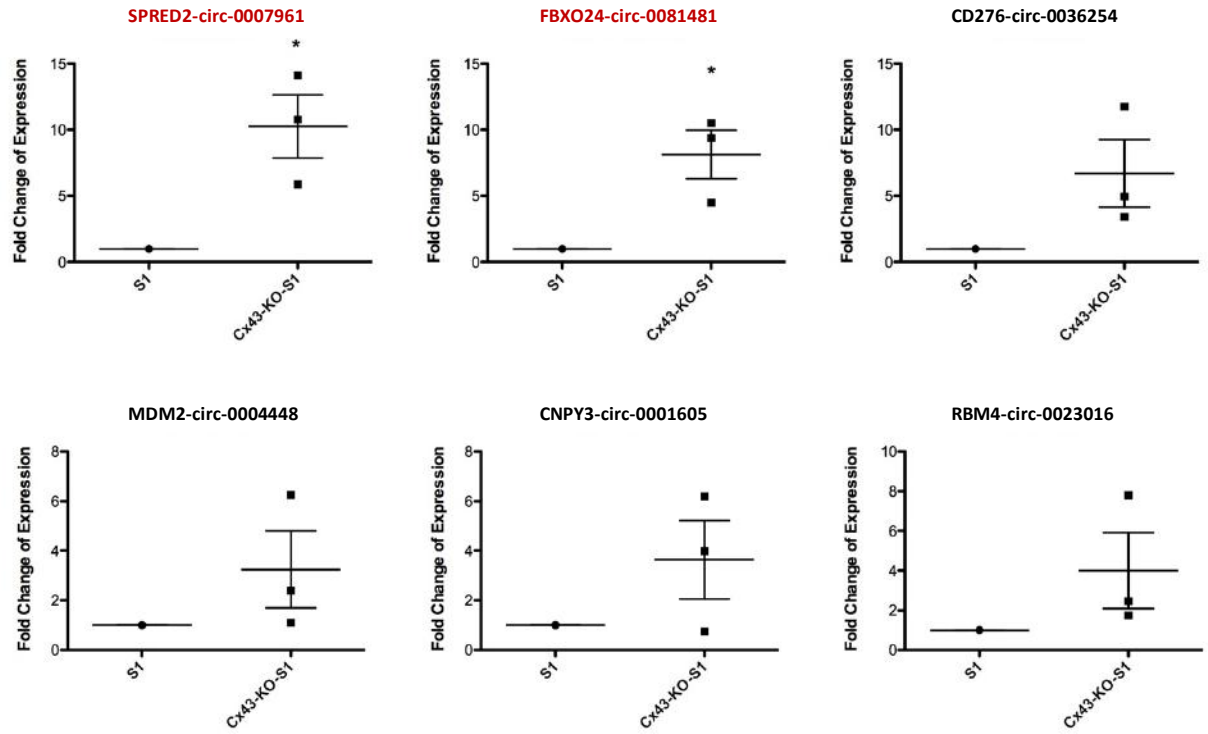
**Figure 5: Microarrays revealed 121 differentially expressed circRNAs in response to Cx43 silencing in Cx43-KO-S1 (pretumorigenic) cells versus S1 (nontumorigenic) breast epithelial cells in 3D.** Triplicates of Cx43-KO-S1 and triplicates of S1 cells were plated on Matrigel™ for 11 days. Total RNA was extracted, digested with RNase R to remove linear RNAs and enrich circRNAs, reverse transcribed and hybridized to Arraystar Human circRNA Array V2 microarrays. **(a) Box plot** after quantile normalization showing the distributions of log2 ratios among the six samples. **(b) Volcano plot** depicting the differential circRNA expression, with the vertical green lines corresponding to 2.0-fold up and down, and the horizontal green line representing a p-value of 0.05. The red points in the plot represent the differentially expressed circRNAs with statistical significance. The circRNAs denoted in black font with arrows highlight the most up-regulated (right) and down-regulated (left) circRNAs, while the circRNAs denoted in red font with arrows highlight the three chosen and validated circRNAs in this study. **(c) Bar graph** showing the chromosomal distributions of the differentially expressed circRNAs. **(d) Hierarchical cluster analysis (heat map)** of microarray data used to assess the significant expression of circRNAs when comparing Cx43-KO-S1 to S1 cells in 3D (the key range (6-10) represents the log2 value of the normalized intensity for each sample and not the fold change). “Red” indicates higher expression level, and “green” indicates lower expression level in Cx43-KO-S1 as compared to S1 cells. Each circRNA is represented by a single row of colored boxes and each sample is represented by a single column.

### ***3. RT-qPCR validation of the 18 selected circRNAs revealed two significantly up-regulated and seven significantly down-regulated circRNAs associated with the loss of Cx43***

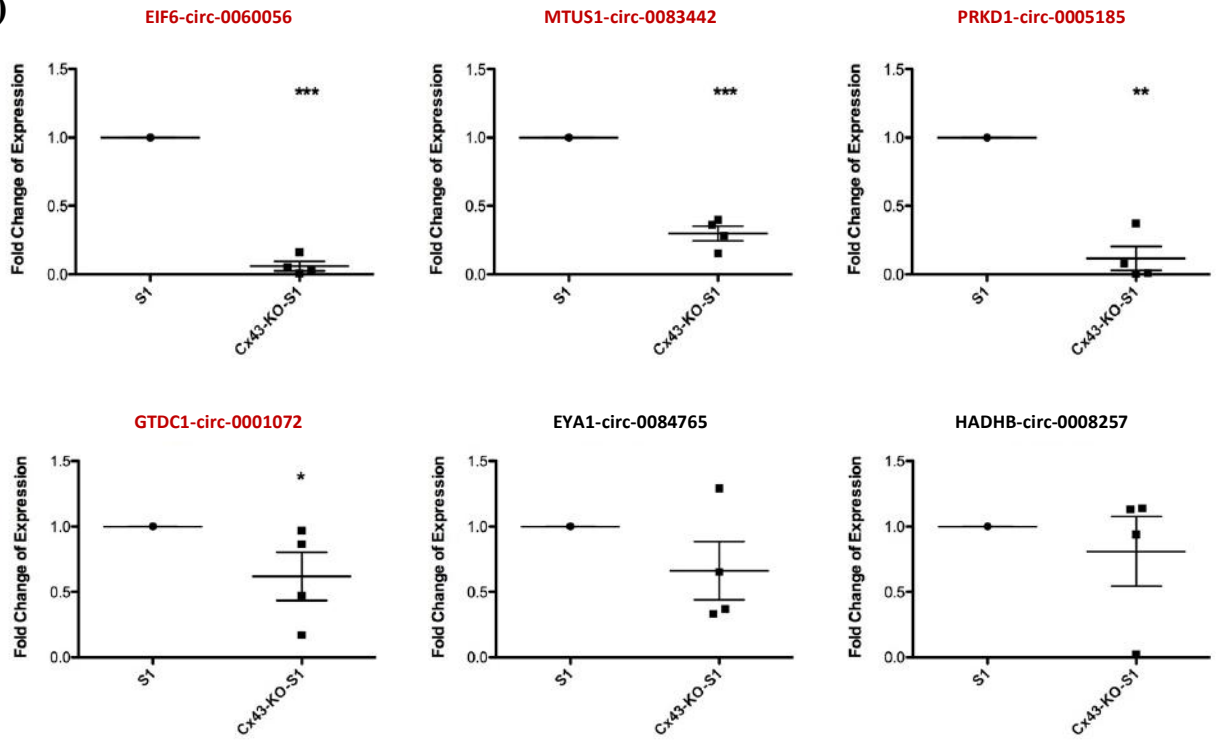
Real time polymerase chain reaction (RT-qPCR) was performed on four replicates of acini obtained from Cx43-KO-S1 and S1 breast epithelial cells in 3D. 18S ribosomal RNA was used as an endogenous control. Two of the ten tested up-regulated circRNAs, hsa\_circ\_0007961 (originating from *SPRED2*) and hsa\_circ\_0081481 (originating from *FBXO24*) were confirmed to be significantly upregulated in Cx43-KO-S1 compared to S1 cells in 3D culture (**Fig. 6a**). Four of the eight tested down-regulated circRNAs, hsa\_circ\_0060056 (from *EIF6*),

hsa\_circ\_0083442 (from *MTUS1*), hsa\_circ\_0005185 (from *PRKDI*) and hsa\_circ\_0001072 (from *GTDC1*) were confirmed to be significantly down-regulated in Cx43-KO-S1 versus S1 breast epithelial cells in 3D (**Fig. 6b**). The rest of the chosen circRNAs did not show significant regulation, thus their data was not presented here. Moreover, all three circRNA isoforms originating from Cx43 (*GJAI*) gene, hsa\_circ\_0077753, hsa\_circ\_0077754 and hsa\_circ\_0077755 were confirmed through RT-qPCR to be significantly down-regulated in Cx43-KO-S1 versus S1 cells (**Fig. 6c**). The next step was to link these circRNAs sponges to their target (predicted and actual) miRNAs.

(a)



(b)



(c)

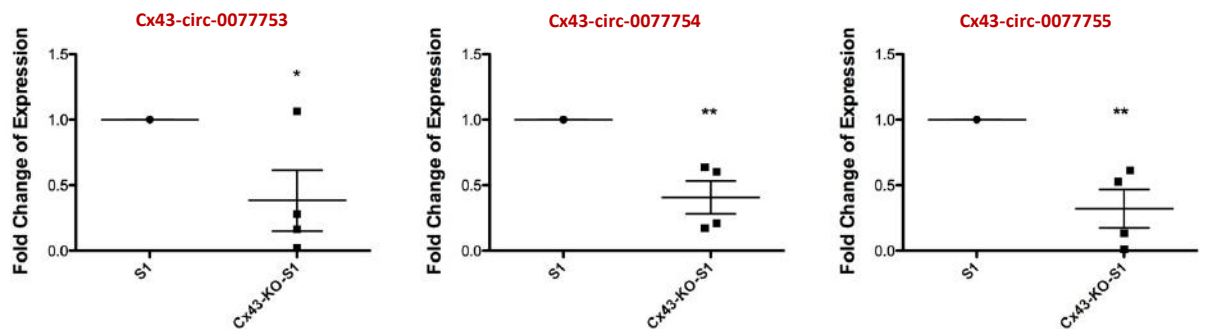


**Figure 6: RT-qPCR validated nine significant differentially expressed circRNAs in the cultured epithelia.** Four replicates of Cx43-KO-S1 and four replicates of S1 cells were plated in Matrigel for 11 days. Total RNA was extracted and RT-qPCR was performed in Cx43-KO-S1 versus S1 breast epithelial cells in 3D using 18S ribosomal RNA as an endogenous control for (a) the selected up-regulated circRNAs and (b) the selected down-regulated circRNAs and (c) the three Cx43 (*GJA1*) derived circRNAs as per microarray results. Dot plot represents the mean fold change with the standard error of mean as error bars of each 74ircRNAs expression in the breast epithelial acini in 3D. The circRNAs highlighted in red font were confirmed to be significantly dysregulated in Cx43-KO-S1 as compared to S1 cells in 3D. \*denotes  $p < 0.05$  and \*\*denotes  $p < 0.01$  and \*\*\* denotes  $p < 0.001$  for Cx43-KO-S1 versus S1 cells using one-tailed unpaired T-test.

**Table 5: Selection of eighteen circRNAs involved in cancer-related and/or epithelial polarity pathways for RT-qPCR validation.** (a) Ten up-regulated (of 75 significantly up-regulated) and eight down-regulated (of 46 significantly down-regulated) circRNAs in Cx43-KO-S1 as compared to S1 cells were chosen for further validation based on whether the genes from which they originate were involved in cancer-related and/or epithelial polarity pathways. (b) The three isoforms of circRNAs that originate from Cx43 (*GJA1*) mRNAs were also chosen due to their relevance to the 3D risk-progression culture model. One Cx43 circRNA isoform, has\_circ\_0077754, was not detected by the microarray due to its short size of 93 bp, since library size-selections usually excludes circRNAs  $< 200$  nt long [244]. **Alias** represents the circRNAs probe name as annotated by CircBase [245]. **Gene Symbol** denotes the gene of the transcript from which this circRNAs originate. Primers were designed using CircularRNA Interactome *in silico* tool [83] and purchased from Eurofins (Canada). The **74ircRNAs fragment size** represents the size of the resulting amplified PCR fragment. The circRNAs highlighted in red font were significantly dysregulated in Cx43-KO-S1 as compared to S1 cells in 3D, as validated through RT-qPCR (shown in Fig. 4).

(a)	Alias	Gene Symbol	Left primer (human)	Right Primer (human)	74ircRNAs fragment size (bp)
Up-regulated circRNAs	has_circ_0001605	<i>CNPY3</i>	AGAGGCAGATCAGGGGGTAT	GAAGGAAGATCCCAGGTGGT	141
	has_circ_0007961	<i>SPRED2</i>	GCCTTGGTCTATGGGTTCAA	TGGTCATAACCACAGCCTTG	120
	has_circ_0081481	<i>FBXO24</i>	ACTACGTGGGGACCCCTCTC	TACAGGCCCTTCGTGTATCC	126
	has_circ_0004448	<i>MDM2</i>	GCTTCAGGAAGAGAAACCTTCA	GTCCGATGATTCTGCTGAT	144
	has_circ_0061251	<i>BAGE2</i>	CTTGCCTGTTCTCAGTGTGG	AAAAATTTCCCACCTCCTG	129
	has_circ_0061405	<i>TIAM1</i>	GCCAGACTTGAATCCTCAG	AGATGTCTTCTCCTCGGGCTGT	140
	has_circ_0004420	<i>C2orf89</i>	GAAGAGCAGTGCCATCCATT	TGTACGGGACATGGATTGTG	124
	has_circ_0036254	<i>CD276</i>	GTGCGAATGGCACCTACAG	ACGCAGCATCTTCTGTGA	141
	has_circ_0011951	<i>HIVEP3</i>	GCCGTAGGAGTGGACATGAA	CGAGGCTCCTCCATGAACTA	134
	has_circ_0023016	<i>RBM4</i>	TCACTGCTCCAGGGTCTCTT	ATTCAGCCCACACACATCC	123

Down-regulated circRNAs	has_circ_0001072	<i>GTDC1</i>	GACCATTCCCATCAGTGAGC	ACTCATTGGCCCATTCAAAC	121
	has_circ_0084765	<i>EYAI</i>	AACCTGGACAGGCACCATAC	TACTGCTCCCAATTGCTGAA	129
	has_circ_0005054	<i>FMN1</i>	CCAGCCTTTCAAGGACAAAC	TGTGCAAGGAGGTGATACCC	139
	has_circ_0008257	<i>HADHB</i>	TTGGAGCTGGCTTCTCTGAC	CATCCACCACCACAACATTC	147
	has_circ_0060056	<i>EIF6</i>	TGCAAAAACCTGCTCTGTTG	AAGCAGCCGATCTCACAGTT	152
	has_circ_0060055	<i>EIF6</i>	TGCAAAAACCTGCTCTGTTG	CTGTTCCCCACACACATGC	193
	has_circ_0005185	<i>PRKD1</i>	AAACAAGAAAGCCAGCTTCG	CATGAGCCCCTGTTCCCTTT	128
	has_circ_0083442	<i>MTUS1</i>	TGGTATCCAGGGCTCATGTT	TGCTGGTTTTGGAGGTTTCT	134

(b)	Alias	Gene Symbol	Left primer (human)	Right Primer (human)	75ircRNAs fragment size (bp)
Up	has_circ_0077753	<i>GJAI</i>	TGTTTCAGCTTCATTGCATGT	GCCTTCCCCCTAATGAAAGA	194
N/A	has_circ_0077754	<i>GJAI</i>	GTGGTGCCCAGGCAACATGG	AGCCACACCTTCCCTCCAGC	93
Down	has_circ_0077755	<i>GJAI</i>	TGTTTCAGCTTCATTGCATGT	CCTCCAGCAGTTGAGTAGGC	180

#### 4. miRNA sequencing revealed 65 differentially expressed miRNAs in Cx43-KO-S1 versus S1 acini specific to Cx43 loss

After identifying the dysregulated circRNAs in response to Cx43 silencing in the cultured epithelia, their miRNA expression profile was studied. Focusing on the sponging activity of circRNAs to their target miRNAs, triplicates of the same 3D drip culture samples were submitted for miRNA sequencing. This was performed to compare dysregulation of actual miRNAs in the cultured epithelia detected through sequencing to the miRNA response elements, MREs, predicted to be “sponged” by the significant circRNAs (shown in **Table 7**) based on Arraystar’s miRNA target prediction software [246, 247]. Sponging refers to circRNAs exhibiting endogenous competing binding sites (one to several) for each specific target miRNA. They covalently bind the mature target miRNA, downregulating its expression, hence preventing it

from binding its own target mRNAs and repressing translation [235]. miRNA sequencing revealed 29 significantly up-regulated (44.6%) and 36 significantly down-regulated (55.4%) mature miRNAs in response to Cx43 silencing in the cultured epithelia. Heat map of hierarchical cluster analysis was used to depict only the differential expression patterns of miRNAs that were both i) significantly detected in miRNA sequencing and ii) predicted to be sponged by (one or more of) all the 121 circRNAs significantly dysregulated in microarray of the same model (**Fig. 7a**). For better selectivity, actual differentially expressed miRNAs from 3D culture model sequencing that are in common with predicted MREs that can be sponged by one or more of only the 18 selected circRNAs were tabulated in **Fig. 7b**, and the MREs sponged by the nine validated circRNAs were highlighted. Of these, eight miRNAs, miR-99a-3p, miR-8072, miR-203a-3p, miR-520g-5p, miR-182-5p, miR-511-5p, miR-653-5p and miR-600 were significantly up-regulated while three miRNAs, miR-520g-3p, miR-520h and miR-3960 were significantly down-regulated in Cx43-KO-S1 versus S1 cells, and were presumably sponged by (one or more of) the nine validated circRNAs by RT-qPCR (**shown in Fig. 6**). Thus, these miRNAs were further considered to function in the potential post-transcriptional axes that might be dysregulated as a result of Cx43 loss in the breast epithelium, and in turn, potentially play a role in heightened risk of breast cancer initiation.

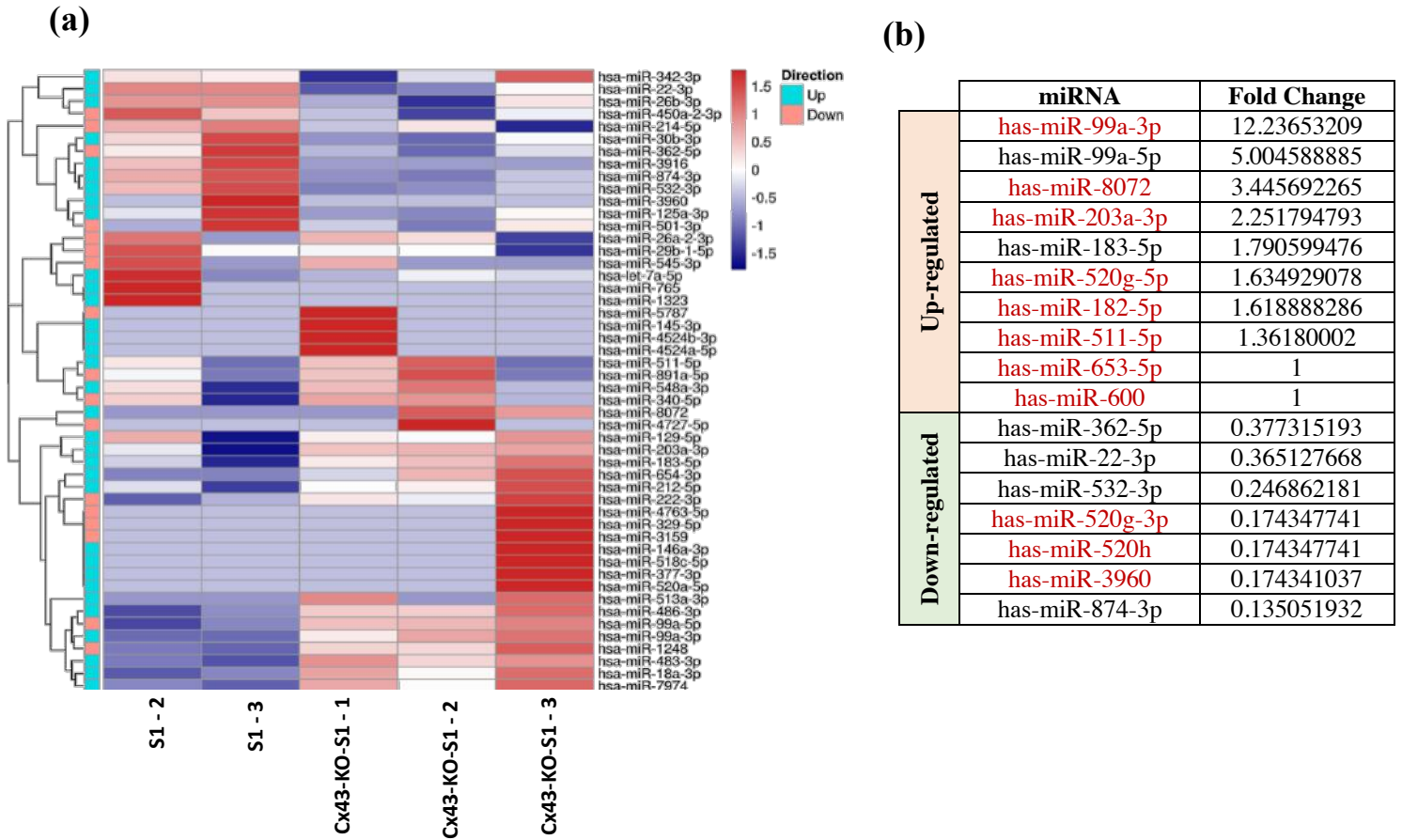


**Figure 7: Sequencing revealed 29 significantly up-regulated and 36 significantly down-regulated mature miRNAs in Cx43-KO-S1 cells as compared to S1 cells in response to Cx43 silencing in cultured epithelia.** Triplicates of Cx43-KO-S1 and triplicates of S1 cells were plated on Matrigel™ for 11 days. Total RNA was extracted, reverse transcribed and hybridized for sequencing using Illumina’s NovaSeq6000. (a) A **heat map** of hierarchical cluster analysis shows for simplicity only miRNAs that were significantly detected from miRNA sequencing data (Fold Change > 2) and are in common with some of the five top miRNA response elements (MREs) for each of the 121 significant differentially expressed circRNAs as predicted by Arraystar’s miRNA target prediction software. Red depicts up-regulated miRNAs and blue depicts down-regulated ones in pretumorigenic Cx43-KO-S1 cells compared to nontumorigenic S1 counterparts. Rows were clustered using hierarchical clustering and are annotated with the direction (up- or down-regulation) of the associated circRNAs in Cx43-KO-S1 samples versus S1 samples. Bright blue boxes (■) annotate miRNAs that are predicted to bind to up-regulated circRNAs, whereas pink

boxes (■) annotate those associated with circRNAs that are down-regulated in Cx43-KO-S1 as compared to S1 acini. (b) **A table** showing the regulation pattern of miRNAs from miRNA sequencing of the 3D culture model that are in common with predicted MREs of only the 18 chosen circRNAs (from **Table 2 &3**), Fold Change  $\geq 1$ . *The miRNAs in red font represent common significant miRNAs from miRNA sequencing results of 3D culture model and MREs that can be sponged by the nine validated circRNAs through RT-qPCR.* Thus, these were selected for investigation in the potential post-transcriptional signature axes in the scope of this paper.

##### ***5. Fifteen tumor-associated miRNAs from microarrays of a validation cohort of early-stage young breast cancer patients exhibited reported involvement in epithelial polarity and cancer-related pathways***

Nassar et al. [29] previously identified 74 dysregulated miRNAs in microarrays from 45 invasive ductal carcinoma (IDC) versus 17 normal adjacent breast tissues from the Lebanese population (Fold Change  $> 2$ ) and compared their profile to 197 American breast cancer patients and 87 normal samples from TCGA (The Cancer Genome Atlas) [29]. All the Lebanese patient cohort were estrogen receptor (ER) positive, 97.8% were progesterone receptor (PR) positive and 24.5% had human epidermal growth factor receptor 2 (HER2) over-expression. The majority of the tumors were of grade 2, and half of them presented with lymph node involvement. Moreover, 42.2% were below the age of 40 and none of the patients had distant metastasis, thus this cohort was categorized into early-stage breast cancers. We uncovered among these miRNAs through a comprehensive literature review fifteen tumor-associated miRNAs involved in early events of breast tumorigenesis that contribute to loss of acinar morphogenesis [104, 248-251]. Among these miRNAs, miR-200c, miR-492, miR-638, miR-663, miR-2861, miR-3960, miR-183, miR-



182) were commonly up-regulated in both Lebanese and US patients while miR-492 and miR-663 were exclusive to the Lebanese population. Seven tumor-associated miRNAs, miR-145, miR-125b, miR-100, miR-139-5p and miR-99a, were commonly down-regulated in both Lebanese and US populations (**Table 6**). Importantly, miR-3960, miR-183, miR-182, miR-145 and miR-99a were in common between patient miRNAs involved in epithelial polarity and MREs predicted to be sponged by the 18 selected circRNAs (as shown in **Table 5 & 7**). However, only miR-3960 and miR-182 belonged to MREs that can be sponged by the validated circRNAs confirmed through RT-qPCR. Thus miR-3960 and miR-182 were considered to function in the potential post-transcriptional axes that might be dysregulated as a result of Cx43 loss in the breast epithelium, and in turn, potentially play a role in heightened risk of breast cancer initiation.

**Table 6: Literature search of tumor-associated miRNAs from microarrays of early-stage Lebanese breast cancer patients [29] uncovered fifteen miRNAs involved in epithelial polarity and cancer pathways.** Building on Nassar et al. [29], 74 miRNAs were differentially expressed in Lebanese patients with early-stage breast cancer with no distant metastasis, of which 42.2% were below the age of 40. We identified through a comprehensive literature review 15 patient tumor-associated miRNAs that are involved in early events of breast tumorigenesis and affect epithelial polarity [104, 248-251]. Eight of these miRNAs are up-regulated and seven are down-regulated in breast cancer tissues as compared to normal adjacent tissues. Orange highlight panel refers to up-regulated miRNAs, green highlight panel represents down-regulated miRNAs, blue highlights refer to miRNAs exclusively dysregulated in the Lebanese population, while miRNAs highlighted in grey refer to miRNAs commonly dysregulated in both Lebanese and matched US patients as reported in Nassar et al. [29]. miRNAs highlighted in yellow are in common between early-stage patient miRNAs involved in epithelial polarity and MREs predicted to be sponged by the selected significant circRNAs (as shown in **Table 5 & 7**). Only miRNAs highlighted in both yellow highlight and red font are implicated in epithelial polarity from patients miRNome and are in common with MREs predicted to be sponged by the RT-qPCR validated

significant circRNAs. Thus, these were selected for investigation in the potential post-transcriptional signature axes in the scope of this paper.

	miRNAs implicated in epithelial polarity (Lebanese patients <40 YO)	Fold Change (From Nassar et al., [29])	Regulation mode – Lebanese versus US Population (From Nassar et al., [29])
Up-regulated	miR-200c	2.075910565	common Lebanon and US
	miR-492	1.681732871	Exclusive to Lebanese patients
	miR-638	1.582078421	common Lebanon and US
	miR-663	1.561979924	Exclusive to Lebanese patients
	miR-2861	1.609109537	common Lebanon and US
	miR-3960	1.503569235	common Lebanon and US
	miR-183	10.03232222	common Lebanon and US
	miR-182	5.958538792	common Lebanon and US
Down-regulated	miR-145	0.433224993	common Lebanon and US
	miR-125b	0.444801522	common Lebanon and US
	miR-100	0.381083182	common Lebanon and US
	miR-99a	0.32225595	common Lebanon and US
	miR-126	0.588181274	common Lebanon and US
	miR-139-5p	0.123421444	common Lebanon and US
	miR-130a	0.323149936	common Lebanon and US

**6. Three mRNA-circRNA-miRNAs axes were proposed, and one axis was validated with potential for risk-assessment of breast cancer initiation**

After analyzing, predicting, selecting, validating and comparing significant circRNAs and miRNAs specific to Cx43 silencing in breast epithelial culture and tumor-associated miRNAs from the early breast cancer patient cohort, three potential mRNA-circRNA-miRNA axes were revealed. Focusing on the possible sponging activity of these circRNAs to their target miRNA, the first proposed axis included hsa\_circ\_0007961 (from *SPRED2*) and its MREs, miR-99a-3p,

miR-653-5p, miR-600 and miR-511-5p that were found dysregulated in the breast epithelial culture miRNome. The second proposed axis included hsa\_circ\_0081481 (from *FBXO24*) and its MREs, miR-3960 (commonly detected in breast epithelial culture and patient miRNome) and miR-8072 (detected in breast epithelial culture miRNome) (**Table 7a**). The third proposed axis denoted hsa\_circ\_0077755 (from *Cx43 (GJAI)*) and its MREs, miR-182, which was commonly detected in breast epithelial culture and patient miRNome as well as miR-203, miR-520g and miR-520h, which were only detected in breast epithelial culture miRNome (**Table 7b**). We next compared the dysregulation pattern of the validated circRNAs in the three potential axes to that of their target MREs that were detected in breast epithelial culture and/or patients miRNomes. Only **Cx43/has\_circ\_0077755/miR-182** axis matched the expected circRNA-miRNA inverse dysregulation levels, suggestive of a possible sponging activity (**Fig. 8a**). Thus, miR-182 expression level was further confirmed to be significantly up-regulated in four samples of Cx43-KO-S1 cells as compared to S1 counterparts using RNU6B as an endogenous control through RT-qPCR (**Fig. 8b**). Moreover, survival analysis for miR-182 was generated using METABRIC dataset in the Kaplan-Meier Plotter [252]. The large patient dataset (460 patients) included long follow-up median of 94 months were 100% ER positive, 12% HER2 positive, all had grade II tumors with no distant metastasis and half of them with lymph node involvement, to match the characteristics of the majority of the early-stage Lebanese validation cohort investigated earlier [29]. Of note, miR-182 seems to associate with poor prognosis when up-regulated in the patients with grade II tumors (**Fig. 8c**). Interestingly, when selecting another dataset of 395 patients with

the exact hormone receptor status, lymph node involvement and no distant metastasis but with grade III breast tumors, the survival analyses for miR-182 showed that miR-182 associates with poor prognosis when down-regulated in grade III tumors of the same characteristics (**Fig. 8d**).

**Table 7: Expression and detection of selected circRNAs (cells microarray) and their target miRNAs (cells sequencing and patients microarray [29]) identified three potential risk-assessment axes for breast cancer initiation. (a)** Listing of the eighteen dysregulated circRNAs chosen for further validation. **(b)** Listing of two of the three isoforms of circRNAs that originate from Cx43 (*GJAI*) mRNAs that were detected in the microarray (hsa\_circ\_0077754 was not detected due to its short size). **Alias** represents circRNAs name as annotated in CircBase [245]. **CircRNAs Size** indicates the mature spliced size of circRNAs, **Fold Change** denotes the absolute ratio (no log scale) of normalized intensities between the two cell lines and **Chrom** represents the chromosomes that from which each circRNA originates. For **circRNAs Type**, exonic represents circRNA arising from an exon, intronic arising from an intron and sense overlapping arising from the same gene locus as the linear transcript, but neither exonic nor intronic. **Gene Symbol** denotes the gene from which circRNA originates. **MREs** represent the predicted miRNA response elements by Arraystar. The MREs highlighted in grey were shown to be differentially expressed in miRNA sequencing results of Cx43-KO-S1 versus S1 breast epithelial cells in 3D (shown in **Fig. 6**). The MREs in green font were found dysregulated in microarrays from the early-stage young Lebanese breast cancer validation patient cohort by Nassar et al. [29] and involved in cancer initiation events (shown in **Table 5**). MREs highlighted in yellow are involved in breast cancer as described in Naser Al Deen et al., 2019 [7]. The circRNAs in red font were confirmed to be significantly dysregulated in Cx43-KO-S1 as compared to S1 cells in 3D through RT-qPCR (shown in **Fig. 7**). The three rows highlighted in light yellow represent the three potential mRNA-circRNA-miRNA breast cancer risk-assessment axes that will be discussed further. These were the only axes with validated circRNAs (RT-qPCR) and with predicted MREs that were also dysregulated in the miRNomes from the cultured epithelia and/or early-stage young patients. *All MREs were predicted using Arraystar's miRNA target prediction software [246, 247], except for the last row in (b), where circRNAs Interactome [83] was used in addition to predict MREs as published in Naser Al Deen et al., 2019 [7] (as shown to be involved in breast cancer initiation pathways and circRNA axes originating from Cx43).*

(a)	Alias	CircRNA Size (bp)	Fold Change	Chrom	circRNA Type	Gene Symbol	miRNA Response Elements (MREs)
Up-regulated circRNAs	hsa_circ_0001605	1600	3.7640541	chr6	intronic	<i>CNPY3</i>	miR-665, miR-129-5p, miR-539-3p, miR-520a-5p, miR-30b-3p
	hsa_circ_0007961	412	3.2491154	chr2	exonic	<i>SPRED2</i>	miR-99a-3p, miR-653-5p, miR-134-3p, miR-600, miR-511-5p
	hsa_circ_0081481	236	2.5544065	chr7	exonic	<i>FBXO24</i>	miR-4467, miR-3960, miR-8072, miR-3915, miR-6880-5p
	hsa_circ_0004448	215	2.294606	chr12	exonic	<i>MDM2</i>	let-7e-5p, miR-532-3p, miR-26b-3p, miR-145-3p, let-7a-5p
	hsa_circ_0061251	444	2.1806787	chr21	exonic	<i>TPTE</i>	miR-203a-3p, miR-513a-3p, miR-212-5p, miR-654-3p, miR-183-5p
	hsa_circ_0061405	603	2.5840028	chr21	exonic	<i>TIAMI</i>	miR-646, miR-4741, miR-7974, miR-4524a-5p, et-7a-2-3p
	hsa_circ_0004420	561	2.246416	chr2	exonic	<i>TRABD2A</i>	miR-2682-3p, miR-1324, miR-6830-5p, miR-1273g-3p, miR-4524b-3p
	hsa_circ_0036254	1423	2.6596151	chr15	exonic	<i>CD276</i>	miR-22-3p, miR-18a-3p, miR-125a-3p, miR-761, miR-874-3p
	hsa_circ_0011951	199	2.2299277	chr1	exonic	<i>HIVEP3</i>	miR-1323, miR-146a-3p, miR-548a-3p, miR-518c-5p, miR-483-3p
	hsa_circ_0023016	447	2.9363024	chr11	exonic	<i>RBM4</i>	miR-3916, miR-765, miR-650, miR-6510-5p, miR-7106-5p
Down-regulated circRNAs	hsa_circ_0001072	267	4.1090007	chr2	exonic	<i>GTDC1</i>	miR-1185-5p, miR-761, miR-340-5p, miR-607, miR-539-5p
	hsa_circ_0084765	432	3.9132515	chr8	exonic	<i>EYA1</i>	miR-3915, miR-539-5p, miR-6864-3p, miR-6738-5p, miR-214-5p
	hsa_circ_0005054	551	2.2480323	chr15	exonic	<i>FMN1</i>	miR-612, miR-6515-3p, miR-4753-5p, miR-362-5p, miR-450a-2-3p
	hsa_circ_0008257	333	3.2325336	chr2	exonic	<i>HADHB</i>	miR-504-3p, miR-545-3p, miR-518e-3p, miR-891a-5p, miR-99a-5p
	hsa_circ_0060056	1018	2.4091004	chr20	sense overlapping	<i>EIF6</i>	miR-5787, miR-4739, miR-4763-5p, miR-4727-5p, miR-3159
	hsa_circ_0060055	906	2.9291354	chr20		<i>EIF6</i>	miR-665, miR-485-5p, miR-501-3p, miR-377-5p, miR-608
	hsa_circ_0005185	920	2.0899337	chr14	exonic	<i>PRKD1</i>	miR-222-3p, miR-7152-5p, miR-1248, miR-4713-5p, miR-3619-3p
	hsa_circ_0083442	174	2.1575894	chr8	exonic	<i>MTUS1</i>	miR-29b-1-5p, miR-329-5p, miR-373-3p, miR-26a-2-3p, miR-607

(b)	Alias	CircRNA Size (bp)	Fold Change	Chrom	circRNA Type	Gene Symbol	miRNA Response Elements (MREs)
Up	hsa_circ_0077753	14129	1.0524777	chr6	exonic	<i>GJA1</i>	miR-4530, miR-6777-3p, miR-524-3p, miR-525-3p, miR-130a-3p
Down	hsa_circ_0077755	2896	1.1941951	chr6	exonic	<i>GJA1</i>	miR-4530, miR-4763-3p, miR-5096, miR-130a-3p, miR-6503-3p
	hsa_circ_0077755	2896	1.1941951	chr6	exonic	<i>GJA1</i>	miR-182, miR-375, miR-203, miR-520g, miR-520h

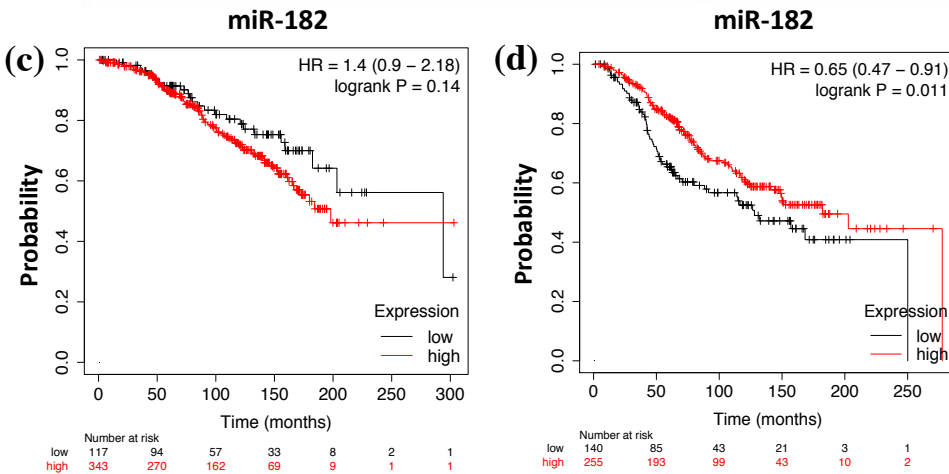
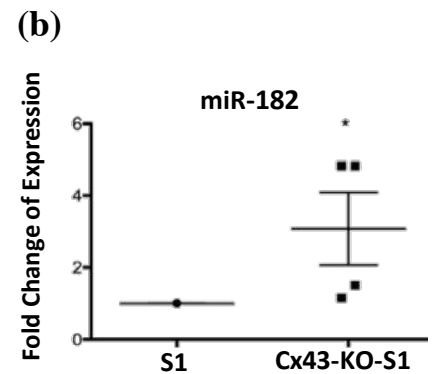
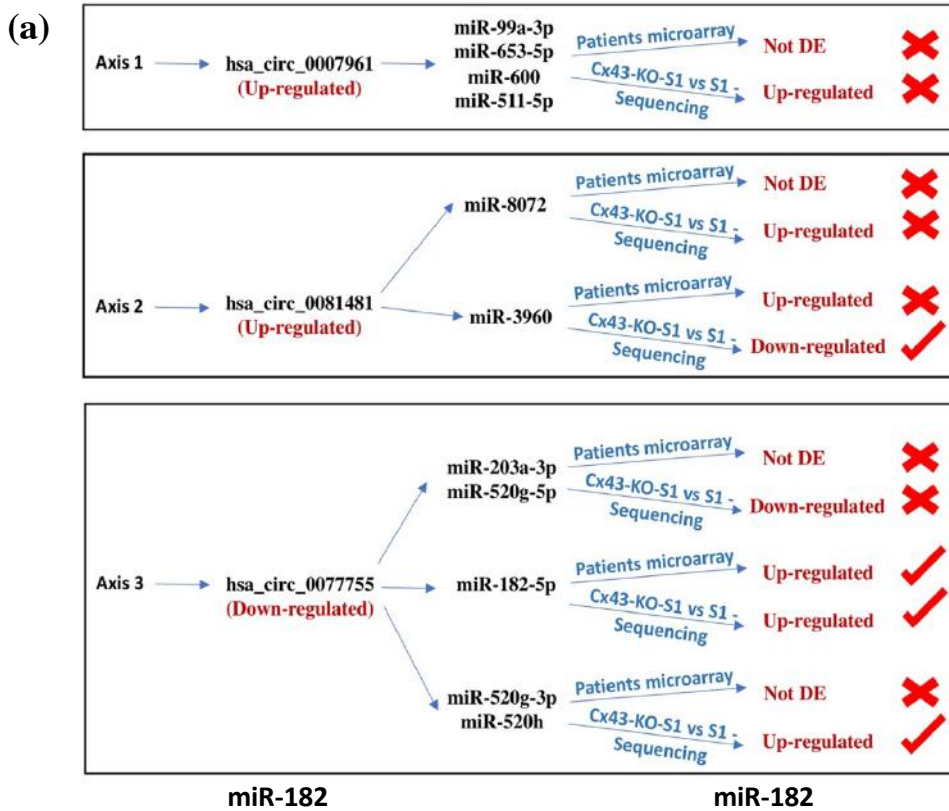


**Figure 8: Selection of one validated mRNA-circRNA-miRNA breast cancer initiation risk-assessment axis. (a) Comparative flow chart representing the dysregulation patterns of the validated circRNAs and that of their target miRNAs, based on i) miRNA sequencing in Cx43-KO-**

S1 cells compared to S1 cells (shown in **Fig. 6**) and ii) tumor-associated miRNAs from microarrays of early-stage young Lebanese breast cancer patient cohort as reported in Nassar et al. [29] (shown in **Table 5**). Only Cx43/has\_circ\_0077755/miR-182 axis exhibits the expected inverse dysregulation pattern between circRNA and their target miRNAs in both cells and patients (when circRNA is down-regulated, its MRE should be up-regulated, and vice versa). **(b)** RT-qPCR further confirmed the upregulation of miR-182 in four samples of Cx43-KO-S1 cells as compared to S1 counterparts using RNU6B as an endogenous control. \* denotes a p.value < 0.05 for Cx43-KO-S1 versus S1 cells using one-tailed unpaired T-test. **(c)** Using METABRIC breast cancer dataset in the Kaplan-Meier Plotter [252], the survival analysis for miR-182 in 460 patients with grade II breast tumors was plotted. miR-182 seems to associate with poor prognosis when up-regulated in grade II breast tumors. **(d)** However, the survival analysis for miR-182 in 395 patients with grade III breast tumors of the same characteristics shows that miR-182 seems to associate with poor prognosis when down-regulated in grade III tumors.

### ***7. Gene co-expression networks associated with Cx43/hsa\_circ\_0077755/miR-182 axis correspond to cancer-related pathways***

We opted to further show that the validated Cx43/has\_circ\_0077755/miR-182 axis, spurred from the comparison between patients and the cell culture risk-progression model, is involved in cancer-related pathways. Thus, sequence pairing using Cytoscape software was utilized to link the top predicted MREs (by ArrayStar), which could be sponged by has\_circ\_0077755 to their predicted mRNA targets by TargetScan within Ingenuity Pathway Analysis (IPA). Only experimentally validated mRNAs involved in cancer-related pathways were kept. The results confirmed that in the gene co-expression network for has\_circ\_0077755, miR-182 exhibited the largest interaction network in cancer-related pathways and exhibited slight interaction network overlap with miR-203 (**Fig. 9**).

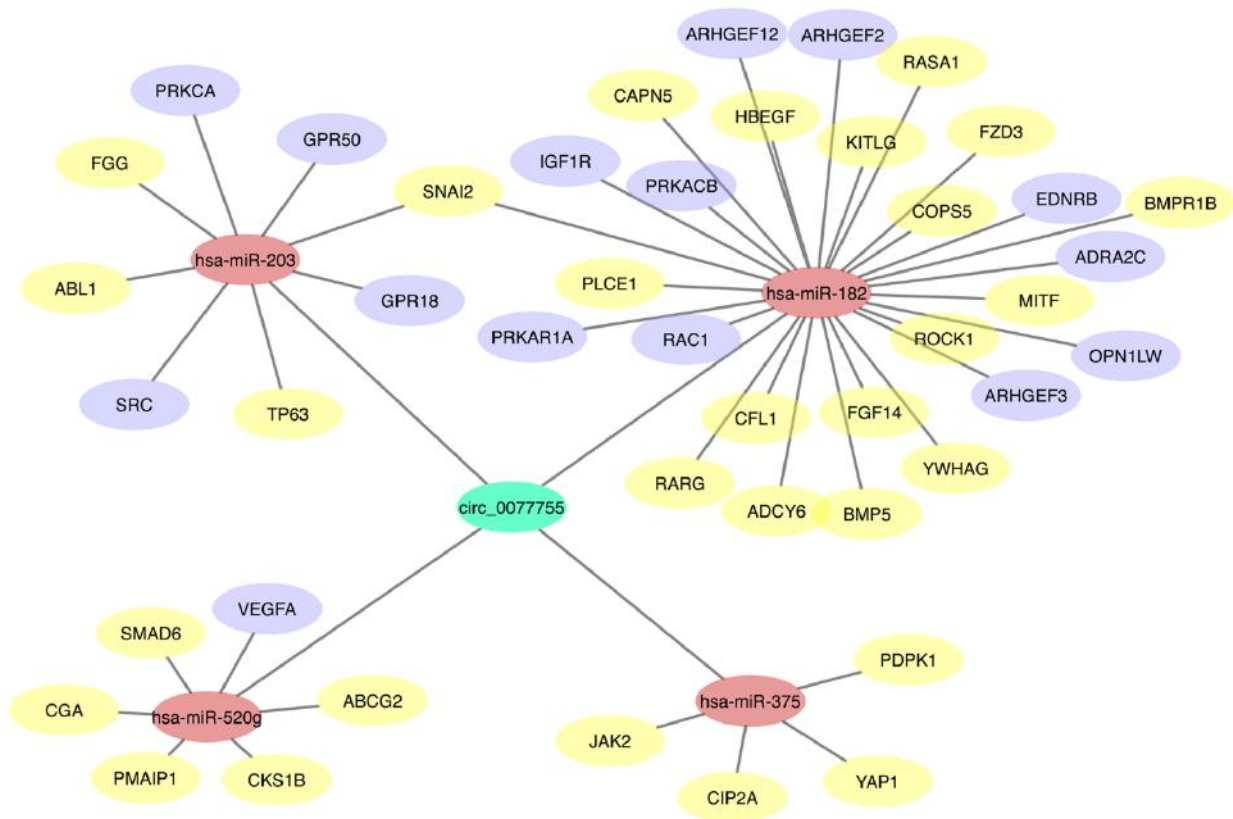


**Figure 9: Gene co-expression networks shows the involvement of the validated Cx43/has\_circ\_0077755/miR-182 axis in cancer-related pathways and in breast cancer.** CircRNA-miRNA-mRNA gene co-expression network for has\_circ\_0077755 was predicted by TargetScan within IPA and Cytoscape was used to draw 86circRNAs-miRNA-mRNA interaction networks. CircRNA is colored in green, miRNAs in pink and mRNAs reported in cancer in yellow and in breast cancer in purple. miR-182 exhibited the largest interaction network with mRNAs involved in cancer-related pathways in the axis.



### 8. Functional analysis for *has\_circ\_0077755* is enriched for cancer-related pathways

Additional *in silico* tools were used to confirm the involvement of the selected axis in cancer-related pathways. Using IPA (Qiagen), a functional enrichment analysis of the predicted target mRNAs (by TargetScan) for the top five MREs associated with *has\_circ\_0077755* was performed (**Fig. 10**). *Hsa\_circ\_0077755* displayed enrichment of biological functions in cancer with pathways mostly enriched in cell movement, migration and proliferation of breast cell lines, formation of focal adhesions, colony formation and cell viability of tumor cell lines and invasion of breast cancer cell lines. This analysis corroborates the strong involvement of the selected axis in cancer-related pathways.

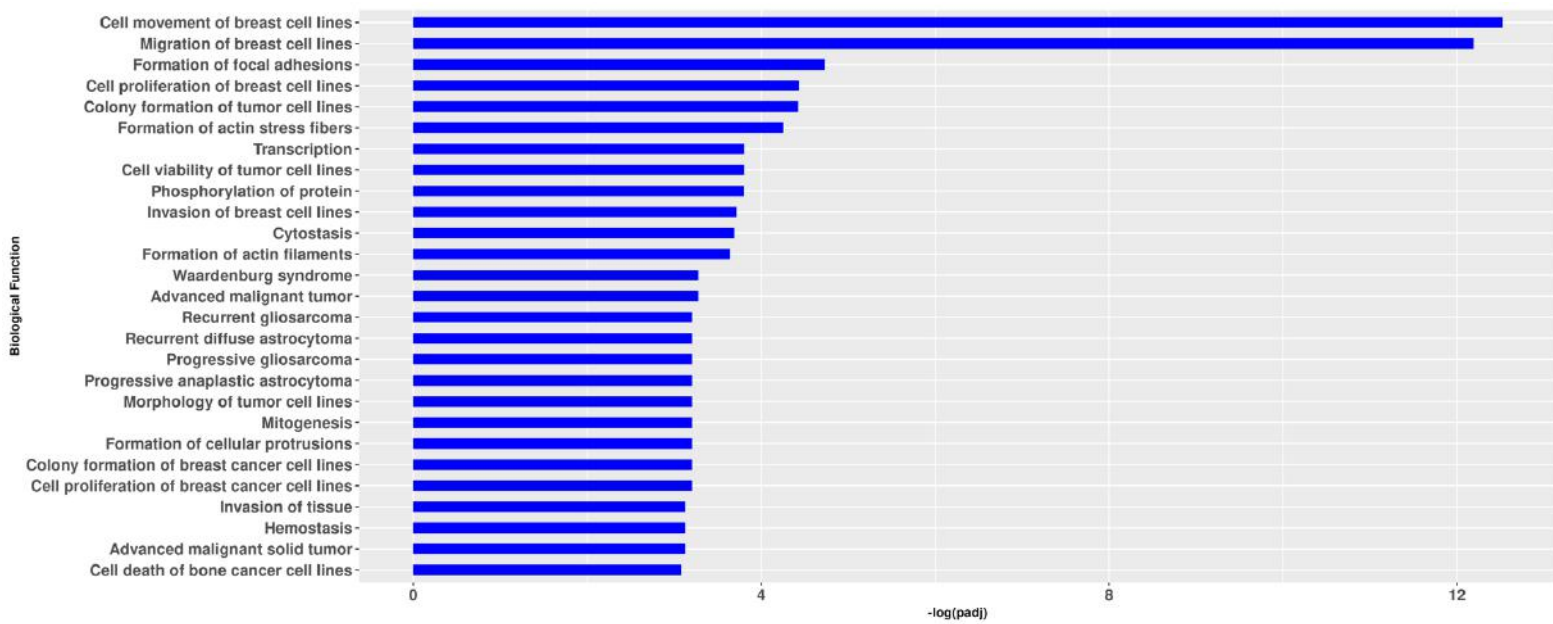


**Figure 10: The chosen and validated hsa\_circ\_0077755 is functionally enriched in cancer-related pathways.** A functional enrichment analysis was performed in Ingenuity Pathway Analysis (IPA) of predicted target mRNAs (by TargetScan) for the top five MREs associated with hsa\_circ\_0077755. P-values were adjusted for multiple testing using the Benjamini-Hochberg method. The bar plot displays the biological functions on the y-axis and the  $-\log$  (adjusted p-value) on the x-axis.

#### **D. Discussion**

Recent studies reported miRNAs and circRNAs as active players in tissue homeostasis, tumorigenesis, therapy resistance and metastasis and as novel noninvasive cancer biomarkers [6, 7, 24, 25] by virtue of their high stability in body fluids [80, 233, 234]. This study brings a novel comprehensive analysis of circRNAs and miRNAs expression axes specific to Cx43 loss and focused on risk assessment of early breast cancer initiation. Acting as endogenous miRNA sponges, circRNAs may also affect breast cancer initiation and progression [8]. CircRNA-miRNA axes have been reported as biomarkers in several cancers [75-77, 238], including breast cancers [9-15] but never specifically in the context of breast premalignant phenotypes and gap junction involvement in breast cancer initiation.

##### ***1. Gap junctions are involved in post-transcriptional regulatory pathways in breast cancer initiation***

A main outcome from this study is the demonstration of Cx43 involvement in post-transcriptional regulatory pathways of heightened risk of breast cancer initiation. Upon silencing

Cx43 in S1 cells, a total of 121 circRNAs and 65 miRNAs were significantly dysregulated in the pretumorigenic phenotype, adding an important post-transcriptional regulatory layer that Cx43 might play in breast epithelia (**Fig. 5 & 7**). Our previous findings implicate Cx43 in fundamental aspects of epithelial homeostasis, mainly in regulating the establishment and maintenance of apical polarity, cell cycle entry and mitotic spindle orientation [26]. Specifically, the loss of Cx43 disrupts apical polarity and mitotic spindle orientation, which contributes to cell multilayering [26], and primes cells for enhanced motility and invasion depending on the microenvironment [26, 27]. These phenotypes represent premalignant mammary lesions (as hallmarks of cancer initiation) like those observed in ductal hyperplasia in a murine model [28]. Recently, we confirmed *in silico* the involvement of Cx43-derived post-transcriptional players as possible biomarker signatures for the risks of early breast cancer. Three Cx43-derived circRNA isoforms (hsa\_circ\_0077753, hsa\_circ\_0077754, and hsa\_circ\_0077755) and a panel of their predicted sponged miRNAs (miR-182 miR-375, miR-203, miR-520g and miR-520h) [7] were proposed to recapitulate phenotypes caused by Cx43 loss when dysregulated [21, 76, 104, 105]. For instance miR-182, miR-203 and miR-375 were up-regulated during breast lobular neoplasia progression and correlated with loss of breast cellular organization and development of hyperplastic phenotypes [104].

In this study, we specifically aimed to validate the actual post-transcriptional axes that might be involved in regulatory pathways contributing to heightened risk of breast cancer initiation upon Cx43 loss. Notably, the choice of validated circRNAs and miRNAs in the axes

was dependent on their involvement in pathways that recapitulate phenotypes observed upon loss of Cx43 (**Table 5**). miR-99a was up-regulated in Cx43-KO-S1 compared to S1 cells. Turcatel et al. [253] reported an involvement of miR-99a in epithelial to mesenchymal transition (EMT) when up-regulated in murine mammary gland, and in driving the progression of breast cancer through cell migration and invasion by regulating TGF- $\beta$  and affecting the phosphorylation of SMAD3. miR-3960, which was commonly up-regulated in early breast cancer Lebanese and US patients, and down-regulated in Cx43-KO-S1 compared to S1 cells was linked to breast cancer-mediated bone metastasis via Runx2/miR-3960/miR-2861 axis [254]. Moreover, miR-182, which was commonly up-regulated in young Lebanese and US patients and in Cx43-KO-S1 compared to S1 cells, was up-regulated in various human breast cancer subtypes and acted as an oncogene [255]. Over-expression of miR-182 *in vitro* enhanced cell migration, invasion and proliferation and increased tumor volume and lung metastasis *in vivo* by regulating FOXF2 [256]. In addition, in an attempt to identify insults that lead to breast cancer initiation, Duforestel et al. revealed that exposing non-neoplastic MCF10A cells to low pressure but sustained DNA hypomethylation, *via* the TET pathway, through repeated exposure to Glyphosate, in combination with over-expression of miR-182 primed tumor-initiation from these non-neoplastic cells *in vivo* [257]. Thus, by sponging these miRNAs, the differentially expressed circRNAs specific to Cx43 loss might drive mammary pretumorigenic phenotypes and cancer initiation, and hence, corroborate gap junction's involvement in post-transcriptional regulatory axes that heighten the risk of breast cancer initiation.

## ***2. One mRNA-circRNA-miRNAs axis act as potential biomarker signatures for heightened-risk of breast cancer initiation***

Only few circRNA biomarker axes have been reported in breast cancers [9-15], but none specific to pre-malignant epithelial polarity transitions that might increase the risk of initiation of the disease. For instance, hsa\_circ\_0001982 was significantly up-regulated *in vivo* and *in vitro*, and its knock-down inhibited proliferation and invasion and promoted apoptosis in breast cancer cells by targeting miR-143 [9]. Hsa\_circ\_0008039/miR-432-5p/E2F3 exhibited oncogenic roles in breast cancer and suppressing hsa\_circ\_0008039 inhibited proliferation and migration and arrested cell cycle through targeting miR-432-5p, in turn targeting E2F3[11]. Circ-Dnmt1 was up-regulated in breast cancer patient samples and in eight cell lines and could bind to oncogenic proteins p53 and AUF1, exhibiting oncogenic potential [13]. Hsa\_circ\_0072309 over-expression dramatically inhibited proliferation, migration and invasion of breast cancer cells *in vitro* and repressed breast cancer growth *in vivo* through sponging miR-492, serving as a prognostic biomarker [14] while hsa\_circ\_0001785 served as a potential plasma diagnostic marker [15].

We investigated potential post-transcriptional axes specific to Cx43 loss that might heighten the risk for breast cancer initiation. The first validated up-regulated hsa\_circ\_0007961 (from *SPRED2*) was predicted to sponge miR-653-5p, miR-99a-3p, miR-134-3p, miR-600 and miR-511-5p (**Table 7a**). Of note, miR-653-5p, miR-99a-3p, miR-600 and miR-511-5p were found dysregulated in miRNA sequencing of the cultured epithelia specific to Cx43 loss (**Fig. 7b**) However, none of these miRNAs matched the expected circRNA-miRNA inverse

dysregulation levels suggestive of a possible sponging activity, and neither of the miRNAs were detected in the early-stage patient validation cohort miRNome. This axis was hence not validated (**Fig. 8a**). The second up-regulated circRNA in our selection, hsa\_circ\_0081481 (from *FBXO24*), was predicted to sponge miR-3960, miR-4467, miR-8072, miR-3915, miR-6880 (**Table 7a**). Of these miRNAs, miR-8072 was found upregulated in miRNome of the cultured epithelia while miR-3960 was found down-regulated in the cultured epithelia and matched the expected circRNA-miRNA inverse dysregulation levels. However, miR-3960 was found up-regulated in the patient validation cohort, contrary to its expected levels, and thus the second axis was also not validated (**Fig. 8a**). As for the down-regulated circRNA, hsa\_circ\_0077755 (originating from Cx43 (*GJA1*), the gene of interest of our previous and current studies [7, 20, 21]), all of the MREs it could sponge, miR-182, miR-203, miR-520g, and miR-520h (except for miR-375) were detected in the miRNome of the cultured epithelia (**Table 7b**). However, only miR-182 was i) found up-regulated in the cultured epithelia, ii) found similarly up-regulated in the patient validation cohort and iii) matched the expected circRNA-miRNA inverse dysregulation levels (**Fig. 8a**). Thus **Cx43/hsa\_circ\_0077755/miR-182** axis was the only validated biomarker axis for heightened-risk of breast cancer initiation.

**3. *Cx43/hsa\_circ\_0077755/miR-182 axis associates with poor prognosis in a differential manner along breast cancer initiation and progression***

To further validate **Cx43/hsa\_circ\_0077755/miR-182 axis**, RT-qPCR confirmed the significant up-regulation of miR-182 in Cx43-KO-S1 cells compared to S1 counterparts (**Fig 8a**). This might imply that the down-regulation of hsa\_circ\_0077755, which is indicative of loss of Cx43 mRNA expression along breast cancer initiation [7], relieves its sponging activity on miR-182 causing an upregulation in its expression, which in turn acts as an oncogene and primers tumor initiation as mentioned earlier [255-257]. In addition, survival analysis for miR-182 in 460 patients with grade II breast tumors showed that miR-182 seems to associate with poor prognosis when up-regulated (**Fig. 8c**) However, when performed on 395 patients with grade III breast tumors with the exact characteristics, survival analysis revealed that miR-182 seems to associate with poor prognosis when down-regulated in grade III tumors (**Fig. 8d**) [252]. Interestingly, low levels of Cx43 in the primary breast tumors at initial stages associate with poor prognosis [25], while high levels of Cx43 in breast cancer patient biopsies at later tumor stages is associated with poor prognosis and is suggestive of enhanced tumor progression and invasion [258]. This is since the tumor epithelial cells reactivate gap junction intercellular communication with endothelial cells, facilitating intravasation and extravasation in order to invade and metastasize [259]. Thus, Cx43 acts as a tumor suppressor, its loss early during tumorigenesis promotes breast cancer initiation [26] and progression [27] and associates with poor prognosis at early stage of the malignancy. Its re-expression at later tumor stages facilitates invasion and metastasis and associates with poor prognosis [259]. Thus, Cx43 (tumor suppressor) down-regulation and miR-182 (oncogene) up-regulation at early tumorigenic stage seem to associate with poor prognosis

while at later advanced tumoral stages they associate with poor prognosis when Cx43 is up-regulated and hence miR-182 is down-regulated.

## **E. Conclusion**

**Cx43/hsa\_circ\_0077755/miR-182** is the only validated post-transcriptional axis specific to Cx43 loss that might serve as a biomarker predictor of heightened risk of breast cancer initiation (**Fig. 19**). Moreover, **Cx43/hsa\_circ\_0077755/miR-182** axis seems to associate with poor prognosis in early-stage breast cancer when the tumor-suppressor Cx43 (and hence hsa\_circ\_0077755) are down-regulated and the onco-miR, miR-182 is up-regulated. Conversely, it associates with poor prognosis and might predict the risk of enhanced invasion and metastasis at later advanced stages of breast cancer when Cx43 (and hence hsa\_circ\_0077755) are up-regulated and miR-182 is down-regulated. Cx43/hsa\_circ\_0077755/miR-182 dysregulation patterns might thus predict prognosis along breast cancer initiation and progression. We previously proposed a possible biomarker signature of Cx43 mRNA-circRNAs-miRNAs axes for detection and prevention of early-onset breast cancer [7], which parallel roles that Cx43 plays along breast tumorigenesis. Here, we confirm the involvement of Cx43 in post-transcriptional regulatory axes in breast cancer initiation, match the miRNA dysregulation pattern to an early-stage young breast cancer patient cohort and propose **Cx43/hsa\_circ\_0077755/miR-182** as a biomarker axis of heightened risk of breast cancer initiation.



## **F. Limitations and future directions**

CircRNAs can sponge tens of different miRNAs, and each miRNA can target hundreds of mRNAs, and hence might affect multiple downstream functional pathways [83, 245, 260]. Thus, it is expected that other pathways might be implicated in the chosen validated axes. However, the 3D culture model that recapitulates heightened risks for cancer development helped us narrow-down these pathways to those downstream (or parallel) to Cx43 loss, since the two cell lines are identical, except for silencing Cx43 (through shRNA). Thus i) by using this breast cancer risk progression culture model and ii) by only choosing miRNAs that matched miRNAs from microarrays of early-stage young Lebanese breast cancer population (that are at most heightened risk of developing this early malignancy in the world [2]), circRNAs and miRNAs selection was carefully chosen to represent what might be reflected in heightened-risk of breast tumors initiation. Future studies should validate this axis in sera of breast cancer-free controls and those at risk and in early-stage and advanced-stage breast cancer patients to test their potential role as noninvasive biomarkers of risk-assessment of initiation and prognosis, respectively.

## **G. Materials and Methods**

### ***1. Three-dimensional cell culture***

Nontumorigenic HMT-3522 S1 (S1) human breast epithelial cells [239] between passages 52 and 60, were routinely maintained as a monolayer on plastic (2D culture) in chemically defined serum-free H14 medium [242, 261] at 37 °C and 5% CO<sub>2</sub> in a humidified

incubator. H14 medium was changed every 2–3 days. For 2D cultures, cells were plated on plastic substrata at a density of  $2.3 \times 10^4$  cells/cm<sup>2</sup>. The drip method of 3D culture was used to induce the formation of acini. Briefly, cells were plated on Matrigel™ (50 µl/cm<sup>2</sup>; BD Biosciences, 354234) at a density of  $4.2 \times 10^4$  cells/cm<sup>2</sup> in the presence of culture medium containing 5% Matrigel™ [242, 262]. The EGF was omitted from the culture medium after day 7 to allow completion of acinar differentiation (usually observed on day 8 or 9) [242]. Cx43 was down-regulated in S1 cells via retroviral delivery of shRNA, as described by Bazzoun et al. [26].

## **2. Total RNA isolation and quality control (QC)**

Total RNA from cells in 3D culture was extracted using TRIzol reagent (Invitrogen, Carlsbad, CA, USA) following the manufacturer's protocol. Purity and concentration of RNA samples were examined spectrophotometrically by absorbance measurements at 260, 280 and 230 nm using the NanoDrop ND-1000 (Thermo Fisher Scientific, Wilmington, DE, USA). OD260/OD280 ratios between 1.8 and 2.1 were deemed acceptable. *Note, same biological 3D culture samples were used for both the 96ircRNAs microarrays and the miRNA sequencing to insure consistency.*

## **3. Sample Preparation and hybridization for circRNAs microarrays**

Sample labeling, and array hybridization were performed according to the manufacturer's protocol (Arraystar Inc.). Briefly, total RNAs were digested with RNase R (Epicentre, Inc.) to

remove linear RNAs and enrich circRNAs. Then, the enriched circRNAs were amplified and transcribed into fluorescent cRNA utilizing a random priming method (Arraystar Super RNA Labeling Kit; Arraystar). Labeled cRNAs were purified by RNeasy Mini Kit (Qiagen). Concentration and specific activity of labeled cRNAs (pmol Cy3/ $\mu\text{g}$  cRNA) were measured by NanoDrop ND-1000. One  $\mu\text{g}$  of each labeled cRNA was fragmented by adding 5  $\mu\text{l}$  10X Blocking Agent and 1  $\mu\text{l}$  of 25X Fragmentation Buffer, then the mixture was heated at 60 °C for 30 min, finally 25  $\mu\text{l}$  2X Hybridization Buffer was added to dilute the labeled cRNA. 50  $\mu\text{l}$  of Hybridization Buffer was dispensed into the gasket slide and assembled to the circRNA expression microarray slide. Slides were incubated for 17 hours at 65°C in an Agilent Hybridization Oven.

#### ***4. Data Processing and Analysis for circRNAs microarrays***

Agilent Feature Extraction software (version 11.0.1.1) was used to analyze acquired array images. Quantile normalization and subsequent data processing were performed using the R software Limma package. Differentially expressed circRNAs with statistical significance between Cx43-KO-S1 and S1 cells were identified through Volcano Plot filtering and Fold Change (i.e. the ratio of the group averages) filtering. The statistical significance was estimated by t-test. circRNAs having fold changes  $\geq 2$  and p-values  $\leq 0.05$  were selected as the significantly differentially expressed. Hierarchical Clustering was performed to show the distinguishable circRNAs expression pattern among samples.

## **5. Annotation for 98ircRNAs/miRNA Interaction**

The 98ircRNAs/microRNA interaction was predicted with Arraystar's home-made miRNA target prediction software based on *TargetScan* [246] & *miRanda* [247] functions, and the differentially expressed circRNAs within all the comparisons were annotated in detail with the 98ircRNAs/miRNA interaction information. *Note: CircRNA sequences were predicted by bioinformatics methods following the approach by Salzman et al. [244].*

## **6. miRNA Library Preparation and Sequencing**

Triplicate samples of S1 cells and triplicates of Cx43-KO-S1 cells were submitted for small RNA-seq. The Purdue Genomics Facility prepared libraries using the NEXTflex Illumina Small RNA Sequencing Kit v3 (Bioo, Austin, TX) with barcoding performed using UDI primers. A total of 15 PCR cycles were performed. 2x50 bp reads were sequenced using the NovaSeq6000. Only one of each read pair was used for analyses, given the short size of miRNAs. Library preparation protocols were modified for the use of unique dual indexes, in order to circumvent index hopping on the Illumina NovaSeq 6000. Before library preparation the RNA quality was checked using an Agilent Nano RNA Chip.

## **7. Heatmap of miRNAs from the breast epithelia that are in common with the MREs sponged by the significant circRNAs**

Counts for miRNAs were obtained using miRNA-seq on a NovaSeq 6000. Data were normalized using DESeq2 [263] and then, the log<sub>2</sub> of 1+ the normalized counts was scaled by row. Rows were clustered using hierarchical clustering and were annotated with the direction (up- or down-regulation) of the associated circRNAs in Cx43 KO S1 samples versus S1 control sample. Cutoff points were set for Fold Change > 2 and p.adjusted value ≤ 0.05.

#### **8. *Functional enrichment of mRNAs associated with 99ircRNAs binding miRNAs***

A functional enrichment analysis was performed in Ingenuity Pathway Analysis (IPA®, QIAGEN Redwood City, [www.qiagen.com/ingenuity](http://www.qiagen.com/ingenuity)) of predicted target mRNAs (predicted by TargetScan) for the top five predicted sponged miRNAs associated with the chosen circRNAs. Due to the high number of predicted mRNA targets for each miRNA, only mRNAs with strong predicted (based on the cumulative weighted context score of -0.4 or lower [109]) or experimental evidence were kept in the analysis. Limiting the number of mRNA targets in this way allows for quantification of the significance of the enrichment via a hypergeometric distribution. An enrichment test was performed to determine which biological functions or diseases associated with mRNA targets are observed in association with these mRNAs more often than we would expect by chance.

#### **9. *RT-qPCR validation of chosen circRNAs (and selection of candidate circRNAs) and divergent primer design***

To validate the expression profiles of circRNAs in four replicates of 3D acini of Cx43-KO-S1 versus S1 cells, QuantiTect® Reverse Transcription Kit (Qiagen cat # 205311) was used for cDNA Synthesis for 1 µg of RNA per sample according to manufacturer's protocol (but optimized for the last steps as follows: after the addition of the RNA samples to the reverse-transcription master mix, the reaction (25 µl per reaction) was incubated at 25°C, 10 min, then at 50°C, 30 min, then at 85°C, 5 min). Specific primers (left and right) for each circRNAs were designed using Circular RNA Interactome built-in divergent primer design tool (based on Primer3 Output) [83] and purchased from Eurofins Genomics (Canada) and were used for the first strand synthesis. 18S ribosomal RNA (TIB Molbiol product no. 1945400 and 1945401) was used as an endogenous control. Real time quantitative polymerase chain reaction (RT-qPCR) was performed as follows: cDNA product was diluted with 75 µl RNase free water. PCR was conducted in a 20-µl reaction volume consisting of the following: 4.0 µl diluted cDNA, 4 µl (total left and right circRNAs primer), 2 µl RNase free water, and 10 µl SYBR® Green JumpStart™ Taq ReadyMix™ (SIGMA S4438). The RT-qPCR reaction was performed using BioRad CFX96 Real Time System, C1000 Thermal Cycler (Germany) as follows: initial denaturation at 95 °C for 5 min, 40 cycles of amplification at 95 °C for 15 sec, annealing and extension at 60 °C for 1 min. Using the  $\Delta\Delta Cq$  equation, relative expression of the experimental circRNA was determined in the Cx43-KO-S1 samples compared to S1 samples using 18S ribosomal RNA as an endogenous control. Normalization of Cx43-KO-S1 samples was based on S1 samples. Statistical analysis was performed using Prism GraphPad software. One-tailed

unpaired t-test was used to compare the circRNA expression in the Cx43-KO-S1 samples versus S1 samples. A p-value < 0.05 was considered statistically significant.

### ***10. Cytoscape analysis***

CircRNA-miRNA-mRNA gene co-expression network was predicted based on sequence-pairing using Cytoscape software (<https://cytoscape.org>). The top four predicted miRNAs (MREs) associated with circRNAs were used to predict mRNA targets by TargetScan within IPA. Only mRNAs involved in cancer-related pathways and shown to be targets experimentally or else high confidence predictions by TargetScan were kept. Cytoscape was used to draw circRNA-miRNA-mRNA interaction networks.

## CHAPTER VI

### MIR-183 AND MIR-492 OVEREXPRESSION TRIGGER INVASION, PROLIFERATION AND LOSS OF POLARITY IN NON-NEOPLASTIC BREAST EPITHELIUM AND IS REPORTED IN EARLY BREAST CANCER PATIENTS

#### A. Abstract

The master gene regulators, microRNAs (miRNAs), exhibit unique dysregulation signatures in cancers, are stable and abundant in body fluids and act as attractive novel noninvasive cancer biomarkers. We performed miRNA-sequencing on 3D acini of a HMT-3522 S1 (S1) breast epithelial risk-progression culture model. Recent studies showed that nontumorigenic S1 cells form a fully polarized epithelium while pretumorigenic counterparts silenced for gap junction Cx43 (Cx43-KO-S1) lose epithelial polarity, multilayer, exhibit proliferative and invasion potential and mimic tumor-initiated *in vivo* mammary epithelial morphology. miRNA sequencing in the cultured epithelial revealed 65 miRNAs that were significantly dysregulated in response to Cx43 silencing. A comparative analysis between the detected miRNAs and 15 tumor-associated miRNAs involved in epithelial polarity disruption from young Lebanese patient cohort was performed. miR-183 was upregulated upon Cx43 loss in the cultured epithelia, was the most up-regulated miRNA in early-stage Lebanese breast cancer patients (and matched US patients) and its up-regulation conferred with the increased risk of cancer progression in the 3D culture model. miR-492 was up-regulated in tumor-associated patient miRNAs involved in epithelial polarity but was not specific to Cx43 loss. Therefore,



ectopic over-expression of miR-183 and miR-492 in nontumorigenic S1 cells through pLenti-III-miR-GFP tagged vectors was performed. The results revealed that over-expression of both miR-183 and miR-492 in nontumorigenic S1 cells resulted in cells formation of larger acini in 3D cultures, devoid of lumen assembly, with disrupted epithelial polarity observed through mislocalization of  $\beta$ -catenin and Scrib's apico-lateral distribution and Cx43's apical distribution. It also triggers enhanced proliferation and invasion capacity, hence recapitulating tumor-initiation phenotypes seen upon Cx43 loss. These tumor-initiation phenotypes seem to be attributed to Scrib's loss (by miR-183) and mis-localization (by miR-492) and through altering the apico-lateral localization of Cx43 and  $\beta$ -catenin. Moreover, miR-183 and miR-492 over-expression might in part affect polarity disruption in a gap junctional dependent manner, through the mislocalization of Cx43 from apical membrane domains in aggregates formed in 3D culture, but not through directly down-regulating Cx43 expression. Therefore, miR-183-5p and miR-492 over-expression in non-neoplastic cells recapitulates tumor-initiation phenotypes observed upon the loss of Cx43.

## **B. Introduction**

Breast cancer is the most common malignancy in Lebanon representing 40.8% and 26.7% of all cancer incidences and mortality, respectively, with the higher incidence in the world for women below the age of 40 [2]. Despite the availability of therapeutic options, poor survival rate and early onset in women make breast cancer a public health concern. These women have low

prevalence of deleterious *BRCA* mutations [3] and present with poor prognosis and aggressive phenotypes due to the lack of diagnostic methods at such an early age [230]. An increased incidence of breast cancer in young women is increasing worldwide [2, 4, 5]. This study brings initial information of the involvement of miRNAs associated with morphological disruptions of the breast epithelium/acini and identified in young women with breast cancer with highest risk of the early malignancy by triggering cancer-initiation phenotypes.

The mammary gland development, differentiation and tumorigenesis is dependent on gap junction organization and proper communication. Gap junction intercellular communication (GJIC) is mediated by transmembrane proteins, called connexins (Cxs) that allow the intercellular exchange of ions, second messengers and metabolites between adjacent cells [16-19]. Cx43, the focus of our previous and current research studies [7, 20, 21] plays essential roles during mammary gland development [22, 23] and differentiation [24] and acts as a tumor suppressor [20, 21, 25]. Its loss and mislocalization influence breast cancer initiation [26], progression [27], increase risk of breast cancer development in overweight women [231, 232] and is associated with markers of poor prognosis, increased metastasis and poor survival in breast cancer patients [25]. We recently showed that Cx43 functions via PI3 Kinase and noncanonical Wnt signaling pathways in priming the breast epithelium for neoplastic behavior [26, 27]. The nontumorigenic luminal human breast epithelial HMT-3522 S1 (S1) cell line, cultured under three-dimensional (3D) conditions, forms growth-arrested and basoapically polarized acini with a central lumen and apicolateral localization of Cx43. Hence S1 cells

recapitulate normal human breast tissue architecture [26]. Silencing Cx43 expression in these nontumorigenic S1 cells via Cx43-shRNA (Cx43-KO-S1) resulted in cell cycle entry, perturbed apical polarity, mitotic spindle misorientation and loss of lumen, causing cell multilayering [26] and priming cells for enhanced motility and invasion [26, 27]. These phenotypic features observed in Cx43-KO-S1 acini represent architectural and phenotypical premalignant mammary lesions, like those observed in ductal hyperplasia in a murine model [28], which increase the risk of breast cancer initiation, thus marking Cx43-KO-S1 as pretumorigenic culture model. Therefore, this 3D risk-progression culture model was used to capture key pretumorigenic changes and cancer initiation phenotypes that might be triggered by miRNA players, heightening the risk of breast cancer development.

miRNAs are small (16–29 nucleotides) endogenous, non-coding, single-stranded RNAs that negatively regulate gene expression at the post-transcriptional level [6]. Several miRNAs are ubiquitously expressed in different tissue types cancers, while others might act in a tissue-specific tumor-specific and at tumoral progression stage-specific manners [8]. miRNAs exert their regulatory functions through mostly downregulating their downstream target genes, by interacting with the 3'UTRs of coding genes, and thus affecting downstream signaling pathways [264]. In order to understand the mechanisms that underlie heightened risk of early breast cancer, preliminary results from the Lebanese population was essential for such investigations. Nassar et al. [29] previously identified 74 dysregulated miRNAs in microarrays from 45 invasive ductal

carcinoma (IDC) versus 17 normal adjacent breast tissues from the Lebanese population (Fold Change > 2) and compared their profile to 197 American breast cancer patients and 87 normal samples from TCGA (The Cancer Genome Atlas) [29]. All the Lebanese patient cohort were estrogen receptor (ER) positive, 97.8% were progesterone receptor (PR) positive and 24.5% had human epidermal growth factor receptor 2 (HER2) over-expression. The majority of the tumors were of grade 2, and half of them presented with lymph node involvement. Moreover, 42.2% were below the age of 40 and none of the patients had distant metastasis, thus this cohort was categorized into early-stage breast cancers. We recently uncovered among these miRNAs through a comprehensive literature review fifteen tumor-associated miRNAs involved in early events of breast tumorigenesis that contribute to loss of acinar morphogenesis [104, 248-251] (Naser Al Deen et al., 2020 submitted). Moreover, the group performed mRNA microarray on young patients below the age of 40. All dysregulated patient mRNAs were mainly involved in cancer-related pathways, cellular growth, proliferation and movement as predicted by Ingenuity Pathway Analysis (IPA) [29]. The mRNA data further classified these patients into the more aggressive Luminal B subtype of ER+ breast cancer that associates with a risk of early relapse.

We therefore performed miRNA sequencing analysis on Cx43-KO-S1 cells as compared to S1 cells and detected 65 miRNAs that were dysregulated as a result of Cx43 loss. We next performed comparative analysis of these dysregulated miRNAs relative to tumor-associated miRNAs from the young Lebanese early breast cancer patient cohort [29] that were implicated in

epithelial polarity loss (Naser AL Deen et al. 2020, submitted), in order to select candidate miRNAs that might recapitulate tumor-initiation phenotypes seen upon Cx43 loss [26, 27]. **miR-183** (downstream of Cx43 loss and commonly upregulated in patient cohort and the breast epithelia) and **miR-492** (not attributed to Cx43 loss, and only up-regulated in the young Lebanese patients) were chosen to be over-expressed in the nontumorigenic S1 cells. Most previous studies introduced miRNA mimics or inhibitors to breast cancer cell lines to trigger cancer-initiation phenotypes [230, 265-269]. Our study introduced stable delivery of miRNAs in **non-neoplastic cells**, and revealed **tumor initiation phenotypes**, similar to those we reported previously upon Cx43 loss

## C. Results

### *1. Comparative analysis from miRNomes of a breast epithelial 3D risk-progression culture model and a young early-stage patient cohort lead to the selection of miR-183 and miR-492 for investigation in the nontumorigenic S1 cells*

Triplicates of pretumorigenic Cx43-KO-S1 cells and nontumorigenic S1 counterparts in 3D drip culture were prepared for miRNA sequencing in the presence of Matrigel™ over 11 days to induce the formation of acinus-like structures. miRNA sequencing revealed 29 significantly up-regulated (44.6%) and 36 significantly down-regulated (55.4%) mature miRNAs in response to Cx43 silencing in the cultured epithelia. Heatmap of hierarchical cluster analysis was used to depict all the differentially expressed miRNAs in Cx43-KO-S1 cells compared to S1 cells (Fold

Change > 2 and adjusted p-value < 0.05) (**Fig. 11a**). Next a comparative analysis of these dysregulated miRNAs and tumor-associated miRNAs from young Lebanese patient cohort with early-stage breast cancer (reported by Nassar et al. [29]) was performed, in an attempt to select candidate miRNAs that might recapitulate tumor-initiation phenotypes seen upon the loss of Cx43 in breast epithelial cells [26, 27]. Fifteen tumor-associated miRNAs from the patient cohort exhibited reported involvement in epithelial polarity and cancer-related pathways (Naser Al Deen et al., 2020, submitted), and thus their dysregulation pattern in the risk-progression culture miRNome was tabulated (**Fig. 11b**). Only miRNAs that were up-regulated in patient tissues as compared to normal adjacent tissues and/or in pretumorigenic Cx43-KO-S1 cells as compared to nontumorigenic S1 cells were considered for potential over-expression in the nontumorigenic cells, in an attempt to study the tumor-initiation potential of such tumor-associated miRNAs in the otherwise nonneoplastic cells. miR-183 was the most upregulated in breast cancer patient samples (fold change = 10) as compared to normal adjacent tissues, was also up-regulated in matched US patients (Nassar et al. [29]) and was commonly upregulated as a result of Cx43 loss in Cx43-KO-S1 cells (fold change  $\approx$  1.8) compared to S1 cells. Interestingly, RT-qPCR validation in 2D cultures of the risk-progression series, using RNU6B as an endogenous control, showed that miR-183 expression increased with the increased progression of the series. Meaning, miR-183 was significantly upregulated by 2.5 folds in Cx43-KO-S1 (pretumorigenic) cells and its expression level was further pronounced by 3.5 folds in T4-2 cells (tumorigenic counterparts) as compared to the nontumorigenic S1 cells (**Fig. 11c**). RT-qPCR validation confirmed the up-

regulated of miR-183 in Cx43-KO-S1 cells cultured in 3D conditions as well (fold change = 3) as compared to S1 cells using RNU6B as an endogenous control (**Fig. 11d**). Therefore, **miR-183** was the first chosen miRNA for overexpression in the nontumorigenic cells since it was upregulated upon Cx43 loss, was the most up-regulated miRNA in early-stage Lebanese breast cancer patient cohort (and matched US patients) and its up-regulation conferred with the increased risk of cancer progression in the 3D culture model. We next opted to choose a tumor-associated miRNA that likely was not attributed to Cx43 loss, and thus only focused on the subset of these miRNAs that were not detected in the sequencing results of the cultured epithelia and were up-regulated in the patient miRNome. Only **miR-492** was i) not detected in the cells' miRNome and ii) the only exclusively up-regulated miRNA in the Lebanese early-stage validation cohort (and not in the US patients). The focus on the profiles of this particular validation cohort of early-stage Lebanese patients is that they are notoriously at highest risk of developing breast cancer [2, 29] with an alarming high percentage diagnosed under the age of 40 (22% of cases compared to 6% in Western populations) and a mean age at diagnosis 10 years younger than in Western countries [2]. RT-qPCR further confirmed that miR-492 was not dysregulated in Cx43-KO-S1 cells cultured in 3D conditions as compared to S1 cells using RNU6B as an endogenous control, and thus, was likely not affected by Cx43 loss (**Fig. 11d**). RT-qPCR analyses for one additional up-regulated (miR-182) and one down-regulated (miR-200c) miRNAs confirmed that miR-182 was significantly up-regulated (2.5 folds) in Cx43-KO-S1 compared to S1 cells, while miR-200c was not significantly dysregulated (**Fig. 11d**).

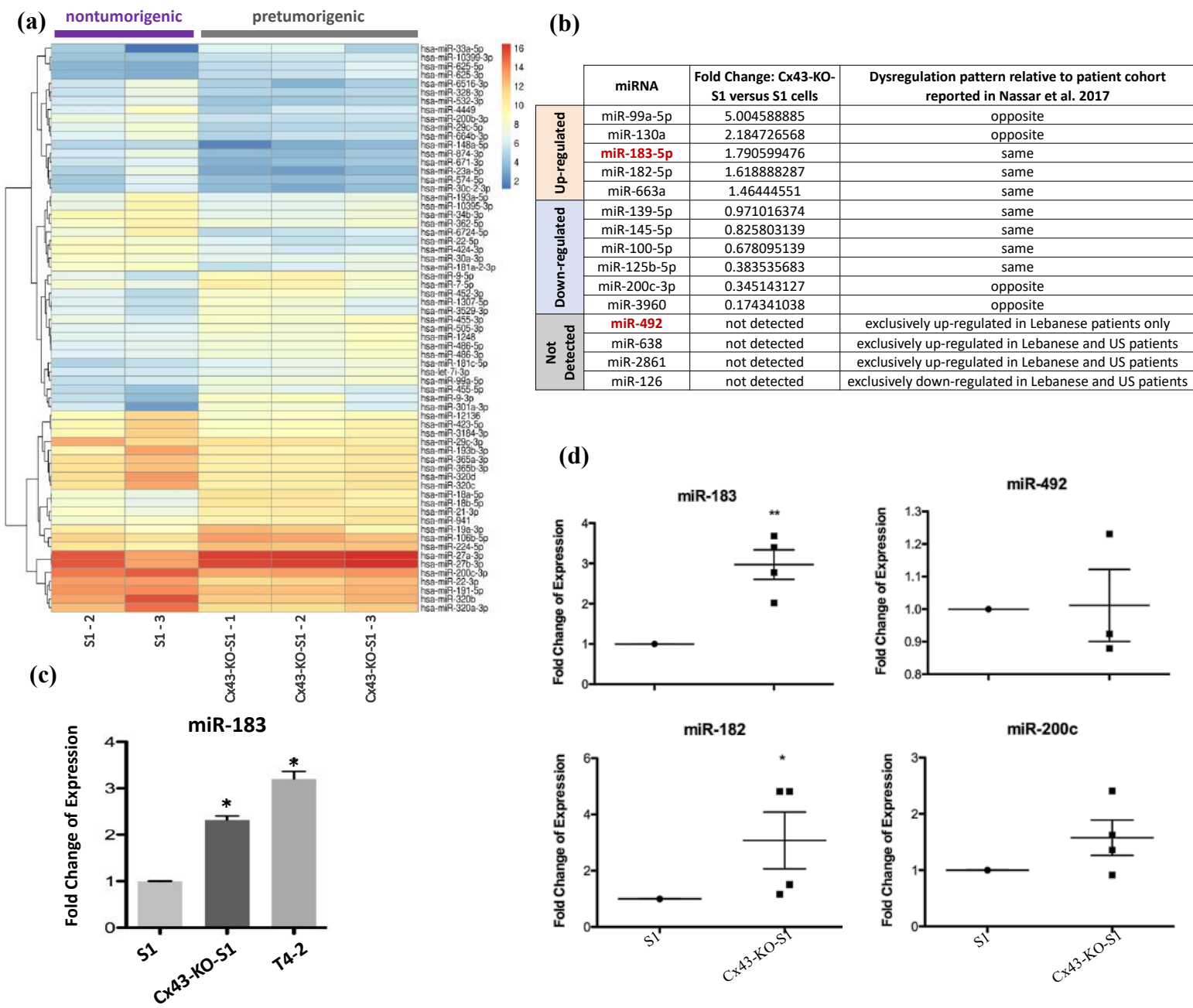


**Figure 11: Comparative analysis from miRNomes of a breast cancer risk-progression 3D culture model and a young early-stage patient cohort and validation of candidate miRNAs. (a) A heatmap of hierarchical cluster analysis revealing a total of 65 significant differentially**

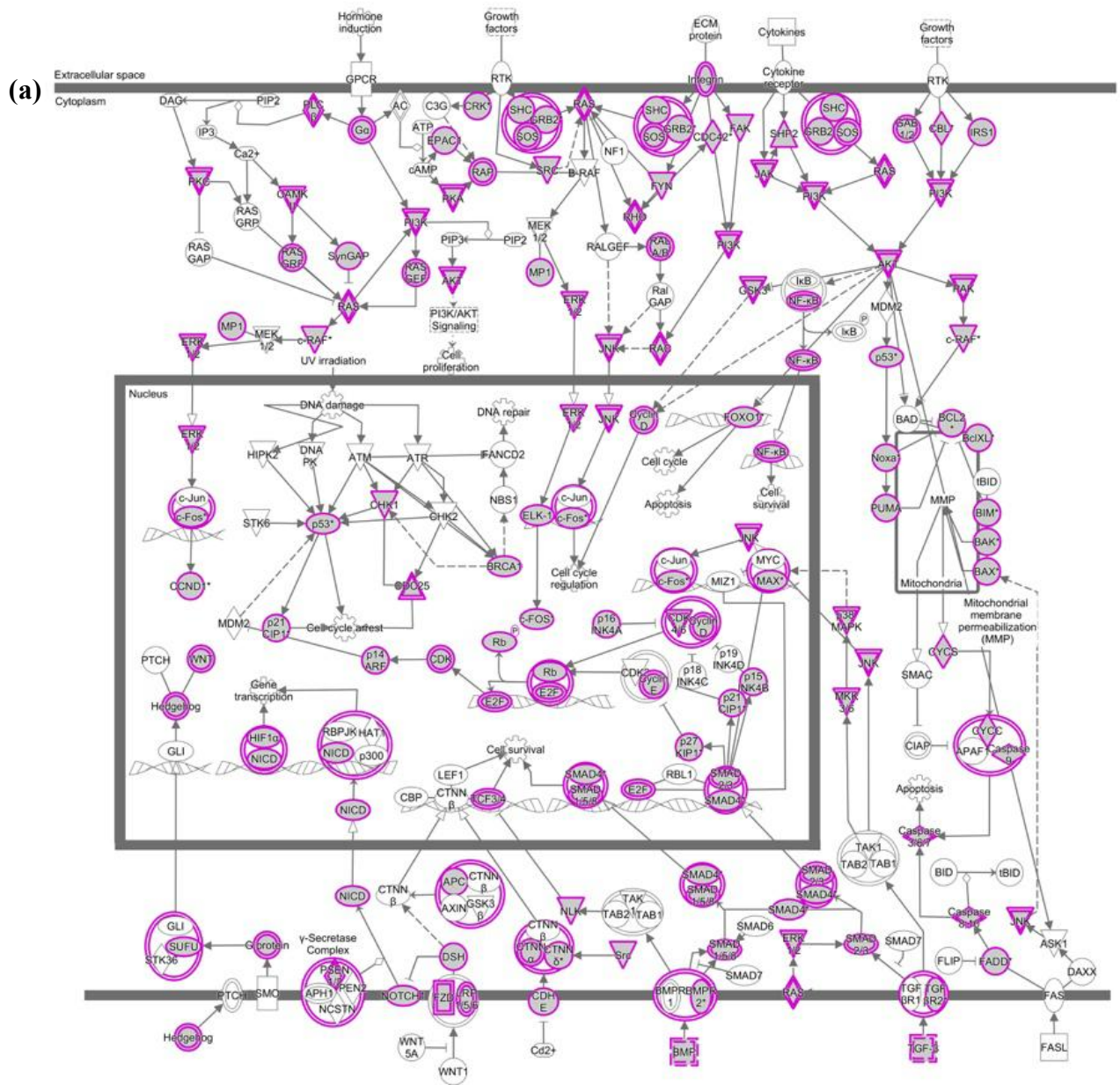


expressed miRNAs (29 upregulated and 36 downregulated) in Cx43-KO-S1 cells compared to S1 cells (Fold Change > 2), attributed to the loss of Cx43. Triplicates of Cx43-KO-S1 and triplicates of S1 cells were plated on Matrigel™ for 11 days. Total RNA was extracted, reverse transcribed and hybridized for sequencing using Illumina's NovaSeq6000. Orange depicts up-regulated miRNAs and blue depicts down-regulated ones in pretumorigenic Cx43-KO-S1 cells compared to nontumorigenic S1 counterparts. **(b) A table** showing the regulation pattern of miRNAs from miRNA sequencing of the 3D culture model as compared to tumor-associated miRNAs from young Lebanese patient cohort with early-stage breast cancer (reported by Nassar et al. (2017)) that are involved in early events of breast tumorigenesis and affect epithelial polarity. Orange highlight panel refers to up-regulated miRNAs and green highlight to down-regulated miRNAs in Cx43-KO-S1 compared to S1 cells. Grey highlights refer to the patient tumor-associated miRNAs that from the list involved in epithelial polarity that were not detected by the cells' miRNA sequencing. **(c) RT-qPCR validation** of miR-183 in the breast epithelial risk progression culture model in 2D cultures shows that miR-183 expression increases with the increased progression of the series (i.e., miR-183 was significantly upregulated by 2.5 folds in Cx43-KO-S1 (pretumorigenic) cells and by 3.5 folds in the tumorigenic counterparts T4-2 cells as compared to the nontumorigenic S1 cells. **(d) RT-qPCR validation** in 3D cultures from four replicates of Cx43-KO-S1 and four replicates of S1 cells plated in Matrigel for 11 days using RNU6B as an endogenous control confirmed that miR-183 and miR-182 were significantly upregulated in Cx43-KO-S1 cells as compared to S1 cells in 3D cultures while miR-200c and miR-492 upregulation was not significant. \*\* denotes a p.value < 0.01, and \* denotes a p.value < 0.05.

## ***2. Functional and gene-set enrichment analyses for the differentially expressed miRNAs in Cx43-KO-S1 compared to S1 cells were enriched in cancer-related pathways***

Of the 65 differentially expressed miRNAs in Cx43-KO-S1 compared to S1 cells, 38 miRNAs (60%) were significantly involved in cancer-related pathways. Using experimentally validated results from Ingenuity Pathway Analysis (IPA), molecular mechanisms of cancer canonical pathways were the most significantly enriched pathways in the miRNAs that were dysregulated in Cx43-KO-S1 cells compared to S1 cells. As a result of Cx43 loss (**Fig. 12a**).

Furthermore, functional enrichment analysis performed in IPA of predicted target mRNAs (by TargetScan) for the top 20 enriched pathways for all dysregulated miRNAs in Cx43-KO-S1 cells compared to S1 cells revealed that molecular mechanisms of cancer, Protein Kinase A signaling, ERK/MAPK signaling, signaling by Rho GTPases, inflammation by IL-8 signaling and regulation of epithelial to mesenchymal transition (EMT) were among the most enriched pathways in the differentially expressed miRNAs upon Cx43 loss (**Fig. 12b**).



(b)

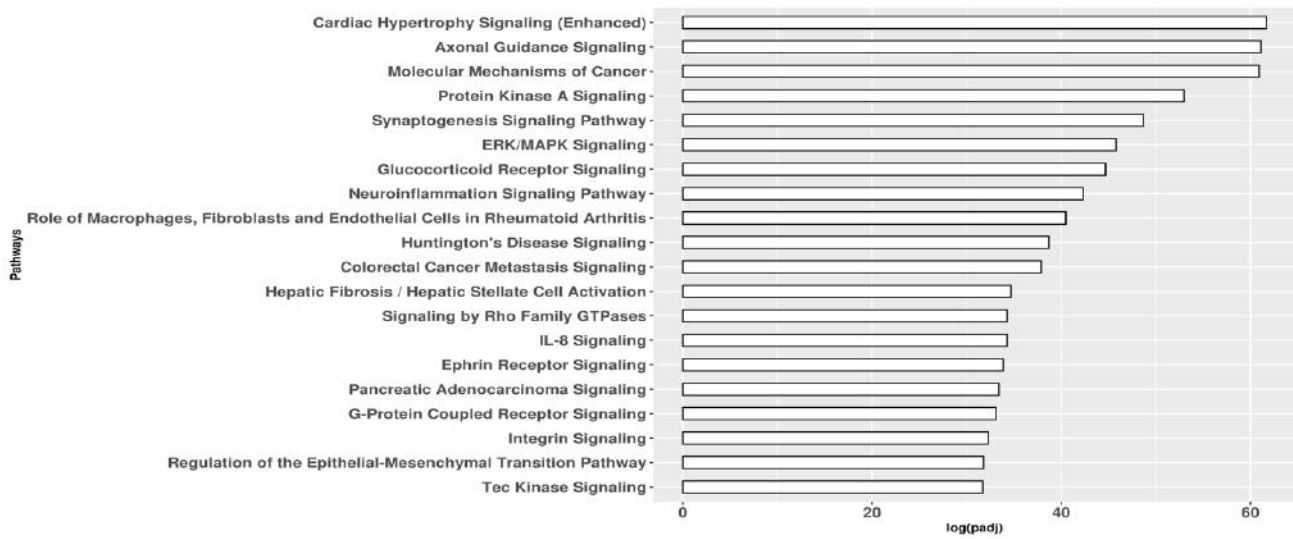


**Figure 12: Functional and gene-set enrichment analyses for differentially expressed miRNAs in (pretumorigenic) Cx43-KO-S1 compared to (nontumorigenic) S1 cells.** (a) Using Ingenuity Pathway Analysis (IPA), molecular mechanisms of cancer canonical pathway was the most significantly enriched pathway in Cx43-KO-S1 cells compared to S1 cells. Colored nodes indicate mRNA targets of miRNAs which were significantly differentially expressed in the comparison. (b) Functional enrichment analysis performed in IPA of predicted target mRNAs (by TargetScan) for the top 20 enriched pathways for all dysregulated miRNAs in Cx43-KO-S1 cells compared to S1 cells revealed mostly pathways in cancer. The y-axis shows the enriched canonical pathway and the x-axis shows the  $\log_{10}$  adjusted p-value, which was adjusted for multiple comparisons using the Benjamini-Hochberg method.

**3. miR-183 and miR-492 were stably over-expressed in nontumorigenic S1 cells using pLenti-III-miR-GPF tagged vectors**

The pLenti-III-miR-GPF tagged plasmids from ABM (Canada) were used to generate stable vectors of the mature miR-183-5p and miR-492 miRNAs, and pLenti-miR-control (empty vector) was used as a control, all exhibiting kanamycin resistance in bacterial culture and

puromycin resistance when infected in human cells. Infection and selection of plenti-miR-183-5p, of plenti-miR-492 and of plenti-miR-Control in S1 cells was assessed by the increased efficiency of GFP labeled cells, implying successful over-expression over time through fluorescent microscopy (**Fig. 13a**). Infection was repeated with polybrene 3 times on days 4, 5, and 6 of culture, and puromycin treatment was started 72 hours after the last day of infection. Puromycin killing curve showed that concentration of 0.5 ug/ul of Puromycin was optimal for selecting the infected cells. RT-qPCR quantification confirmed that over-expressing miR-183 in S1 cells significantly upregulated the expression of miR-183 by an average of 32 folds while miR-492 over-expression in S1 cells was significantly achieved with an average of 6 fold increase in three separate replicates as compared to un-infected S1 controls and pLenti-miR-control infected S1 cells in 3D cultures using RNU6B as an endogenous control (**Fig. 13b**).

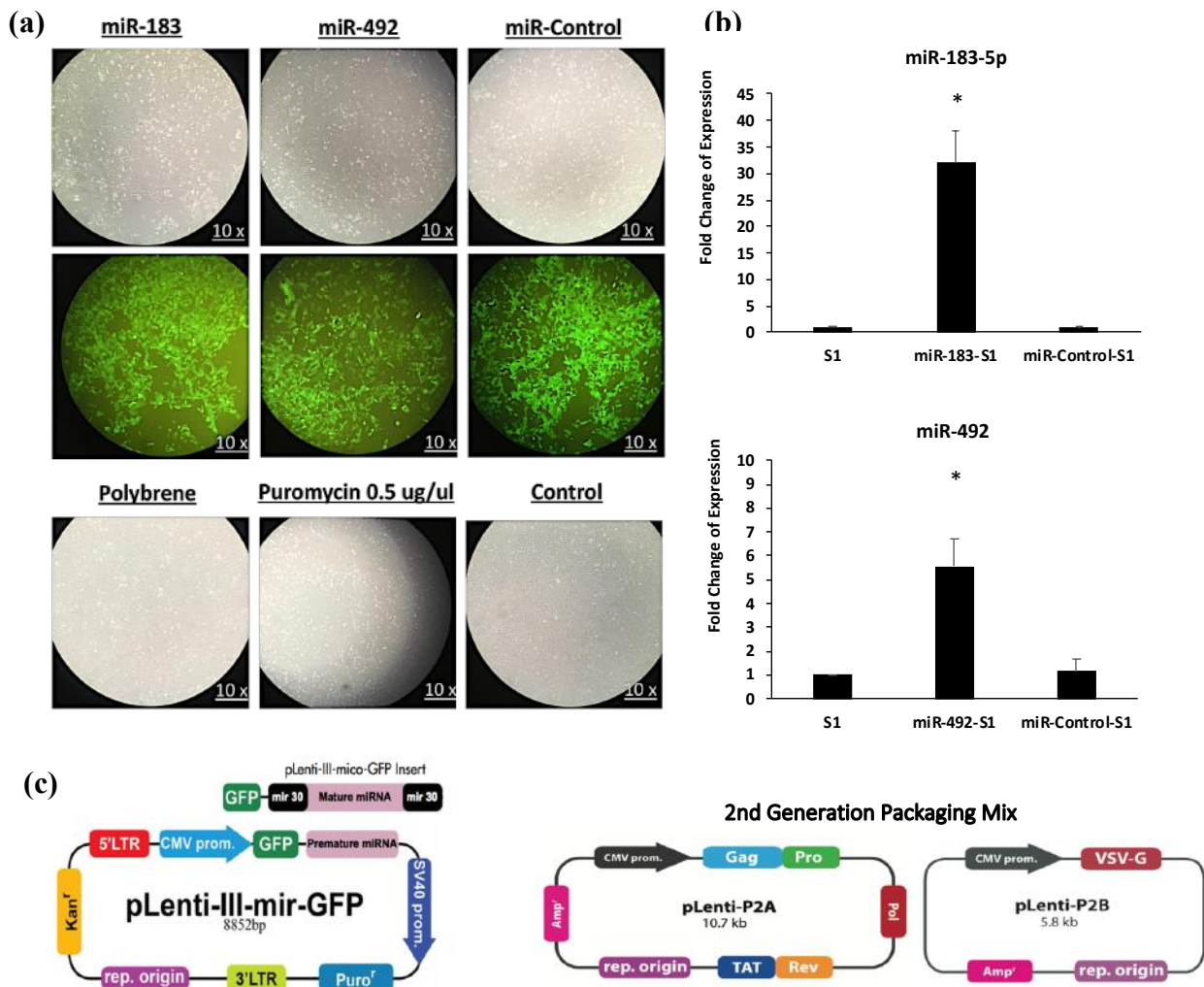
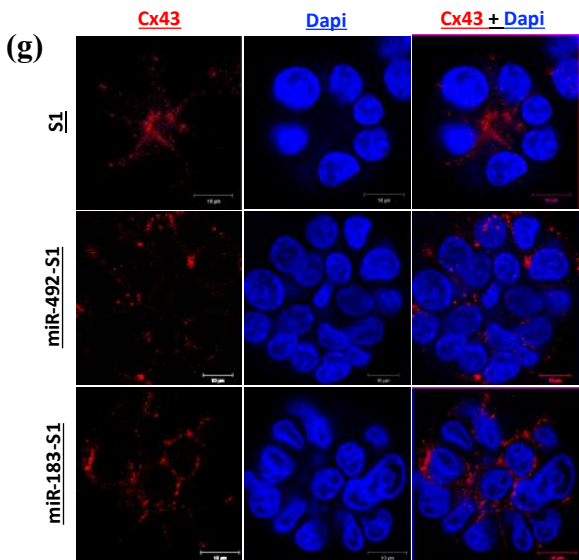
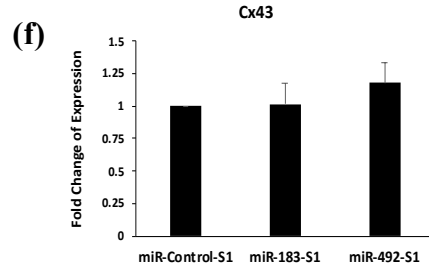
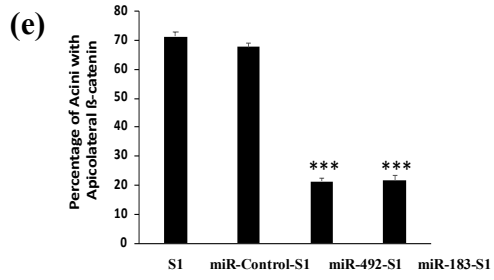
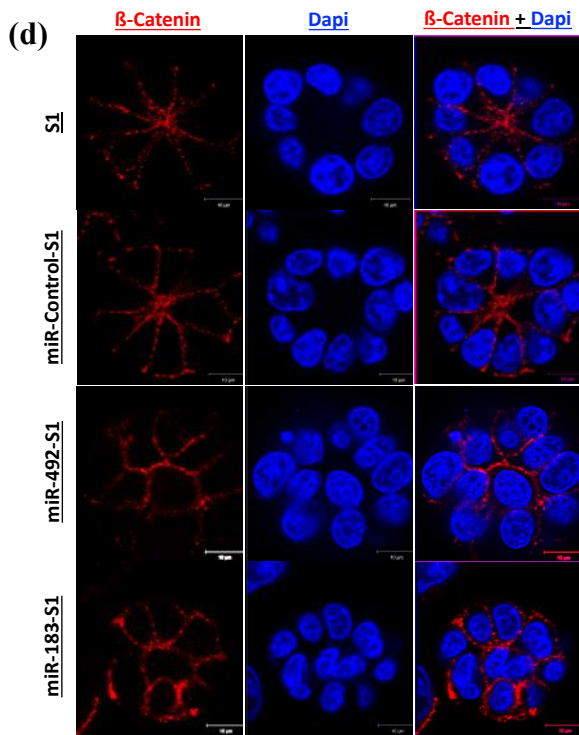
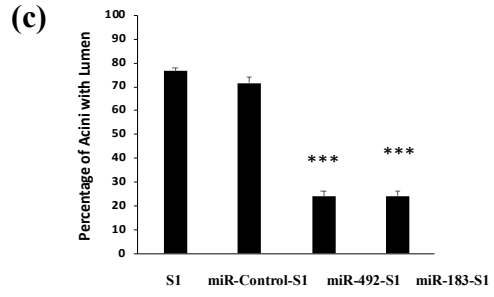
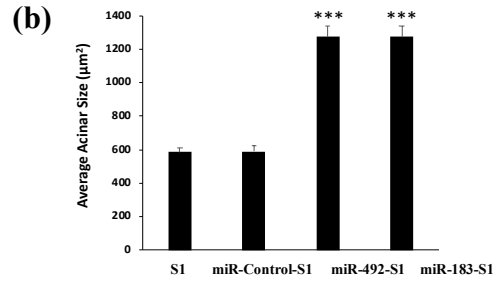
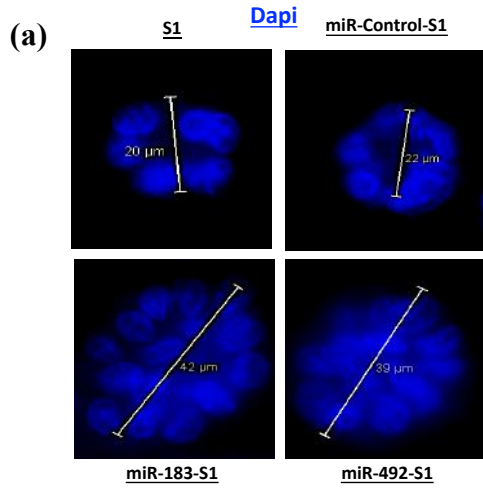


**Figure 13: Stable over-expression of miR-183 and miR-492 in nontumorigenic S1 cells using pLenti-III-miR-GPF tagged vectors.** (a) microscopy images showing the successful pLenti-III-miR-GPF viral infection in both miR-183-S1 and miR-492-S1 infected cells on day 25 in culture (16 days post-puromycin treatment). pLenti-miR-control (empty vector) was used as a control. Puromycin killing curve showed that concentration of 0.5 ug/ul of Puromycin was optimal for selecting the infected cells. (b) RT-qPCR quantification showed that over-expressing miR-183 in S1 cells through pLenti-III-miR-183-GPF significantly upregulated the expression of miR-183 by 32 average folds while miR-492 over-expression in S1 cells was significantly achieved with a 6 folds average increase in three different replicates as compared to un-infected S1 controls and pLenti-miR-control infected S1 cells in 3D cultures using RNU6B as an endogenous control. \* denotes a p.value < 0.05 for Cx43-KO-S1 versus S1 cells using one-tailed unpaired T-test. (c) The map specific to pLenti-III-miR-GPF tagged vectors from ABM (Canada) used to generate lenti-miR-183, lenti-miR-492, and lenti-miR-control (empty vector) with kanamycin resistance in bacterial culture and puromycin resistance when infected in human cells (left panel) and the map of the 2<sup>nd</sup> Generation Packaging Mix used with the amphoteric 293T cells to package the viruses.

**4. *Over-expression of miR-183-S1 and miR-492-S1 in S1 cells disrupts epithelial polarity, causes loss in lumen assembly, increases acinar sizes and alters the localization of junctional and polarity proteins***

S1 nontumorigenic cells [239] have been used in 3D cell culture, in the presence of Matrigel, as a model of phenotypically normal differentiation of breast luminal epithelium [240, 241], forming a fully polarized epithelium [242, 243]. Previous work has shown that Cx43 drives apical polarity *in vivo*, and that it controls the distribution of tight junction proteins and of adherens junction component  $\beta$ -catenin [26]. Its loss is associated with cell multilayering and polarity disruption as reported in the S1 cells silenced for Cx43 and in archival biopsy tissue samples [26]. This *in vitro* 3D risk-progression culture model was used to study the effect of candidate tumor-associated miRNAs over-expression (miR-183 and miR-492) on the otherwise

phenotypically polarized S1 cells. The results revealed that over-expressing both miR-183 and miR-492 resulted in larger acini when cultured in Matrigel with an average size of  $\approx 1300 \mu\text{m}^2$  compared to  $\approx 590 \mu\text{m}^2$  in S1 and miR-Control-S1 cells (**Fig. 14 a & b**). The larger acini in miR-183-S1 and miR-492-S1 cells were also devoid of lumen formation (and showed cell multi-layering), with only 24% of acini forming a lumen, compared to 71.5% in miR-Control-S1 cells and 76% in S1 cells (**Fig. 14 a & c**). Over-expression of miR-183 and miR-492 in S1 cells resulted in disruption of the apicolateral distribution of the adherens junction component  $\beta$ -catenin with only 20% of the acini exhibiting apico-lateral distribution compared to 70% in S1 cells (**Fig. 14 d & e**), similar to what was previously reported in the Cx43-KO-S1 cells [26, 27]. To check whether miR-183 and miR-492 might be causing the disruption of polarity in S1 cells via Cx43 loss, cells were stained for Cx43 and RT-qPCR validation for Cx43 mRNA levels of miR-183-S1 and miR-492 S1 cells in 3D culture was performed using GAPDH as an endogenous control. The results revealed non effect on the mRNA levels of Cx43 in miR-183-S1 and miR-492-S1 cells as compared to miR-Control-S1 cells (**Fig. 14f**). However, alteration in the apical localization of Cx43 in both miR-183-S1 and miR-492-S1 cells as compared to the phenotypically normal S1 cells was observed (**Fig. 14g**). Previous results showed that total levels of Scrib, a key regulator of apical polarity in epithelia, were not altered in Cx43-KO-S1 cells under 2D and 3D conditions, while its apicolateral distribution was altered in Cx43-KO-S1 under 3D conditions [26, 27]. Here, Scrib apicolateral distribution was altered in the miR-492-S1 cells, while it was not detected entirely in the miR-183-S1 cells as compared to S1 cells (**Fig. 14h**).



117

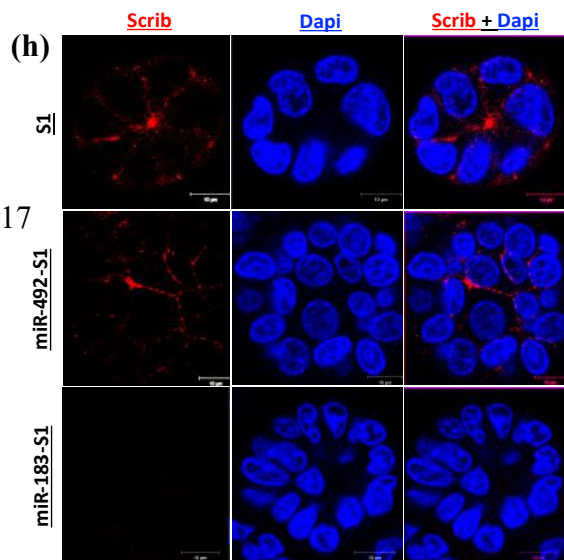


**Figure 14: Immunofluorescence (IF) staining characterizing the (nontumorigenic) S1 cells upon miR-183 and miR-492 over-expression as compared to control S1 cells infected with miRNA empty vectors and un-infected S1 cells.** (a) Representative images of each of the cell lines with their acinar diameter (b) and bar graph showing sizes reported as acinar areas ( $\mu\text{m}^2$ ) and (c) scored for the presence/absence of lumen formation. Size measurements and scoring was taken from at least 100 acini across 12 regions. (d) Localization of  $\beta$ -catenin (red) with nuclei counterstained with Dapi (blue) and (e) scoring for acini with apico-lateral  $\beta$ -catenin distribution, reported as percentages. (f) RT-qPCR validation for Cx43 mRNA levels in 3D cultures from three replicates of miR-183-S1 and miR-492 S1 cells was performed in comparison to miR-Control-S1 cells using GAPDH as an endogenous control. (g) Localization of Cx43 (red) and (h) Scrib (red) with nuclei counterstained with Dapi (blue). \*\*\* denotes a p.value < 0.001, \*\* denotes a p.value < 0.01 and \* denotes a p.value < 0.05 by unpaired *t*-test.

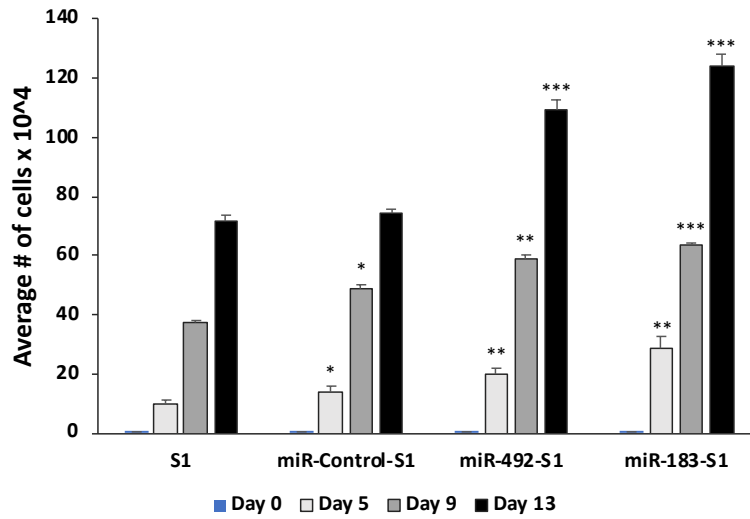
### ***5. Over-expressing miR-183 and miR-492 in nontumorigenic S1 cells resulted in significant enhanced proliferation and invasion potential***

The 2D cultures of miR-183-S1 cells revealed a significant increase in cell counts, by 188%, 69% and 73% on days 5, 9 and 13, respectively, compared to control cells and for and miR-492-S1 cells revealed a significant increase in cell counts, by 102%, 56.5% and 52% on days 5, 9 and 13, respectively, while miR-Control-S1 cells only revealed a significant increase in cell counts, by 37% and 30% on days 5 and 9 and 13, respectively, but by day 13 (after cells become quiescent), there was no significant difference in the cell count between miR-Control-S1 cells and S1 cells (**Fig. 15a**). The number of dead cells was negligible and did not differ between the two groups at the different time points (data not shown). In addition, in transwell cell invasion assay, miR-183-S1 cells showed a significant increase of 2.56 folds in the number of Matrigel-invading cells and miR-492-S1 cells showed a significant increase of 2 folds in the

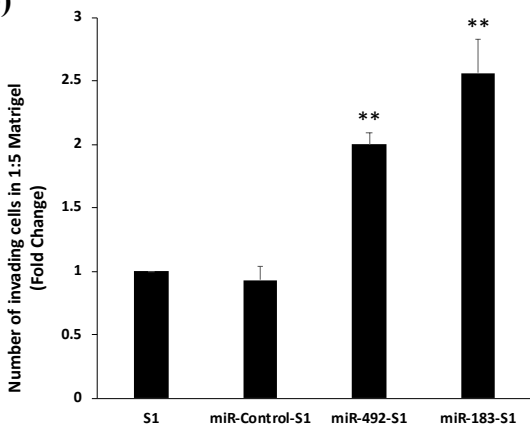


number of Matrigel-invading cells compared to control S1 cells. miR-Control-S1 cells did not show any significant increase in invading cells compared to S1 cells.

(a)



(b)



(c)

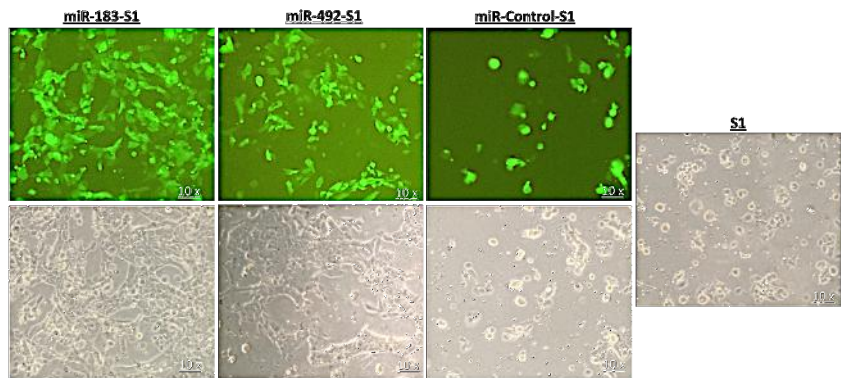


**Figure 15: Proliferation and invasion potential assessment upon over-expressing miR-183 and miR-492 in nontumorigenic S1 cells. (a) All four samples (S1, miR-Control-S1, miR-492-**

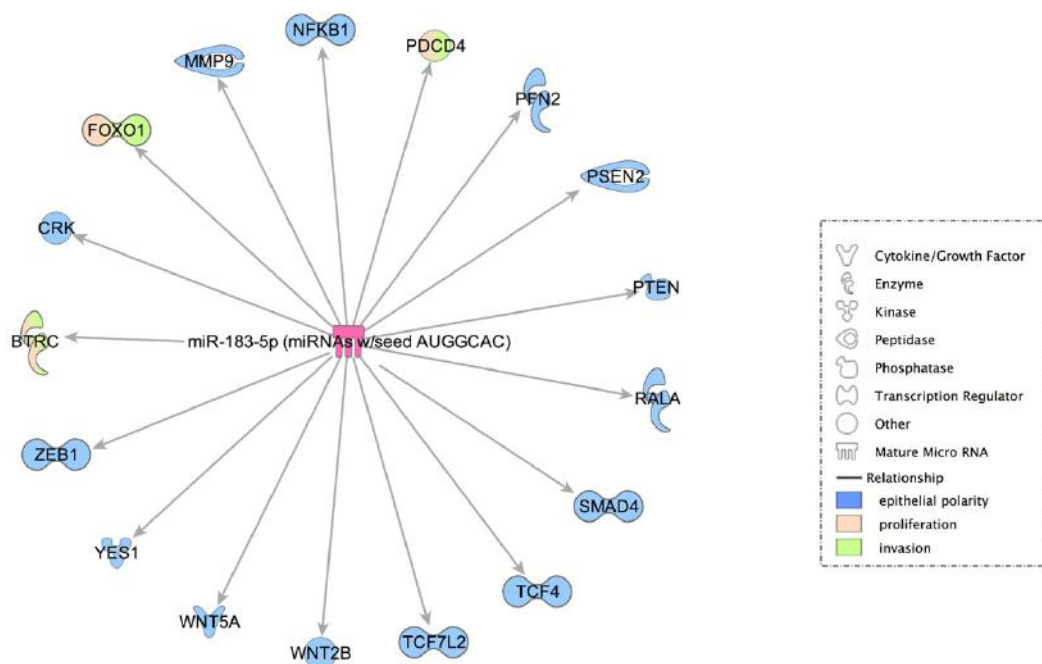
S1 and miR-183-S1) were cultured in 2D conditions in 12 well plate. Proliferation rate was assessed by cell counting on days 5, 9 and 13 and repeated at least three times. The values depicted in the histogram are the means ( $\pm$  standard error of the mean, SEM) of cell counts  $\times 10^4$  using hemocytometer. **(b)** Invasion of S1, miR-Control-S1, miR-492-S1 and miR-183-S1 cells cultured in diluted Matrigel (1:5) for 72 hours. Invasion was assessed by transwell invasion assay; invading cells were counted after fixation and Hoechst staining. The values depicted are the fold change of the number of invading cells ( $\pm$ SEM) from three separate experiments. \*\*\* denotes a p.value  $< 0.001$ , \*\* denotes a p.value  $< 0.01$  and \* denotes a p.value  $< 0.05$  by unpaired *t*-test. **(c)** Representative images of the invading cells after 72hr of being cultured in diluted Matrigel (1:5).

#### ***6. Potential downstream targets of miR-183 and miR-492 that might drive the pretumorigenic phenotypes observed***

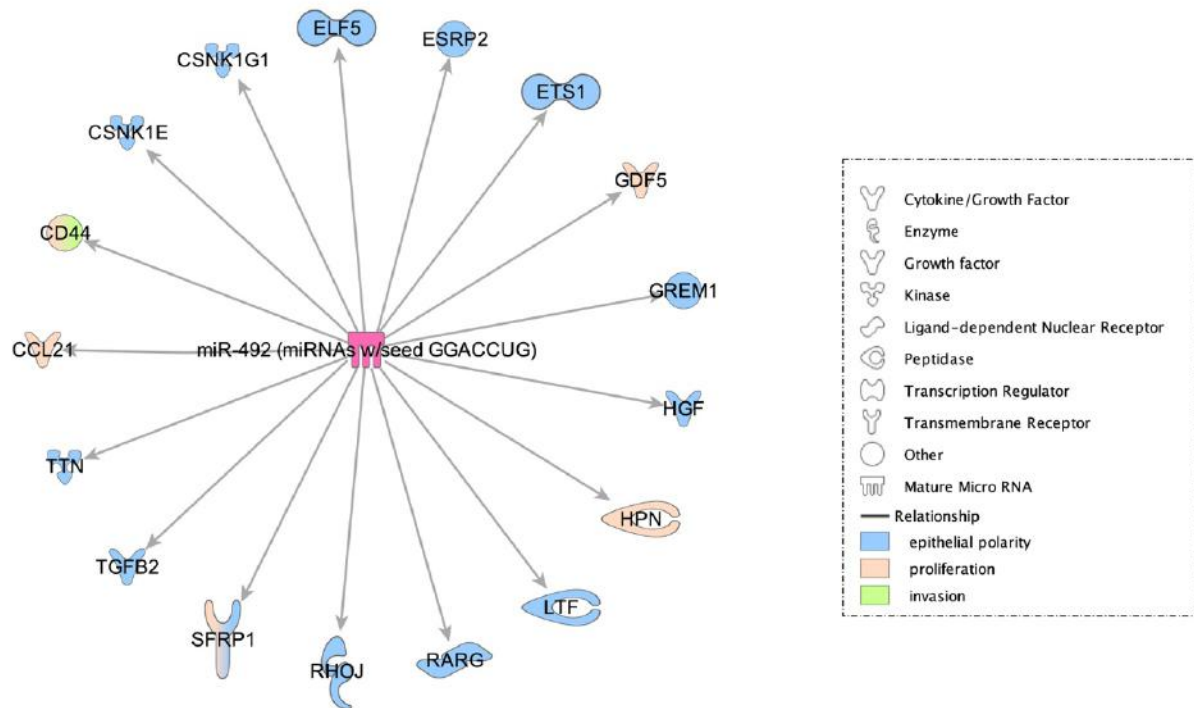
Recent research from our group reported enhanced proliferation and cell cycle entry, upregulation of c-Myc and cyclin D1 in Cx43-KO-S1 cells upon the loss of Cx43, mislocalization of  $\beta$ -catenin and Scrib from apicolateral membrane domains in 3D cultures resulting in loss of polarity, upregulation in the activity of Rho GTPases (RhoA, Rac1, and Cdc42) and thus triggering the noncanonical Wnt pathway and enhanced ERK1/2 activity [26, 27]. To identify potential downstream targets of miR-183 and miR-492 that might be driving pretumorigenic phenotypes, similar to what was reported upon the loss of Cx43 IPA was used. Experimentally validated and predicted (with high or moderate confidence) mRNA targets downstream of miR-183 (**Fig. 16a**) and miR-492 (**Fig. 16b**) that are implicated in invasion, proliferation and/or epithelial polarity pathways in breast cells and tissues were illustrated. The results showed that PDCD4, FOXO1 and BTRC downstream of miR-183 were involved in both invasion and proliferation pathways, while the rest of the mRNAs were implicated in epithelial polarity, like MMP9, NFKB1, PTEN,

SMAD4, TCF4, WNT2B, WNT5A and ZEB-1(**Fig. 16a**). Moreover, potential targets downstream of miR-492 represented CD44 to be involved in both invasion and proliferation pathways and CCL21, HPN and GDF5 in proliferative pathways. The mRNAs downstream of miR-492 and implicated in epithelial polarity included ETS1, LTF, RARG, RHOJ, TGFB2 and ELF5 (**Fig. 16b**). In addition, TargetScan was used to predict all downstream targets of miR-183-5p and miR-492, respectively to be compared to the targets reported by Fostok et al. [27] and Bazzoun et al. [26] downstream of Cx43 loss, which contributed to the observed pretumorigenic phenotypes. The results showed overlap in pathways and players along Cx43 loss and miR-183-5p and miR-492 over-expression (**Table 8**), however these were not experimentally validated.

(a)



(b)



© 2000-2020 QIAGEN. All rights reserved.

**Figure 16: Potential downstream targets of miR-183 and miR-492 that might be driving pretumorigenic phenotypes. IPA was used to plot the predicted (with high and moderate confidence) and experimentally validated mRNA targets downstream of (a) miR-183-5p and (b) miR-492, that might be driving the pretumorigenic phenotypes implicated in epithelial polarity, invasion and proliferation pathways in breast cells and tissues.**

	Targets dysregulated due to Cx 43 loss (Fostok et. al 2019)	Targets downstream of miR-183-5p		Targets downstream of miR-492	
	gene name	gene symbol	gene name	gene symbol	gene name
Cyclins	Cyclin D1	CCND2 CCNB1 CDK5R1 RUNX1T1	cyclin D2 cyclin B1 cyclin-dependent kinase 5, regulatory subunit 1 (p35) runt-related transcription factor 1; translocated to, 1 (cyclin D-related)	CCNDBP1 CNNM2 CNNM4 CCN12 CDK9 CDK13	cyclin D-type binding-protein 1 cyclin M2 cyclin M4 cyclin I family, member 2 cyclin-dependent kinase 9 cyclin-dependent kinase 13
Gap Junctions	Cx43	GJD2	gap junction protein, delta 2, 36kDa	GJB4 GJB7 GJD3	gap junction protein, beta 4, 30.3kDa gap junction protein, beta 7, 25kDa gap junction protein, delta 3, 31.9kDa
Catenins	Beta-catenin			CTNND2	catenin (cadherin-associated protein), delta 2
Rho GTPase binding proteins	Cdc42			CDC42EP4 PAK6	CDC42 effector protein (Rho GTPase binding) 4 p21 protein (Cdc42/Rac)-activated kinase 6
Rac	Rac1	ARHGEF18	Rho/Rac guanine nucleotide exchange factor (GEF) 18		
Rho GTPases	RhoA	ARHGAP18 ARHGAP21 ARHGAP26 ARHGAP6	Rho GTPase activating protein 18 Rho GTPase activating protein 21 Rho GTPase activating protein 26 Rho GTPase activating protein 6	ARHGAP27 ARHGAP28 ARHGAP29 ARHGAP30 ARHGAP31 ARHGAP36 ARHGAP44	Rho GTPase activating protein 27 Rho GTPase activating protein 28 Rho GTPase activating protein 29 Rho GTPase activating protein 30 Rho GTPase activating protein 31 Rho GTPase activating protein 36 Rho GTPase activating protein 44
Others	C-myc	FOXO1	forkhead box O1	WNT2B	wingless-type MMTV integration site family, member 2B
	ZO-1	PDCD4	programmed cell death 4 (neoplastic transformation inhibitor)	WNT3A	wingless-type MMTV integration site family, member 3A
	Scrib	TCF4	transcription factor 4	WNT4	wingless-type MMTV integration site family, member 4
	ERK1/2	ZEB1	zinc finger E-box binding homeobox 1	WNT7A	wingless-type MMTV integration site family, member 7A
		ZEB2	zinc finger E-box binding homeobox 2	WNT7B	wingless-type MMTV integration site family, member 7B
				WNT8B	wingless-type MMTV integration site family, member 8B
				WNT9B	wingless-type MMTV integration site family, member 9B
				WISP1	WNT1 inducible signaling pathway protein 1

**Table 8: Comparative analysis of targets dysregulated downstream of Cx43 loss as reported by Fostok et al. [27] and Bazzoun et al. [26] that contribute to pretumorigenic phenotypes in Cx43-KO-S1 cells as compared to targets downstream of miR-183-5p and miR-492.** To further check whether miR-183 and/or miR-492 might be triggering the loss of polarity, invasion and proliferation phenotypes through targeting Cx43 levels or mislocalization, TargetScan was used to predict all downstream targets of miR-183-5p and miR-492, respectively. These targets were extracted and compared to targets reported by Fostok et al. [27] and Bazzoun et al. [26] downstream of Cx43 loss, which contributed to the observed pretumorigenic phenotypes. Targets highlighted in orange were found up-regulated, in blue were down-regulated and the ones in grey, their levels were unaffected, but their cellular distribution was significantly altered in Cx43-KO-S1 cells compared to S1 cells upon Cx43 loss.

## D. Discussion

S1 nontumorigenic cells [239] have been used previously in 3D cell culture, in the presence of extracellular matrix of basement membrane type, as a model of phenotypically normal differentiation of breast luminal epithelium [240, 241]. They form a fully polarized epithelium that displays apicolateral distribution of tight junction proteins ZO-1 and ZO-2 [242, 243]. We have shown in recent studies that Cx43 drives apical polarity *in vivo*, and that it controls the distribution of tight junction proteins and of adherens junction component  $\beta$ -catenin [26]. Its loss is associated with cell multilayering and polarity disruption as reported in the S1 epithelium silenced for Cx43 (pretumorigenic Cx43-KO-S1 cells) and in archival biopsy tissue samples [26]. This *in vitro* 3D risk-progression culture model was used here to study the effect of the candidate tumor-associated miRNA over-expression (miR-183 and miR-492) on the otherwise phenotypically polarized S1 epithelial cells. Recent research from our group reported enhanced proliferation and cell cycle entry through the upregulation of c-Myc and cyclin D1 in Cx43-KO-S1 cells upon the loss of Cx43. In addition,  $\beta$ -catenin and Scrib mislocalized from apicolateral membrane domains in 3D cultures, indicating loss of epithelial polarity. No apparent activation of Wnt/ $\beta$ -catenin signaling was reported, however, the the expression and activity of Rho GTPases (RhoA, Rac1, and Cdc42) were upregulated due to the loss of Cx43, thus activating the noncanonical Wnt pathway and enhancing ERK1/2 activity. Moreover, Cx43-KO-S1 cells possessed migratory and invasive capacity when cultured under conditions mimicking permissive, or reduced, ECM stiffness. Therefore, Cx43 was reported to regulate proliferation

and invasion pathways in the non-neoplastic mammary epithelial cells in part through regulating noncanonical Wnt signaling [27]. This nontumorigenic *in vitro* 3D culture model was used here to study the effect of the candidate tumor-associated miRNAs over-expression (miR-183 and miR-492) on the otherwise phenotypically polarized nontumorigenic S1 epithelial cells.

***1. miR-183 over-expression promotes cell proliferation, invasion and loss of epithelial polarity in nonneoplastic breast epithelial cells***

The first miRNA was chosen from the tumor-associated patient miRNAs that were involved in epithelia polarity pathways and were downstream of Cx43 loss. miR-183 was thus selected for overexpression in the nontumorigenic S1 cells. It was upregulated upon Cx43 loss in Cx43-KO-S1 cells compared to S1 cells (**Fig. 11b & d**), was the most up-regulated miRNA in early-stage Lebanese breast cancer patient cohort (and matched US patients) [29] and its up-regulation conferred with the increased risk of cancer progression in the 3D culture model (**Fig. 11c**). miR-183 over-expression in S1 cells (miR-183-S1) resulted in similar pretumorigenic phenotypes observed upon Cx43 loss in Cx43-KO-S1 cells [26, 27]. miR-183-S1 cells exhibited formation of larger acini in 3D cultures (**Fig. 14a & b**) devoid of lumen assembly (**Fig. 14a & c**) with disrupted epithelial polarity observed via alteration of  $\beta$ -catenin apico-lateral distribution (**Fig. 14d & e**), alteration of apical Cx43 distribution (**Fig. 14g**) but without affecting the total mRNA levels of Cx43 (**Fig. 14f**), complete loss of Scrib apico-lateral expression (**Fig. 14h**). miR-183 over-expression also revealed enhanced proliferation (**Fig. 15a**) and invasion capacity

(**Fig. 15b & c**), hence recapitulating tumor-initiation phenotypes seen upon Cx43 loss [26, 27]. Therefore, loss of Scrib in miR-183-S1 cells seems to play a role in driving the corresponding tumor-initiation phenotype. For instance, Zhan et al. reported that up-regulation of the cell polarity Scrib inhibits breast cancer formation while its loss promotes tumor initiation and uncontrolled proliferation as a result of disrupting cellular morphology and reducing apoptosis through associating with the oncogene Myc in mammary epithelial cells and *in vivo*. Importantly, the team also indicated that Scrib mislocalization was sufficient to promote tumor initiation [30]. In another study, miR-183 was confirmed among a biomarker panel of miRNAs whose up-regulation predicted the tumor progression of lobular neoplasia from an *in situ* to a malignant transformation brought by loss of cellular polarity and acquisition of a hyperplastic phenotypes [104].

Using IPA, experimentally validated and predicted (with high or moderate confidence) mRNA targets downstream of miR-183 in breast cells and tissues that were involved in invasion and proliferation pathways were PDCD4, FOXO1 and BTRC. As for mRNAs implicated in epithelial polarity, MMP9, NFKB1, PTEN, SMAD4, TCF4, WNT2B, WNT5A and ZEB-1 were the most relevant targets (**Fig. 16a**). Lu et al. showed that miR-183 up-regulation increased pancreatic cancer cell proliferation, migration and invasion, by inhibiting the tumor suppressor *PDCD4* (programmed cell death 4) mRNA and protein levels [270]. The invasion capacity was further enhanced upon knocking down *PDCD4* via the up-regulation of urokinase-type plasminogen activator receptor (u-PAR) and c-Myc expression [271]. Based on these studies,



one can speculate that miR-183 might be driving these tumor-initiation phenotypes through similar pathways. However, these require further validation. Therefore, loss of Scrib and alteration in the localization of Cx43 and  $\beta$ -catenin seem to trigger the tumor-initiation phenotypes upon the over-expression of miR-183.

## ***2. miR-492 over-expression promotes cell proliferation, invasion and loss of epithelial polarity in nonneoplastic breast epithelial cells***

The second miRNA was chosen from the tumor-associated patient miRNAs that were involved in epithelia polarity pathways but were not downstream of Cx43 loss. Therefore, **miR-492** was selected from the subset of the up-regulated tumor-associated patient miRNAs that were not detected in the miRNome of the cultured epithelia specific to Cx43 loss. Like miR-183-S1 cells, miR-492-S1 cells also exhibited formation of larger acini in 3D cultures (**Fig. 14a & b**) devoid of lumen assembly (**Fig. 14a & c**) with disrupted epithelial polarity observed through alteration in  $\beta$ -catenin apico-lateral distribution (**Fig. 14d & e**), alteration of apical Cx43 distribution (**Fig. 14g**) without affecting its total expression levels (**Fig. 14f**), and mis-localization of Scrib apico-lateral expression (**Fig. 14h**). miR-492 over-expression also resulted in enhanced proliferation (**Fig. 15a**) and invasion capacity (**Fig. 15b & c**) in the nontumorigenic S1 cells. Hence, these cells recapitulated the tumor-initiation phenotypes seen upon Cx43 loss. While complete loss of Scrib in miR-183-S1 cells seems to play role in driving epithelial polarity loss, mislocalization of Scrib was also reported to sufficiently promote tumor loss of polarity

[30]. Hence the observed mislocalization of Scrib, Cx43 and  $\beta$ -catenin in miR-492-S1 cells seem to recapitulate the tumor-initiation phenotypes seen upon Cx43 loss.

Using IPA, experimentally validated and predicted (with high or moderate confidence) mRNA targets downstream of miR-492 in breast cells and tissues that were involved in invasion and proliferation pathways was CD44, while CCL21, HPN and GDF5 were implicated in proliferation. The rest of the mRNAs were implicated in epithelial polarity, like ETS1, LTF, RARG, RHOJ, TGFB2 and ELF5 (**Fig. 16b**). Although, miR-492 has not been widely studied in breast cancer, it seems to play an essential role in cancer initiation of various cancer cells. For instance, Shen et al. [272] showed that miR-492 was significantly up-regulated in breast cancer tissues and cells, and its over-expression in cells triggered proliferation and anchorage-independent growth by downregulating SOX7 protein, in turn upregulating cyclin D1 and c-Myc. miR-492 was proposed as an onco-miR that drives breast cancer initiation through associating with cyclin D1 and c-Myc [272]. Moreover, Sui et al. [273] proposed SOX7 as a potential prognostic marker and a tumor suppressor in breast cancer [274]. These studies suggest that miR-183 might be driving these tumor-initiation phenotypes through similar pathways. However, these require further validation. Therefore, alteration in the localization of Scrib, Cx43 and  $\beta$ -catenin seem to trigger the tumor-initiation phenotypes upon the over-expression of miR-492 in the otherwise nontumorigenic cells.

### ***3. miR-183 and miR-492 over-expression might drive pre-tumorigenic phenotypes through possible involvement with gap junction proteins***

Connexins provide the communication of small molecules between neighboring cells by establishing gap junction intercellular communication (GJIC), and thus play important roles along development, differentiation and tumorigenesis. Cx43 (GJA1) was not a down-stream target of miR-183 nor miR-492, as validated by RT-qPCR (**Fig. 14f**) and predicted by TargetScan (**Table 8**). Since miR-183 was found up-regulated in Cx43-KO-S1 cells as compared to S1 cells (**Fig. 11b & d**), this adds a direct link between Cx43 down-regulation and miR-183 up-regulation. This might imply that Cx43 down-regulation results in miR-183 up-regulation, and not the converse (as seen in **Fig. 14f**). However, miR-183 up-regulation causes alteration in the distribution of Cx43 (**Fig. 14g**). miR-492 was not found dysregulated in sequencing or RT-qPCR analysis upon Cx43 loss. However, over-expression of miR-492 was able to alter the localization of Cx43 in the epithelial aggregates (**Fig. 14g**). Therefore, miR-183 and miR-492 over-expression might in part affect polarity disruption in a gap junctional dependent manner, through the mislocalization of Cx43 from apical membrane domains in glandular structures or acini formed in 3D culture (**Fig. 14g**), but not through directly down-regulating the expression of Cx43.

## E. Conclusion

Ectopic over-expression of miR-183 and miR-492 in nontumorigenic S1 cells resulted in cells formation of larger acini in 3D cultures, devoid of lumen assembly, with disrupted epithelial polarity observed through mislocalization of  $\beta$ -catenin and Scrib's apico-lateral distribution and Cx43's apical distribution. It also triggers enhanced proliferation and invasion capacity, hence recapitulating tumor-initiation phenotypes seen upon Cx43 loss [26, 27]. miR-183 was chosen for overexpression in the nontumorigenic S1 cells since it was upregulated upon Cx43 loss, was the most up-regulated miRNA in early-stage Lebanese breast cancer patients (and matched US patients) [29] and its up-regulation conferred with the increased risk of cancer progression in the 3D culture model. Tumor-initiation phenotypes attributed to miR-183 over-expression seem to be due to complete loss of Scrib in miR-183-S1 and mis-localization of the distribution of  $\beta$ -catenin and Cx43 in the cultured epithelia. While loss of Scrib in miR-183-S1 cells seems to drive tumor-initiation phenotypes, its mis-localization was also reported to be sufficient in promoting tumorigenesis [30]. Therefore, tumor-initiation phenotypes attributed to miR-492 over-expression seem to be due to mislocalization Scrib,  $\beta$ -catenin and Cx43 in the cultured epithelia. Moreover, while miR-183 was found up-regulated in response to Cx43 loss, adding a direct link between Cx43 down-regulation and miR-183 up-regulation, the contrary was not observed. Therefore, miR-183 and miR-492 over-expression might in part be affecting polarity disruption in a gap junctional dependent manner, through the mislocalization of Cx43 from apical membrane domains in aggregates formed in 3D culture, but not through directly

down-regulating Cx43 expression. Although each miRNA is predicted to affect different downstream targets and pathways along breast cancer initiation, both miR-183 and miR-492 ectopic over-expression triggers enhanced proliferation and invasion and loss of apical polarity through Scrib's loss/mis-localization and through altering the distribution of Cx43 and  $\beta$ -catenin in the cultured epithelia.

## **F. Materials and Methods**

### ***1. Three-dimensional cell culture***

Nontumorigenic HMT-3522 S1 (S1) human breast epithelial cells [239] between passages 52 and 60, were routinely maintained as a monolayer on plastic (2D culture) in chemically defined serum-free H14 medium [242, 261] at 37 °C and 5% CO<sub>2</sub> in a humidified incubator. H14 medium was changed every 2–3 days. For 2D cultures, cells were plated on plastic substrata at a density of  $2.3 \times 10^4$  cells/cm<sup>2</sup>. The drip method of 3D culture was used to induce the formation of acini. Briefly, cells were plated on Matrigel™ (50  $\mu$ l/cm<sup>2</sup>; BD Biosciences, 354234) at a density of  $4.2 \times 10^4$  cells/cm<sup>2</sup> in the presence of culture medium containing 5% Matrigel™ [242, 262]. The EGF was omitted from the culture medium after day 7 to allow completion of acinar differentiation (usually observed on day 8 or 9) [242]. Cx43 was down-regulated in S1 cells via retroviral delivery of shRNA, as described by Bazzoun et al. [26].

### ***2. Total RNA isolation and quality control (QC)***

Total RNA from cells in 3D culture was extracted using TRIzol reagent (Invitrogen, Carlsbad, CA, USA) following the manufacturer's protocol. Purity and concentration of RNA samples were examined spectrophotometrically by absorbance measurements at 260, 280 and 230 nm using the NanoDrop ND-1000 (Thermo Fisher Scientific, Wilmington, DE, USA). OD260/OD280 ratios between 1.8 and 2.1 were deemed acceptable.

### **3. *miRNA Library Preparation and Sequencing***

Triplicate samples of S1 cells and triplicates of Cx43-KO-S1 cells were submitted for small RNA-seq. The Purdue Genomics Facility prepared libraries using the NEXTflex Illumina Small RNA Sequencing Kit v3 (Bioo, Austin, TX) with barcoding performed using UDI primers. A total of 15 PCR cycles were performed. 2x50 bp reads were sequenced using the NovaSeq6000. Only one of each read pair was used for analyses, given the short size of miRNAs. Library preparation protocols were modified for the use of unique dual indexes, in order to circumvent index hopping on the Illumina NovaSeq 6000. Before library preparation the RNA quality was checked using an Agilent Nano RNA Chip.

### **4. *Heatmap of miRNAs from the breast epithelia that are in common with the MREs sponged by the significant circRNAs***

Counts for miRNAs were obtained using miRNA-seq on a NovaSeq 6000. Data were normalized using DESeq2 [263] and then, the log<sub>2</sub> of 1+ the normalized counts was scaled by

row. Rows were clustered using hierarchical clustering and were annotated with the direction (up- or down-regulation) of the associated circRNAs in Cx43 KO S1 samples versus S1 control sample. Cutoff points were set for Fold Change > 2 and p.adjusted value ≤ 0.05.

### **5. *Functional enrichment of mRNAs associated with circRNA binding miRNAs***

A functional enrichment analysis was performed in Ingenuity Pathway Analysis (IPA®, QIAGEN Redwood City, [www.qiagen.com/ingenuity](http://www.qiagen.com/ingenuity)) of predicted target mRNAs (predicted by TargetScan) for the top five predicted sponged miRNAs associated with the chosen circRNAs. Due to the high number of predicted mRNA targets for each miRNA, only mRNAs with strong predicted (based on the cumulative weighted context score of -0.4 or lower [109]) or experimental evidence were kept in the analysis. Limiting the number of mRNA targets in this way allows for quantification of the significance of the enrichment via a hypergeometric distribution. An enrichment test was performed to determine which biological functions or diseases associated with mRNA targets are observed in association with these mRNAs more often than we would expect by chance.

### **6. *miRNA Expression by Quantitative Real Time-Polymerase Chain Reaction***

Reverse transcription of ten nanograms of the total RNA was performed using the TaqMan® MicroRNA Reverse Transcription Kit (Applied Biosystems, USA) according to the manufacturer's instructions. Small nuclear RNA RNU6B, miR-183-5p and miR-492 primers and

probes were purchased as part of the TaqMan® microRNA Assays Kit (Applied Biosystems, USA) with validated efficiency. cDNA synthesis was carried out in a multiplex reaction set up whereby two miRNA primers (for example miR-183-5p and miR-492) were used in each reaction with the endogenous control, RNU6B. RT-qPCR was performed using BioRad CFX96 Real Time System, C1000 Thermal Cycler (Germany). Reactions using 10µl of 2x TaqMan® Universal Master Mix with no Amperase Uracil N-glycosylase (UNG) (Applied Biosystems, USA), 1µl of the corresponding 20x microRNA probe, 4µl of DEPC treated water, and 5µl of cDNA were performed in duplicates for each miRNA probe. cDNA Synthesis and RT-qPCR were repeated twice for each sample and each plate included: no reverse transcription control (NRT), no template control (NTC) and normal breast tissue samples. The normalization of the Cx43-KO-S1 or miR-183-S1 or miR-492-S1 cells was based on the S1 control or miR-Control-S1 cells present in the RT-qPCR plate to ensure inter-run calibration. The cycling conditions were 95 °C for 10 min and 40 cycles of 95 °C for 15 seconds and an annealing temperature of 60 °C for 60 seconds. Using the  $\Delta\Delta C_t$  equation, the relative expression of the experimental miRNA was determined in the tumor samples compared to the normal tissue specimens using RNU6B as an endogenous control.

### ***7. Lentiviral Infection for Delivery of mature miRNAs into S1 cells***

The pLenti-III-miR-GPF tagged vectors from ABM (Canada) were used to generate lenti-miR-183-5p, lenti-miR-492, and lenti-miR-control (empty vector) with kanamycin resistance for



over-expression in S1 cells in bacterial culture and puromycin resistance to infect S1 cells and generate stable miR-183-S1 and miR-492-S1. Briefly, plasmids were streaked in an agar plat and grown overnight in a humidified incubator at 37C, a single colony was selected and amplified in agar broth overnight in an incubator shaker, and then purified using Qiagen Midi-Prep Kit as per the company's protocol. Briefly, lentiviral vectors (10 µg) containing pLenti-III-miR-GPF tagged vectors for each of the mature transcript of miR-183, miR-492 or the miR-Control (empty vector) were transfected into the amphoteric 293T packaging cells using Invitrogen™ Lipofectamine™ 2000 (ThermoFisher Scientific, USA) according to manufacturer's protocol (80 µL). and a 2nd Generation Packaging Mix (10 µg) in 1 mL of serum-free, antibiotic-free medium for each 10 cm dish and incubated at 37 °C for 5-8 hours, then 0.65mL FBS was added to the 10 cm dish and incubated overnight at 37 °C. The transfection media was replaced with complete media and incubated overnight at 37°C. The first viral harvest in the supernatant was collected at 3000 rpm for 15 min at 4 °C, filtered and stored at 4 °C for the next day. Complete media was added again to the cells and a second harvest was collected and filtered the next day and added to the first harvest that was kept at 4°C. The pooled harvest was aliquoted and stored at -80°C until use. The viral titer of the first harvest is approximately 106 IU/mL. Puromycin drug selection killing curve showed that concentration of 0.5 ug/ul of Puromycin was optimal for selecting the infected cells as per manufacturer's protocol (ABM, Canada). Multiplicity of Infection, MOI was calculated as:  $\text{Product Titer (IU/ml)} \times \text{Virus Volume (ml)} / \text{Total Cell Number}$ , and 3 MOI was used for the S1 cells, as recommended by ABM for breast cell lines. For infection, filtered

lentiviral supernatants were applied to monolayers of S1 cells on day 3. Cells were incubated with hexadimethrine bromide (Polybrene; 8  $\mu\text{g}/\text{mL}$ ; Sigma, St. Louis, MO, USA) for 8 h. The infection medium was removed, and cells were incubated in regular H14 medium for 24 h. Infection was repeated two additional times, and selection with puromycin dihydrochloride (0.5  $\mu\text{g}/\text{ul}$ ; Gibco™, USA, A-1113803) was started 72 h after the last infection. miRNA-infected cells (miR-183-S1, miR-492-S1 and miR-Control-S1) cells were maintained, propagated, and plated similarly to S1 cells, but the H14 medium was supplemented with puromycin for selection. The stability of the over-expression was regularly assessed in different cell passages with fluorescence microscopy and RT-qPCR throughout this study.

#### **8. Immunofluorescence**

S1, miR-183-S1, miR-492-S1 and miR-Control-S1 cells were plated on coverslips 4-well chamber slides (3D) and were stained by immunofluorescence on day 11 as described earlier [60]. Briefly, cells were washed with 1  $\times$  PBS and permeabilized with 0.5% peroxide and carbonyl-free Triton X-100 in cytoskeleton buffer (100 mM NaCl, 300 mM sucrose, 10 mM PIPES, pH 6.8, 5 mM  $\text{MgCl}_2$ , 1 mM pefabloc, 10  $\mu\text{g}/\text{mL}$  aprotinin, 250  $\mu\text{M}$  NaF). Cells were washed twice with cytoskeleton buffer and fixed in 4% formaldehyde. Cells were subsequently washed thrice with 50 mM glycine in 1x PBS and blocked. Primary antibodies used were mouse monoclonal  $\beta$ -catenin (200  $\mu\text{g}/\text{mL}$ ; Santa Cruz Biotechnology, Dallas, TX, USA, sc-7963), mouse monoclonal Scrib (200  $\mu\text{g}/\text{mL}$ ; Santa Cruz Biotechnology, Dallas, TX, USA, sc-55543)

and mouse monoclonal Connexin 43 (200 µg/mL; Santa Cruz Biotechnology, Dallas, TX, USA, sc-271837) all at dilutions (1:200). Secondary antibody conjugated to Alexa Fluor 568 (red), goat anti-mouse (Invitrogen, Waltham, MA, USA, A-11004) was used at the manufacturer's proposed dilutions (1:1000). Nuclei were counterstained with 0.5 µg/mL Hoechst 33342, and cells were mounted in ProLong® Gold antifade reagent, allowed to dry overnight and sealed. The slides were then examined and imaged with a laser scanning confocal microscope (Zeiss, LSM710). A minimum of 100 acini were analyzed per group.

### ***9. Diameter measurements, lumen assembly and apico-lateral polarity markers scoring***

The fixed slides were examined with an upright fluorescent microscope (Leica, DF7000 T) using a 40x oil immersion objective to measure the diameter of 3D cultures, assess lumen assembly, and score for the apicolateral distribution of  $\beta$ -catenin. A minimum of 100 acini were analyzed per group. The size of acini was measured manually by recording the diameter of each acinus or nodule using LAS X software. Lumen assembly was scored visually. Apicolateral distribution of  $\beta$ -catenin was scored visually from acini having proper apico-lateral distribution. At least 100 acini were included in the measurements and scoring.

### ***10. Trypan Blue Exclusion Method***

S1, miR-183-S1, miR-492-S1 and miR-Control- cells were plated in 12-well tissue culture plates (2D). The medium was removed, and the cells were subsequently trypsinized and

collected. Cells were then diluted in trypan blue at 1:1 ratio (vol/vol) and counted using a hemocytometer. The cells were counted from triplicates on days 5, 9 and 13. The counts from each well were repeated at least three times.

### ***11. Transwell Cell Invasion Assay***

Six-well format cell culture inserts (8  $\mu\text{m}$  pore size) were coated with 400  $\mu\text{L}$  of 1:5 diluted Matrigel<sup>TM</sup> and incubated at 37 °C for 4 h.  $3 \times 10^5$  S1, miR-183-S1, miR-492-S1 and miR-Control-S1 cells were plated in the inserts in DMEM:F-12 supplemented with 1% fetal bovine serum (FBS; Sigma, F-9665). DMEM:F-12 supplemented with 10% FBS was added below the insert. Cells were incubated for 72 h and were then fixed using 4% formaldehyde in 1x PBS for 20 min at room temperature. The cells towards the inside of the insert were removed using a cotton swab, and nuclei of invading cells were stained with 1  $\mu\text{g}/\text{mL}$  Hoechst 33342 (Molecular Probes, H3570) in 1  $\times$  PBS for 10 min at room temperature. The insert was then cut, mounted on a microscope slide in ProLong<sup>®</sup> Gold antifade reagent (Molecular Probes, P36930), allowed to dry overnight and sealed. The inserts were examined with a fluorescence microscope, and the number of invading cells was counted and reported as fold change.

## CHAPTER VII

### CONCLUSION

The mammary gland development, differentiation and tumorigenesis is dependent on gap junction organization and proper communication, especially Cxs. Cx43 plays essential roles during mammary gland development [22, 23] and differentiation [24] and acts as a tumor suppressor [20, 21, 25]. Its loss and mislocalization influence breast cancer initiation [26], progression [27], increase risk of breast cancer development in overweight women [231, 232] and is associated with markers of poor prognosis, increased metastasis and poor survival in breast cancer patients [25]. We recently showed that Cx43 functions via PI3 Kinase and noncanonical Wnt signaling pathways in priming the breast epithelium for neoplastic behavior [26, 27]. The nontumorigenic luminal human breast epithelial HMT-3522 S1 (S1) cell line, cultured under 3D conditions, forms growth-arrested and basoapically polarized acini with a central lumen and apicolateral localization of Cx43. S1 cells recapitulate normal human breast tissue architecture [26]. Silencing Cx43 expression in these nontumorigenic S1 cells via Cx43-shRNA (Cx43-KO-S1) resulted in cell cycle entry, perturbed apical polarity, mitotic spindle misorientation and loss of lumen, causing cell multilayering [26] and priming cells for enhanced motility and invasion [26, 27]. These phenotypic features observed in Cx43-KO-S1 acini represent architectural and phenotypical premalignant mammary lesions, like those observed in

ductal hyperplasia in a murine model [28], which increase the risk of breast cancer initiation, thus marking Cx43-KO-S1 as pretumorigenic culture model. Therefore, this 3D risk-progression culture model was used to capture key pretumorigenic changes and cancer initiation phenotypes that might be triggered by miRNA players, heightening the risk of breast cancer development.

This study brings initial information of the involvement of miRNAs associated with morphological disruptions of the breast epithelium/acini and identified in young women with breast cancer as triggers of cancer-initiation phenotypes. Through performing miRNA-sequencing on 3D acini of a HMT-3522 S1 (S1) breast epithelial risk-progression culture model we revealed 65 miRNAs that were significantly dysregulated in response to Cx43 silencing. A comparative analysis between the detected miRNAs and 15 tumor-associated miRNAs involved in epithelial polarity disruption from young Lebanese patient validation cohort was performed [29]. miR-183 was upregulated upon Cx43 loss in the cultured epithelia, was the most up-regulated miRNA in early-stage Lebanese breast cancer patients (and matched US patients) and its up-regulation conferred with the increased risk of cancer progression in the 3D culture model. miR-492 was up-regulated in tumor-associated patient miRNAs involved in epithelial polarity but was not specific to Cx43 loss. Ectopic over-expression of miR-183 and miR-492 in nontumorigenic S1 cells through pLenti-III-miR-GFP tagged vectors was performed. The results revealed that over-expression of both miR-183 and miR-492 in nontumorigenic S1 cells resulted in cells formation of larger acini in 3D cultures, devoid of lumen assembly, with disrupted epithelial polarity observed through mislocalization of  $\beta$ -catenin and Scrib's apico-lateral

distribution and Cx43's apical distribution. It also triggers enhanced proliferation and invasion capacity, hence recapitulating tumor-initiation phenotypes seen upon Cx43 loss. These tumor-initiation phenotypes seem to be attributed to Scrib's loss (by miR-183) and mis-localization (by miR-492) and through altering the apico-lateral localization of Cx43 and  $\beta$ -catenin. Moreover, miR-183 and miR-492 over-expression might in part affect polarity disruption in a gap junctional dependent manner, through the mislocalization of Cx43 from apical membrane domains in aggregates formed in 3D culture, but not through directly down-regulating Cx43 expression. Therefore, miR-183-5p and miR-492 over-expression in non-neoplastic cells recapitulates tumor-initiation phenotypes observed upon the loss of Cx43. Although each miRNA is predicted to affect different downstream targets and pathways along breast cancer initiation (**Fig. 17**), both miR-183 and miR-492 ectopic over-expression triggers enhanced proliferation and invasion and loss of apical polarity through Scrib's loss/mis-localization and through altering the distribution of Cx43 and  $\beta$ -catenin in the cultured epithelia.

We also revealed **Cx43/hsa\_circ\_0077755/miR-182** as the only validated post-transcriptional axis specific to Cx43 loss that might serve as a biomarker predictor of heightened risk of breast cancer initiation (**Fig. 18**). Moreover, **Cx43/hsa\_circ\_0077755/miR-182** axis seems to associate with poor prognosis in early-stage breast cancer when the tumor-suppressor Cx43 (and hence hsa\_circ\_0077755) are down-regulated [25] and the onco-miR, miR-182 is up-regulated. Conversely, it associates with poor prognosis and might predict the risk of enhanced invasion and metastasis at later advanced stages of breast cancer when Cx43 (and hence

hsa\_circ\_0077755) are up-regulated [258] and miR-182 is down-regulated [252].

Cx43/hsa\_circ\_0077755/miR-182 dysregulation patterns might thus predict prognosis along breast cancer initiation and progression. We previously proposed a possible biomarker signature of Cx43 mRNA-circRNAs-miRNAs axes for detection and prevention of early-onset breast cancer through three “initiation circRNAs” and a panel of their sponged miRNAs (identified to date in the literature), miR-182, miR-375, miR-203, miR-520g and miR-520h [7], which parallel roles that Cx43 plays along breast tumorigenesis. Here, we confirm the involvement of Cx43 in post-transcriptional regulatory axes in breast cancer initiation, match the miRNA dysregulation pattern to an early-stage young breast cancer patient cohort and propose

**Cx43/hsa\_circ\_0077755/miR-182** as a biomarker axis of heightened risk of breast cancer initiation.

We also highlighted through a literature review the novelty of utilizing miRNAs to serve not only as biomarkers for breast cancer progression, invasiveness, drug resistance and metastasis, but also as potential key players in re-sensitizing breast cancer cells to chemo/targeted/hormonal therapies and/or potentially blocking metastasis. The focus for BC understanding should be on the original molecular triggers for cellular transformation prior to cancer progression, drug resistance and metastasis. In other terms, it is essential to focus research on the basic molecular mechanisms that trigger cancer.



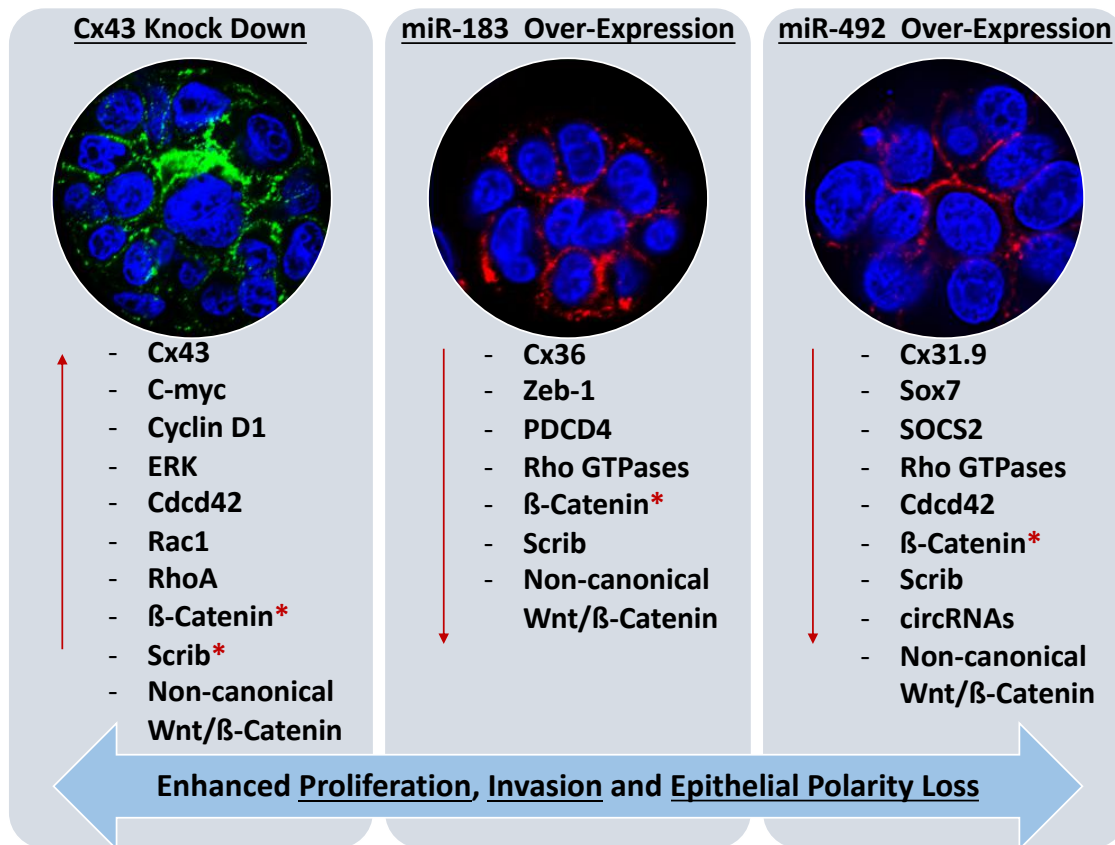


**Figure 17. Comparative summary of major players driving proliferation, invasion and epithelial polarity loss upon loss of Cx43, over-expression of miR-183 and over-expression of miR-492, respectively.** The first panel represents major players/pathways that drive the pretumorigenic phenotypes observed in Cx43-KO-S1 cells upon Cx43 loss, as reported by Fostok et al. [27] and Bazzoun et al. [26]. All proteins were up-regulated upon Cx43 loss. The second panel represents major players/pathways that are predicted to drive the pretumorigenic phenotypes observed in miR-183-S1 cells upon over-expression of miR-183. All reported genes were down-regulated. The third panel represents major players/pathways that drive the pretumorigenic phenotypes observed in miR-492-S1 cells upon over-expression of miR-492. All reported genes were down-regulated. \* denotes that total levels were unaffected but their localization along the cell was altered. Each cell line is illustrated by a representative acinus devoid of lumen formation and with mislocalization of  $\beta$ -catenin (green first panel and red for the rest) from apicolateral membrane domains in glandular structures or acini formed in 3D culture, suggesting the loss of apical polarity. Nuclei were counterstained with Dapi (blue).

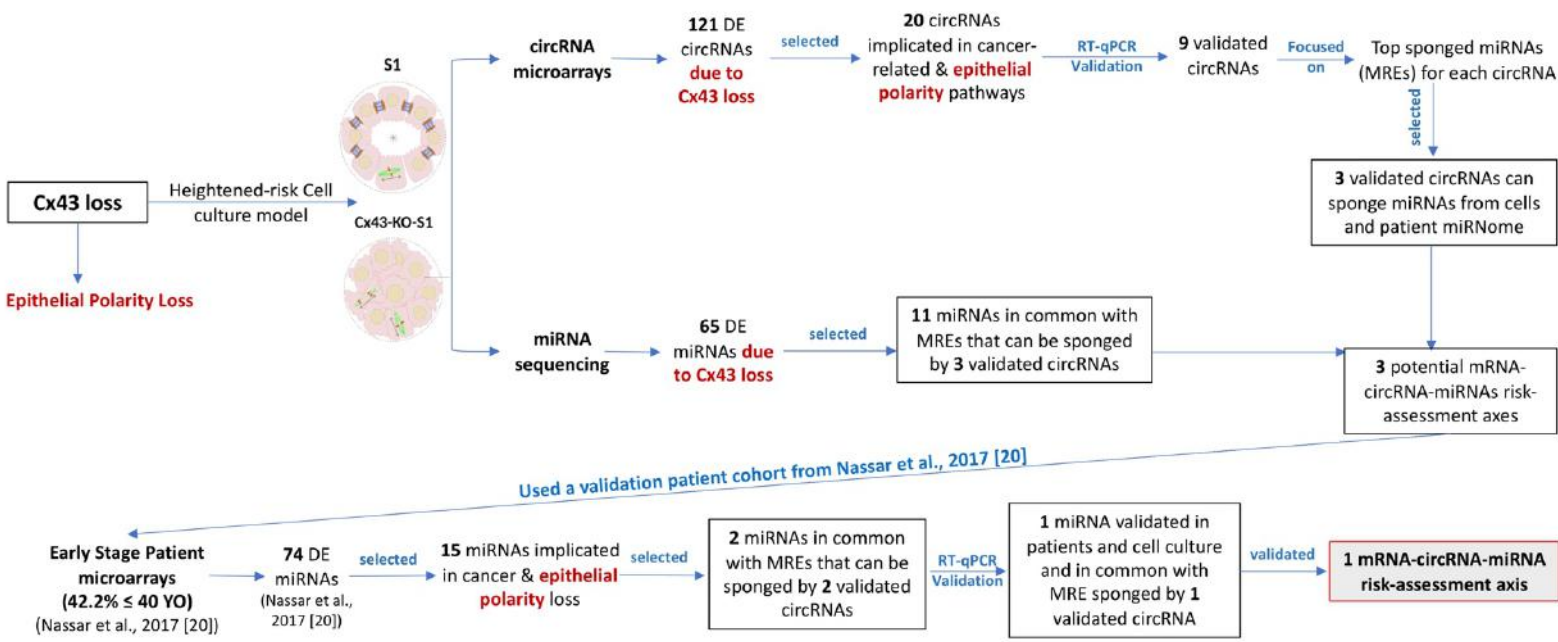


**Figure 18.** A graphical abstract summarizing the methodology used to select **Cx43/has\_circ\_0077755/miR-182** as the only validated risk-assessment axis for breast cancer initiation. Using the circRNA microarrays and miRNA sequencing results of Cx43-KO-S1 compared to S1 cells and focusing mainly only on Cx43 loss (and hence epithelial polarity loss) and on the sponging activity of circRNAs to miRNAs, three axes were predicted for breast cancer risk-assessment. After using a validation early-stage young breast cancer patient cohort as published in Nassar et al. [29], the list was narrowed down to only Cx43/has\_circ\_0077755/miR-182 axis.

## BIBLIOGRAPHY

1. Bray, F., et al., *Global cancer statistics 2018: GLOBOCAN estimates of incidence and mortality worldwide for 36 cancers in 185 countries*. CA: a cancer journal for clinicians, 2018. **68**(6): p. 394-424.
2. SHAMS, A.A. and K.M. MUSALLAM, *Cancer epidemiology in Lebanon*. 2010.
3. El Saghir, N.S., et al., *BRCA1 and BRCA2 mutations in ethnic Lebanese Arab women with high hereditary risk breast cancer*. The oncologist, 2015. **20**(4): p. 357.
4. DeSantis, C.E., J. Ma, and A. Jemal, *Trends in stage at diagnosis for young breast cancer patients in the United States*. Breast cancer research and treatment, 2019. **173**(3): p. 743-747.
5. Anderson, L.N., et al., *Phytoestrogen intake from foods, during adolescence and adulthood, and risk of breast cancer by estrogen and progesterone receptor tumor subgroup among Ontario women*. International journal of cancer, 2013. **132**(7): p. 1683-1692.
6. Bartel, D.P., *MicroRNAs: genomics, biogenesis, mechanism, and function*. cell, 2004. **116**(2): p. 281-297.
7. Naser Al Deen, N.M., M.G. AbouHaidar, and R.S. Talhouk, *Connexin43 as a tumor suppressor: Proposed Connexin43 mRNA-circularRNAs-microRNAs axis towards prevention and early detection in breast cancer*. Frontiers in medicine, 2019. **6**: p. 192.
8. Al Deen, N.N., et al., *Cross-roads to drug resistance and metastasis in breast cancer: miRNAs regulatory function and biomarker capability*, in *Breast Cancer Metastasis and Drug Resistance*. 2019, Springer. p. 335-364.
9. Tang, Y.-Y., et al., *Circular RNA hsa\_circ\_0001982 promotes breast cancer cell carcinogenesis through decreasing miR-143*. DNA and cell biology, 2017. **36**(11): p. 901-908.
10. Liu, Y., et al., *Circular RNA-MTO1 suppresses breast cancer cell viability and reverses monastrol resistance through regulating the TRAF4/Eg5 axis*. International journal of oncology, 2018. **53**(4): p. 1752-1762.
11. Liu, Y., et al., *Circular RNA hsa\_circ\_0008039 promotes breast cancer cell proliferation and migration by regulating miR-432-5p/E2F3 axis*. Biochemical and biophysical research communications, 2018. **502**(3): p. 358-363.
12. Gao, D., et al., *Screening circular RNA related to chemotherapeutic resistance in breast cancer*. Epigenomics, 2017. **9**(9): p. 1175-1188.
13. Du, W.W., et al., *A circular RNA circ-DNMT1 enhances breast cancer progression by activating autophagy*. Oncogene, 2018. **37**(44): p. 5829-5842.

14. Yan, L., M. Zheng, and H. Wang, *Circular RNA hsa\_circ\_0072309 inhibits proliferation and invasion of breast cancer cells via targeting miR-492*. *Cancer management and research*, 2019. **11**: p. 1033.
15. Yin, W.-B., et al., *Circulating circular RNA hsa\_circ\_0001785 acts as a diagnostic biomarker for breast cancer detection*. *Clinica chimica acta*, 2018. **487**: p. 363-368.
16. Dbouk, H.A., et al., *Connexins: a myriad of functions extending beyond assembly of gap junction channels*. *Cell Communication and signaling*, 2009. **7**(1): p. 4.
17. Leithe, E., M. Mesnil, and T. Aasen, *The connexin 43 C-terminus: A tail of many tales*. *Biochimica et Biophysica Acta (BBA)-Biomembranes*, 2018. **1860**(1): p. 48-64.
18. Su, V. and A.F. Lau, *Connexins: mechanisms regulating protein levels and intercellular communication*. *FEBS letters*, 2014. **588**(8): p. 1212-1220.
19. Grek, C.L., et al., *Connexin 43, breast cancer tumor suppressor: Missed connections?* *Cancer letters*, 2016. **374**(1): p. 117-126.
20. Bazzoun, D., S. Lelièvre, and R. Talhouk, *Beyond the Channel: Role of Connexins in Regulating Normal and Cancerous Processes in the Mammary Gland*, in *Intercellular Communication in Cancer*. 2015, Springer. p. 1-28.
21. Fostok, S.F., et al., *Gap junctions and Wnt signaling in the mammary gland: a cross-talk?* *Journal of mammary gland biology and neoplasia*, 2019. **24**(1): p. 17-38.
22. Paine, I.S. and M.T. Lewis, *The terminal end bud: The little engine that could*. *Journal of mammary gland biology and neoplasia*, 2017. **22**(2): p. 93-108.
23. Musumeci, G., et al., *Mammary gland: From embryogenesis to adult life*. *Acta histochemica*, 2015. **117**(4-5): p. 379-385.
24. Talhouk, R.S., et al., *Heterocellular interaction enhances recruitment of  $\alpha$  and  $\beta$ -catenins and ZO-2 into functional gap-junction complexes and induces gap junction-dependant differentiation of mammary epithelial cells*. *Experimental cell research*, 2008. **314**(18): p. 3275-3291.
25. Chasampalioti, M., et al., *Connexin 43 is an independent predictor of patient outcome in breast cancer patients*. *Breast cancer research and treatment*, 2019. **174**(1): p. 93-102.
26. Bazzoun, D., et al., *Connexin 43 maintains tissue polarity and regulates mitotic spindle orientation in the breast epithelium*. *Journal of cell science*, 2019. **132**(10): p. jcs223313.
27. Fostok, S., et al., *Connexin 43 loss triggers cell cycle entry and invasion in non-neoplastic breast epithelium: a role for noncanonical wnt signaling*. *Cancers*, 2019. **11**(3): p. 339.
28. Godde, N.J., et al., *Scribble modulates the MAPK/Fra1 pathway to disrupt luminal and ductal integrity and suppress tumour formation in the mammary gland*. *PLoS genetics*, 2014. **10**(5).
29. Nassar, F.J., et al., *microRNA Expression in Ethnic Specific Early Stage Breast Cancer: An Integration and Comparative Analysis*. *Scientific reports*, 2017. **7**(1): p. 1-12.
30. Zhan, L., et al., *Deregulation of scribble promotes mammary tumorigenesis and reveals a role for cell polarity in carcinoma*. *Cell*, 2008. **135**(5): p. 865-878.

31. Bray, F., et al., *Global cancer statistics 2018: GLOBOCAN estimates of incidence and mortality worldwide for 36 cancers in 185 countries*. CA Cancer J Clin, 2018. **68**(6): p. 394-424.
32. Musallam, K.M. and A.I. Shamseddine, *Cancer Epidemiology in Lebanon*. Middle East Journal of Cancer, 2010. **1**(1): p. 41-44.
33. Porter, P., "Westernizing" women's risks? *Breast cancer in lower-income countries*. New England Journal of Medicine, 2008. **358**(3): p. 213-216.
34. Fostok, S.F., et al., *Gap Junctions and Wnt Signaling in the Mammary Gland: a Cross-Talk?* Journal of mammary gland biology and neoplasia, 2018: p. 1-22.
35. Howard, B.A. and B.A. Gusterson, *Human breast development*. Journal of mammary gland biology and neoplasia, 2000. **5**(2): p. 119-137.
36. Dbouk, H.A., et al., *Connexins: a myriad of functions extending beyond assembly of gap junction channels*. Cell Commun Signal, 2009. **7**: p. 4.
37. Leithe, E., M. Mesnil, and T. Aasen, *The connexin 43 C-terminus: A tail of many tales*. Biochim Biophys Acta Biomembr, 2018. **1860**(1): p. 48-64.
38. Calle, E.E. and R. Kaaks, *Overweight, obesity and cancer: epidemiological evidence and proposed mechanisms*. Nat Rev Cancer, 2004. **4**(8): p. 579-91.
39. Deng, T., et al., *Obesity, Inflammation, and Cancer*. Annu Rev Pathol, 2016. **11**: p. 421-49.
40. Talhouk, R.S., et al., *Developmental expression patterns and regulation of connexins in the mouse mammary gland: expression of connexin30 in lactogenesis*. Cell and tissue research, 2005. **319**(1): p. 49-59.
41. Talhouk, R.S., et al., *Context dependent reversion of tumor phenotype by connexin-43 expression in MDA-MB231 cells and MCF-7 cells: role of  $\beta$ -catenin/connexin43 association*. Experimental cell research, 2013. **319**(20): p. 3065-3080.
42. Talhouk, R.S., et al., *Gap junctions mediate STAT5-independent  $\beta$ -casein expression in CID-9 mammary epithelial cells*. Cell communication & adhesion, 2011. **18**(5): p. 104-116.
43. Zhang, Z., T. Yang, and J. Xiao, *Circular RNAs: promising biomarkers for human diseases*. EBioMedicine, 2018.
44. El-Saghir, J.A., et al., *Connexins: a junctional crossroad to breast cancer*. Int J Dev Biol, 2011. **55**(7-9): p. 773-80.
45. Kelly, J.J., J. Simek, and D.W. Laird, *Mechanisms linking connexin mutations to human diseases*. Cell Tissue Res, 2015. **360**(3): p. 701-21.
46. Laird, D.W., et al., *Deficiency of connexin43 gap junctions is an independent marker for breast tumors*. Cancer research, 1999. **59**(16): p. 4104-4110.
47. Naus, C.C. and D.W. Laird, *Implications and challenges of connexin connections to cancer*. Nature reviews Cancer, 2010. **10**(6): p. 435.

48. Roarty, K., et al., *Ror2 regulates branching, differentiation, and actin-cytoskeletal dynamics within the mammary epithelium*. J Cell Biol, 2015. **208**(3): p. 351-366.
49. Stewart, M.K., et al., *The severity of mammary gland developmental defects is linked to the overall functional status of Cx43 as revealed by genetically modified mice*. Biochemical Journal, 2013. **449**(2): p. 401-413.
50. Mroue, R., et al., *Asymmetric expression of connexins between luminal epithelial-and myoepithelial-cells is essential for contractile function of the mammary gland*. Developmental biology, 2015. **399**(1): p. 15-26.
51. Plum, A., et al., *Unique and shared functions of different connexins in mice*. Current biology, 2000. **10**(18): p. 1083-1091.
52. Kanczuga-Koda, L., et al., *Expression of connexin 43 in breast cancer in comparison with mammary dysplasia and the normal mammary gland*. Folia Morphol (Warsz), 2003. **62**(4): p. 439-42.
53. Kanczuga-Koda, L., et al., *Increased expression of gap junction protein--connexin 32 in lymph node metastases of human ductal breast cancer*. Folia Histochem Cytobiol, 2007. **45 Suppl 1**: p. S175-80.
54. Kanczuga-Koda, L., et al., *Increased expression of connexins 26 and 43 in lymph node metastases of breast cancer*. Journal of clinical pathology, 2006. **59**(4): p. 429-433.
55. Kanczuga-Koda, L., et al., *Connexins 26 and 43 correlate with Bak, but not with Bcl-2 protein in breast cancer*. Oncology reports, 2005. **14**(2): p. 325-329.
56. Singal, R., et al., *Modulation of the connexin26 tumor suppressor gene expression through methylation in human mammary epithelial cell lines*. Anticancer research, 2000. **20**(1A): p. 59-64.
57. McLachlan, E., et al., *Connexins act as tumor suppressors in three-dimensional mammary cell organoids by regulating differentiation and angiogenesis*. Cancer research, 2006. **66**(20): p. 9886-9894.
58. Lesko, A.C., et al., *The APC tumor suppressor is required for epithelial cell polarization and three-dimensional morphogenesis*. Biochimica Et Biophysica Acta (BBA)-Molecular Cell Research, 2015. **1853**(3): p. 711-723.
59. Teleki, I., et al., *The potential prognostic value of connexin 26 and 46 expression in neoadjuvant-treated breast cancer*. BMC cancer, 2013. **13**(1): p. 50.
60. Teleki, I., et al., *Correlations of differentially expressed gap junction connexins Cx26, Cx30, Cx32, Cx43 and Cx46 with breast cancer progression and prognosis*. PloS one, 2014. **9**(11): p. e112541.
61. Conklin, C., et al., *Tissue microarray analysis of connexin expression and its prognostic significance in human breast cancer*. Cancer letters, 2007. **255**(2): p. 284-294.
62. Jamieson, S., et al., *Expression of gap junction proteins connexin 26 and connexin 43 in normal human breast and in breast tumours*. J Pathol, 1998. **184**(1): p. 37-43.

63. Naoi, Y., et al., *Connexin26 expression is associated with lymphatic vessel invasion and poor prognosis in human breast cancer*. Breast cancer research and treatment, 2007. **106**(1): p. 11-17.
64. Lin, Z.J., et al., *Mechanism of Regulatory Effect of MicroRNA-206 on Connexin 43 in Distant Metastasis of Breast Cancer*. Chin Med J (Engl), 2016. **129**(4): p. 424-34.
65. Chang, C.W., et al., *MicroRNA-30a increases tight junction protein expression to suppress the epithelial-mesenchymal transition and metastasis by targeting Slug in breast cancer*. Oncotarget, 2016. **7**(13): p. 16462-78.
66. Valiunas, V., et al., *Connexin - specific cell - to - cell transfer of short interfering RNA by gap junctions*. The Journal of physiology, 2005. **568**(2): p. 459-468.
67. Thuringer, D., et al., *Transfer of functional microRNAs between glioblastoma and microvascular endothelial cells through gap junctions*. Oncotarget, 2016. **7**(45): p. 73925.
68. Shao, Y., et al., *Elevated levels of serum tumor markers CEA and CA15-3 are prognostic parameters for different molecular subtypes of breast cancer*. PloS one, 2015. **10**(7): p. e0133830.
69. Dobbe, E., et al., *Gene-expression assays: new tools to individualize treatment of early-stage breast cancer*. Am J Health Syst Pharm, 2008. **65**(1): p. 23-8.
70. Boyd, N.F., et al., *Mammographic density and the risk and detection of breast cancer*. N Engl J Med, 2007. **356**(3): p. 227-36.
71. Checka, C.M., et al., *The relationship of mammographic density and age: implications for breast cancer screening*. AJR Am J Roentgenol, 2012. **198**(3): p. W292-5.
72. Asaga, S., et al., *Direct serum assay for microRNA-21 concentrations in early and advanced breast cancer*. Clin Chem, 2011. **57**(1): p. 84-91.
73. Wu, X., et al., *De novo sequencing of circulating miRNAs identifies novel markers predicting clinical outcome of locally advanced breast cancer*. J Transl Med, 2012. **10**: p. 42.
74. Sahlberg, K.K., et al., *A serum microRNA signature predicts tumor relapse and survival in triple-negative breast cancer patients*. Clinical cancer research, 2015. **21**(5): p. 1207-1214.
75. Hansen, T.B., J. Kjems, and C.K. Damgaard, *Circular RNA and miR-7 in cancer*. Cancer research, 2013. **73**(18): p. 5609-5612.
76. Li, F., et al., *Circular RNA ITCH has inhibitory effect on ESCC by suppressing the Wnt/ $\beta$ -catenin pathway*. Oncotarget, 2015. **6**(8): p. 6001.
77. Wang, X., et al., *Decreased expression of hsa\_circ\_001988 in colorectal cancer and its clinical significances*. International journal of clinical and experimental pathology, 2015. **8**(12): p. 16020.
78. Zhang, M., et al., *A novel protein encoded by the circular form of the SHPRH gene suppresses glioma tumorigenesis*. Oncogene, 2018. **37**(13): p. 1805.
79. Cocquerelle, C., et al., *Mis-splicing yields circular RNA molecules*. FASEB J, 1993. **7**(1): p. 155-60.

80. Hansen, T.B., et al., *miRNA -dependent gene silencing involving Ago2 -mediated cleavage of a circular antisense RNA*. The EMBO journal, 2011. **30**(21): p. 4414-4422.
81. Nigro, J., et al., *Vogelstein. B. 1991. Scrambled exons*. Cell. **64**: p. 607-613.
82. Du, W.W., et al., *Foxo3 circular RNA retards cell cycle progression via forming ternary complexes with p21 and CDK2*. Nucleic acids research, 2016. **44**(6): p. 2846-2858.
83. Dudekula, D.B., et al., *CircInteractome: a web tool for exploring circular RNAs and their interacting proteins and microRNAs*. RNA biology, 2016. **13**(1): p. 34-42.
84. Armakola, M., et al., *Inhibition of RNA lariat debranching enzyme suppresses TDP-43 toxicity in ALS disease models*. Nature genetics, 2012. **44**(12): p. 1302.
85. Li, Z., et al., *Corrigendum: Exon-intron circular RNAs regulate transcription in the nucleus*. Nature structural & molecular biology, 2017. **24**(2): p. 194.
86. Meng, S., et al., *CircRNA: functions and properties of a novel potential biomarker for cancer*. Molecular cancer, 2017. **16**(1): p. 94.
87. Ashwal-Fluss, R., et al., *circRNA biogenesis competes with pre-mRNA splicing*. Molecular cell, 2014. **56**(1): p. 55-66.
88. Lu, W.-Y., *Roles of the circular RNA circ-Foxo3 in breast cancer progression*. Cell cycle, 2017. **16**(7): p. 589.
89. Lasda, E. and R. Parker, *Circular RNAs Co-Precipitate with Extracellular Vesicles: A Possible Mechanism for circRNA Clearance*. PLoS One, 2016. **11**(2): p. e0148407.
90. Memczak, S., et al., *Identification and characterization of circular RNAs as a new class of putative biomarkers in human blood*. PloS one, 2015. **10**(10): p. e0141214.
91. Xie, R., et al., *Silencing of hsa\_circ\_0004771 inhibits proliferation and induces apoptosis in breast cancer through activation of miR-653 by targeting ZEB2 signaling pathway*. Bioscience reports, 2019. **39**(5): p. BSR20181919.
92. Xu, J.-Z., et al., *circTADA2As suppress breast cancer progression and metastasis via targeting miR-203a-3p/SOCS3 axis*. Cell death & disease, 2019. **10**(3): p. 175.
93. Lü, L., et al., *Identification of circular RNAs as a promising new class of diagnostic biomarkers for human breast cancer*. Oncotarget, 2017. **8**(27): p. 44096.
94. Nair, A.A., et al., *Circular RNAs and their associations with breast cancer subtypes*. Oncotarget, 2016. **7**(49): p. 80967.
95. Du, W.W., et al., *Induction of tumor apoptosis through a circular RNA enhancing Foxo3 activity*. Cell death and differentiation, 2017. **24**(2): p. 357.
96. Liang, H.-F., et al., *Circular RNA circ-ABCB10 promotes breast cancer proliferation and progression through sponging miR-1271*. American journal of cancer research, 2017. **7**(7): p. 1566.
97. Kristensen, L., et al., *Circular RNAs in cancer: opportunities and challenges in the field*. Oncogene, 2018. **37**(5): p. 555.
98. Yang, Q., et al., *A circular RNA promotes tumorigenesis by inducing c-myc nuclear translocation*. Cell death and differentiation, 2017. **24**(9): p. 1609.



99. Zhang, H., et al., *Exosomal circRNA derived from gastric tumor promotes white adipose browning by targeting the miR - 133/PRDM16 pathway*. International journal of cancer, 2019. **144**(10): p. 2501-2515.
100. Zhang, H., et al., *Exosome circRNA secreted from adipocytes promotes the growth of hepatocellular carcinoma by targeting deubiquitination-related USP7*. Oncogene, 2018: p. 1.
101. Salzman, J., et al., *Circular RNAs are the predominant transcript isoform from hundreds of human genes in diverse cell types*. PLoS one, 2012. **7**(2): p. e30733.
102. Xia, S., et al., *CSCD: a database for cancer-specific circular RNAs*. Nucleic acids research, 2017. **46**(D1): p. D925-D929.
103. Lu, T.P., et al., *miRSystem: an integrated system for characterizing enriched functions and pathways of microRNA targets*. PLoS One, 2012. **7**(8): p. e42390.
104. Giricz, O., et al., *Hsa - miR - 375 is differentially expressed during breast lobular neoplasia and promotes loss of mammary acinar polarity*. The Journal of pathology, 2012. **226**(1): p. 108-119.
105. O'Day, E. and A. Lal, *MicroRNAs and their target gene networks in breast cancer*. Breast cancer research, 2010. **12**(2): p. 201.
106. Dragomir, M. and G.A. Calin, *Corrigendum: Circular RNAs in Cancer - Lessons Learned From microRNAs*. Front Oncol, 2018. **8**: p. 307.
107. Brisset, A.C., B.E. Isakson, and B.R. Kwak, *Connexins in vascular physiology and pathology*. Antioxid Redox Signal, 2009. **11**(2): p. 267-82.
108. Glazar, P., P. Papavasileiou, and N. Rajewsky, *circBase: a database for circular RNAs*. RNA, 2014. **20**(11): p. 1666-70.
109. Agarwal, V., et al., *Predicting effective microRNA target sites in mammalian mRNAs*. elife, 2015. **4**: p. e05005.
110. Grimson, A., et al., *MicroRNA targeting specificity in mammals: determinants beyond seed pairing*. Molecular cell, 2007. **27**(1): p. 91-105.
111. Salzman, J., et al., *Cell-type specific features of circular RNA expression*. PLoS genetics, 2013. **9**(9): p. e1003777.
112. Siegel, R.L., K.D. Miller, and A. Jemal, *Cancer statistics, 2016*. CA: a cancer journal for clinicians, 2016. **66**(1): p. 7-30.
113. Sørlie, T., et al., *Gene expression patterns of breast carcinomas distinguish tumor subclasses with clinical implications*. Proceedings of the National Academy of Sciences, 2001. **98**(19): p. 10869-10874.
114. Liu, Z., X.-S. Zhang, and S. Zhang, *Breast tumor subgroups reveal diverse clinical prognostic power*. Scientific reports, 2014. **4**.
115. Prat, A., et al., *Clinical implications of the intrinsic molecular subtypes of breast cancer*. The Breast, 2015. **24**: p. S26-S35.

116. Spitale, A., et al., *Breast cancer classification according to immunohistochemical markers: clinicopathologic features and short-term survival analysis in a population-based study from the South of Switzerland*. *Annals of Oncology*, 2008. **20**(4): p. 628-635.
117. Bhattacharyya, M., J. Nath, and S. Bandyopadhyay, *MicroRNA signatures highlight new breast cancer subtypes*. *Gene*, 2015. **556**(2): p. 192-198.
118. Adams, B.D., et al., *miR-34a silences c-SRC to attenuate tumor growth in triple-negative breast cancer*. *Cancer research*, 2016. **76**(4): p. 927-939.
119. Fidler, I.J., *The pathogenesis of cancer metastasis: the 'seed and soil' hypothesis revisited*. *Nature Reviews Cancer*, 2003. **3**(6): p. 453-458.
120. Polyak, K. and R.A. Weinberg, *Transitions between epithelial and mesenchymal states: acquisition of malignant and stem cell traits*. *Nature Reviews Cancer*, 2009. **9**(4): p. 265-273.
121. McGuire, A., J.A. Brown, and M.J. Kerin, *Metastatic breast cancer: the potential of miRNA for diagnosis and treatment monitoring*. *Cancer and Metastasis Reviews*, 2015. **34**(1): p. 145-155.
122. Nassar, F.J., R. Nasr, and R. Talhouk, *MicroRNAs as biomarkers for early breast cancer diagnosis, prognosis and therapy prediction*. *Pharmacology & therapeutics*, 2017. **172**: p. 34-49.
123. Dobbe, E., et al., *Gene-expression assays: New tools to individualize treatment of early-stage breast cancer*. *American Journal of Health-System Pharmacy*, 2008. **65**(1).
124. Dai, X., et al., *Breast cancer intrinsic subtype classification, clinical use and future trends*. *American journal of cancer research*, 2015. **5**(10): p. 2929.
125. BoydNF, G., *Mammographic density and the risk and detection of breast cancer*. *NEngl J Med*, 2007. **356**: p. 227-236.
126. Checka, C.M., et al., *The relationship of mammographic density and age: implications for breast cancer screening*. *American Journal of Roentgenology*, 2012. **198**(3): p. W292-W295.
127. Singh, S.K., et al., *MicroRNAs—micro in size but macro in function*. *The FEBS journal*, 2008. **275**(20): p. 4929-4944.
128. Winter, J., et al., *Many roads to maturity: microRNA biogenesis pathways and their regulation*. *Nature cell biology*, 2009. **11**(3): p. 228-234.
129. Kutanzi, K.R., et al., *MicroRNA-mediated drug resistance in breast cancer*. *Clinical epigenetics*, 2011. **2**(2): p. 171.
130. Pink, R.C., et al., *The passenger strand, miR-21-3p, plays a role in mediating cisplatin resistance in ovarian cancer cells*. *Gynecologic oncology*, 2015. **137**(1): p. 143-151.
131. He, L. and G.J. Hannon, *MicroRNAs: small RNAs with a big role in gene regulation*. *Nature Reviews Genetics*, 2004. **5**(7): p. 522-531.
132. Eulalio, A., et al., *Deadenylation is a widespread effect of miRNA regulation*. *Rna*, 2009. **15**(1): p. 21-32.

133. Vasudevan, S., Y. Tong, and J.A. Steitz, *Switching from repression to activation: microRNAs can up-regulate translation*. *Science*, 2007. **318**(5858): p. 1931-1934.
134. Li, M., et al., *microRNA and cancer*. *The AAPS journal*, 2010. **12**(3): p. 309-317.
135. Raza, U., et al., *The miR-644a/CTBP1/p53 axis suppresses drug resistance by simultaneous inhibition of cell survival and epithelial-mesenchymal transition in breast cancer*. *Oncotarget*, 2016. **7**(31): p. 49859.
136. Chim, S.S., et al., *Detection and characterization of placental microRNAs in maternal plasma*. *Clinical chemistry*, 2008. **54**(3): p. 482-490.
137. Lawrie, C.H., et al., *Detection of elevated levels of tumour - associated microRNAs in serum of patients with diffuse large B - cell lymphoma*. *British journal of haematology*, 2008. **141**(5): p. 672-675.
138. Weber, J.A., et al., *The microRNA spectrum in 12 body fluids*. *Clinical chemistry*, 2010. **56**(11): p. 1733-1741.
139. Lima, L.G., et al., *Tumor-derived microvesicles modulate the establishment of metastatic melanoma in a phosphatidylserine-dependent manner*. *Cancer letters*, 2009. **283**(2): p. 168-175.
140. Turchinovich, A., et al., *Characterization of extracellular circulating microRNA*. *Nucleic acids research*, 2011. **39**(16): p. 7223-7233.
141. Merkerova, M., et al., *MicroRNA expression profiles in umbilical cord blood cell lineages*. *Stem cells and development*, 2010. **19**(1): p. 17-26.
142. Wu, K., et al., *Exosomal miR-19a: a novel communicator between cancer cell and osteoclast in osteolytic bone metastasis of breast cancer*. 2017, AACR.
143. Zhong, S., et al., *MicroRNA expression profiles of drug-resistance breast cancer cells and their exosomes*. *Oncotarget*, 2016. **7**(15): p. 19601-19609.
144. Le, M.T., et al., *miR-200-containing extracellular vesicles promote breast cancer cell metastasis*. *The Journal of clinical investigation*, 2014. **124**(12): p. 5109.
145. Ma, R., T. Jiang, and X. Kang, *Circulating microRNAs in cancer: origin, function and application*. *Journal of experimental & clinical cancer research*, 2012. **31**(1): p. 38.
146. LI, Z., et al., *Global Analysis of miRNA-mRNA Interaction Network in Breast Cancer with Brain Metastasis*. *Anticancer Research*, 2017. **37**(8): p. 4455-4468.
147. Mohammadi-Yeganeh, S., et al., *MicroRNA-340 inhibits the migration, invasion, and metastasis of breast cancer cells by targeting Wnt pathway*. *Tumor Biology*, 2016. **37**(7): p. 8993-9000.
148. Madhavan, D., et al., *Circulating miRNAs with prognostic value in metastatic breast cancer and for early detection of metastasis*. *Carcinogenesis*, 2016. **37**(5): p. 461-470.
149. Markou, A., et al., *Direct comparison of metastasis-related miRNAs expression levels in circulating tumor cells, corresponding plasma, and primary tumors of breast cancer patients*. *Clinical chemistry*, 2016. **62**(7): p. 1002-1011.

150. Peng, F., et al., *Isoliquiritigenin modulates miR-374a/PTEN/Akt axis to suppress breast cancer tumorigenesis and metastasis*. Scientific Reports, 2017. **7**.
151. Teoh, S. and S. Das, *The Role of MicroRNAs in Diagnosis, Prognosis, Metastasis and Resistant Cases in Breast Cancer*. Current pharmaceutical design, 2017. **23**(12): p. 1845.
152. Miao, Y., et al., *MicroRNA-130b targets PTEN to mediate drug resistance and proliferation of breast cancer cells via the PI3K/Akt signaling pathway*. Scientific Reports, 2017. **7**.
153. Cortez, M.A., et al., *MicroRNAs in body fluids—the mix of hormones and biomarkers*. Nature reviews Clinical oncology, 2011. **8**(8): p. 467-477.
154. Roth, C., et al., *Circulating microRNAs as blood-based markers for patients with primary and metastatic breast cancer*. Breast Cancer Research, 2010. **12**(6): p. R90.
155. Chen, W., et al., *The level of circulating miRNA-10b and miRNA-373 in detecting lymph node metastasis of breast cancer: potential biomarkers*. Tumor Biology, 2013. **34**(1): p. 455-462.
156. Schwarzenbach, H., et al., *Diagnostic potential of PTEN-targeting miR-214 in the blood of breast cancer patients*. Breast cancer research and treatment, 2012. **134**(3): p. 933-941.
157. Ahmad, A., et al., *Up-regulation of microRNA-10b is associated with the development of breast cancer brain metastasis*. American journal of translational research, 2014. **6**(4): p. 384.
158. Zhao, F., et al., *Serum overexpression of microRNA-10b in patients with bone metastatic primary breast cancer*. Journal of International Medical Research, 2012. **40**(3): p. 859-866.
159. Madhavan, D., et al., *Circulating miRNAs as surrogate markers for circulating tumor cells and prognostic markers in metastatic breast cancer*. Clinical Cancer Research, 2012. **18**(21): p. 5972-5982.
160. Zhou, W., et al., *Cancer-secreted miR-105 destroys vascular endothelial barriers to promote metastasis*. Cancer cell, 2014. **25**(4): p. 501-515.
161. Eichelser, C., et al., *Deregulated serum concentrations of circulating cell-free microRNAs miR-17, miR-34a, miR-155, and miR-373 in human breast cancer development and progression*. Clinical chemistry, 2013. **59**(10): p. 1489-1496.
162. Gasparri, M.L., et al., *Beyond circulating microRNA biomarkers: Urinary microRNAs in ovarian and breast cancer*. Tumor Biology, 2017. **39**(5): p. 1010428317695525.
163. Zheng, R., et al., *Prognostic value of miR-106b expression in breast cancer patients*. journal of surgical research, 2015. **195**(1): p. 158-165.
164. Sahlberg, K.K., et al., *A serum microRNA signature predicts tumor relapse and survival in triple negative breast cancer patients*. Clinical cancer research, 2014: p. clincanres. 2011.2014.
165. Halvorsen, A.R., et al., *Profiling of microRNAs in tumor interstitial fluid of breast tumors—a novel resource to identify biomarkers for prognostic classification and detection of cancer*. Molecular oncology, 2017. **11**(2): p. 220-234.

166. Lánczky, A., et al., *miRpower: a web-tool to validate survival-associated miRNAs utilizing expression data from 2178 breast cancer patients*. Breast cancer research and treatment, 2016. **160**(3): p. 439-446.
167. Guestini, F., et al., *Triple negative breast cancer chemosensitivity and chemoresistance: current advances in biomarkers identification*. Expert opinion on therapeutic targets, 2016. **20**(6): p. 705-720.
168. Chen, X., et al., *The role of miRNAs in drug resistance and prognosis of breast cancer formalin-fixed paraffin-embedded tissues*. Gene, 2016. **595**(2): p. 221-226.
169. Erbes, T., et al., *Feasibility of urinary microRNA detection in breast cancer patients and its potential as an innovative non-invasive biomarker*. BMC cancer, 2015. **15**: p. 193-193.
170. Pecot, C.V., et al., *Tumour angiogenesis regulation by the miR-200 family*. Nature communications, 2013. **4**: p. 2427.
171. Sarkar, F.H., et al., *Implication of microRNAs in drug resistance for designing novel cancer therapy*. Drug Resistance Updates, 2010. **13**(3): p. 57-66.
172. Ellis, L.M. and D.J. Hicklin, *Resistance to targeted therapies: refining anticancer therapy in the era of molecular oncology*. Clinical Cancer Research, 2009. **15**(24): p. 7471-7478.
173. Sorrentino, A., et al., *Role of microRNAs in drug-resistant ovarian cancer cells*. Gynecologic oncology, 2008. **111**(3): p. 478-486.
174. Allen, K.E. and G.J. Weiss, *Resistance may not be futile: microRNA biomarkers for chemoresistance and potential therapeutics*. Molecular cancer therapeutics, 2010: p. molcanther. 0397.2010.
175. Liang, Z., et al., *Involvement of miR-326 in chemotherapy resistance of breast cancer through modulating expression of multidrug resistance-associated protein 1*. Biochemical pharmacology, 2010. **79**(6): p. 817-824.
176. Kovalchuk, O., et al., *Involvement of microRNA-451 in resistance of the MCF-7 breast cancer cells to chemotherapeutic drug doxorubicin*. Molecular cancer therapeutics, 2008. **7**(7): p. 2152-2159.
177. Yang, S.-j., et al., *Predictive role of GSTP1-containing exosomes in chemotherapy-resistant breast cancer*. Gene, 2017. **623**: p. 5-14.
178. Wu, Q., et al., *Multi-drug resistance in cancer chemotherapeutics: mechanisms and lab approaches*. Cancer letters, 2014. **347**(2): p. 159-166.
179. Zhao, J.-J., et al., *MicroRNA-221/222 negatively regulates estrogen receptors and is associated with tamoxifen resistance in breast cancer*. Journal of Biological Chemistry, 2008. **283**(45): p. 31079-31086.
180. Lau, L.-y. and 劉麗儀., *Identification of microRNAs associated with tamoxifen resistance in breast cancer*. HKU Theses Online (HKUTO), 2011.
181. Hong, L., et al., *MicroRNA-21: a therapeutic target for reversing drug resistance in cancer*. Expert opinion on therapeutic targets, 2013. **17**(9): p. 1073-1080.

182. Wang, Z.-X., et al., *MicroRNA-21 modulates chemosensitivity of breast cancer cells to doxorubicin by targeting PTEN*. Archives of medical research, 2011. **42**(4): p. 281-290.
183. Bourguignon, L.Y., et al., *Stem cell marker (Nanog) and Stat-3 signaling promote MicroRNA-21 expression and chemoresistance in hyaluronan/CD44-activated head and neck squamous cell carcinoma cells*. Oncogene, 2012. **31**(2): p. 149-160.
184. Mei, M., et al., *Downregulation of miR-21 enhances chemotherapeutic effect of taxol in breast carcinoma cells*. Technology in cancer research & treatment, 2010. **9**(1): p. 77-86.
185. Zhou, M., et al., *Mir-125b confers the resistance of cancer cells to Taxol through suppression of Bak1*. 2010, AACR.
186. Luqmani, Y.A. and N. Alam-Eldin, *Overcoming resistance to endocrine therapy in breast cancer: new approaches to a nagging problem*. Medical Principles and Practice, 2016. **25**(Suppl. 2): p. 28-40.
187. Joshi, T., et al., *Integrative analysis of miRNA and gene expression reveals regulatory networks in tamoxifen-resistant breast cancer*. Oncotarget, 2016. **7**(35): p. 57239-57253.
188. Sachdeva, M. and Y.-Y. Mo, *miR-145-mediated suppression of cell growth, invasion and metastasis*. American journal of translational research, 2010. **2**(2): p. 170.
189. Rehman, S.K., W.-C. Huang, and D. Yu, *MiR-21 upregulation in breast cancer cells leads to PTEN loss and Herceptin resistance*. 2010, AACR.
190. Gong, C., et al., *Up-regulation of miR-21 mediates resistance to trastuzumab therapy for breast cancer*. Journal of Biological Chemistry, 2011. **286**(21): p. 19127-19137.
191. Scott, G.K., et al., *Coordinate suppression of ERBB2 and ERBB3 by enforced expression of micro-RNA miR-125a or miR-125b*. Journal of Biological Chemistry, 2007. **282**(2): p. 1479-1486.
192. del Pilar Camacho-Leal, M., M. Sciortino, and S. Cabodi, *ErbB2 Receptor in Breast Cancer: Implications in Cancer Cell Migration, Invasion and Resistance to Targeted Therapy*, in *Breast Cancer-From Biology to Medicine*. 2017, InTech.
193. Lowery, A.J., et al., *MicroRNA signatures predict oestrogen receptor, progesterone receptor and HER2/neureceptor status in breast cancer*. Breast cancer research, 2009. **11**(3): p. R27.
194. Mattie, M.D., et al., *Optimized high-throughput microRNA expression profiling provides novel biomarker assessment of clinical prostate and breast cancer biopsies*. Molecular cancer, 2006. **5**(1): p. 1-14.
195. Breunig, C., et al., *MicroRNA-519a-3p mediates apoptosis resistance in breast cancer cells and their escape from recognition by natural killer cells*. Cell Death & Disease, 2017. **8**(8): p. e2973.
196. Anastasov, N., et al., *Radiation resistance due to high expression of miR-21 and G2/M checkpoint arrest in breast cancer cells*. Radiation oncology, 2012. **7**(1): p. 206.
197. Liang, Z., et al., *MicroRNA-302 replacement therapy sensitizes breast cancer cells to ionizing radiation*. Pharmaceutical research, 2013. **30**(4): p. 1008-1016.

198. Raza, U., J.D. Zhang, and Ö. Şahin, *MicroRNAs: master regulators of drug resistance, stemness, and metastasis*. *Journal of molecular medicine*, 2014. **92**(4): p. 321-336.
199. Gupta, G.P. and J. Massagué, *Cancer metastasis: building a framework*. *Cell*, 2006. **127**(4): p. 679-695.
200. Ma, L., J. Teruya-Feldstein, and R.A. Weinberg, *Tumour invasion and metastasis initiated by microRNA-10b in breast cancer*. *Nature*, 2008. **455**(7210): p. 256-256.
201. Luqmani, Y.A. and M.A. Khajah, *MicroRNA in Breast Cancer—Gene Regulators and Targets for Novel Therapies*, in *A Concise Review of Molecular Pathology of Breast Cancer*. 2015, InTech.
202. Ma, L., et al., *miR-9, a MYC/MYCN-activated microRNA, regulates E-cadherin and cancer metastasis*. *Nature cell biology*, 2010. **12**(3): p. 247-256.
203. Korpala, M., et al., *Direct targeting of Sec23a by miR-200s influences cancer cell secretome and promotes metastatic colonization*. *Nature medicine*, 2011. **17**(9): p. 1101-1108.
204. Orso, F., et al., *miR-214 and miR-148b targeting inhibits dissemination of melanoma and breast cancer*. *Cancer research*, 2016. **76**(17): p. 5151-5162.
205. Zou, Q., et al., *MicroRNA-22 inhibits cell growth and metastasis in breast cancer via targeting of SIRT1*. *Experimental and Therapeutic Medicine*.
206. Li, W., et al., *Tumor-suppressive microRNA-452 inhibits migration and invasion of breast cancer cells by directly targeting RAB11A*. *Oncology Letters*, 2017. **14**(2): p. 2559-2565.
207. Kong, W., et al., *MicroRNA-155 is regulated by the transforming growth factor  $\beta$ /Smad pathway and contributes to epithelial cell plasticity by targeting RhoA*. *Molecular and cellular biology*, 2008. **28**(22): p. 6773-6784.
208. Valastyan, S., et al., *RETRACTED: A pleiotropically acting MicroRNA, miR-31, inhibits breast cancer metastasis*. *Cell*, 2009. **137**(6): p. 1032-1046.
209. Valastyan, S., et al., *Concurrent suppression of integrin  $\alpha 5$ , radixin, and RhoA phenocopies the effects of miR-31 on metastasis*. *Cancer research*, 2010. **70**(12): p. 5147-5154.
210. Valastyan, S. and R.A. Weinberg, *miR-31: a crucial overseer of tumor metastasis and other emerging roles*. *Cell Cycle*, 2010. **9**(11): p. 2124-2129.
211. Körner, C., et al., *MicroRNA-31 Sensitizes Human Breast Cells to Apoptosis by Direct Targeting of Protein Kinase C  $\epsilon$  (PKC $\epsilon$ )*. *Journal of Biological Chemistry*, 2013. **288**(12): p. 8750-8761.
212. Li, H., et al., *miR-17-5p promotes human breast cancer cell migration and invasion through suppression of HBPI*. *Breast cancer research and treatment*, 2011. **126**(3): p. 565-575.
213. Lu, Y., et al., *MicroRNA-140-5p inhibits invasion and angiogenesis through targeting VEGF-A in breast cancer*. *Cancer gene therapy*, 2017.
214. Mertens-Talcott, S.U., et al., *The oncogenic microRNA-27a targets genes that regulate specificity protein transcription factors and the G2-M checkpoint in MDA-MB-231 breast cancer cells*. *Cancer research*, 2007. **67**(22): p. 11001-11011.

215. Lee, D.Y., et al., *MicroRNA-378 promotes cell survival, tumor growth, and angiogenesis by targeting SuFu and Fus-1 expression*. Proceedings of the National Academy of Sciences, 2007. **104**(51): p. 20350-20355.
216. Soria-Valles, C., et al., *The anti-metastatic activity of collagenase-2 in breast cancer cells is mediated by a signaling pathway involving decorin and miR-21*. Oncogene, 2014. **33**(23): p. 3054-3063.
217. Croset, M., et al., *TWIST1 expression in breast cancer cells facilitates bone metastasis formation*. Journal of Bone and Mineral Research, 2014. **29**(8): p. 1886-1899.
218. Bishopric, N., et al., *Abstract P4-07-03: Dynamic regulation of a microRNA-mRNA network during breast cancer metastasis reveals an essential tumor-promoting role for miR-203*. 2017, AACR.
219. Blevins, M.A., et al., *Small molecule, NSC95397, inhibits the CtBP1-protein partner interaction and CtBP1-mediated transcriptional repression*. Journal of biomolecular screening, 2015. **20**(5): p. 663-672.
220. Okuda, H., et al., *miR-7 suppresses brain metastasis of breast cancer stem-like cells by modulating KLF4*. Cancer research, 2013. **73**(4): p. 1434-1444.
221. Zare, M., et al., *Aberrantly miRNA promoter methylation and EMT - involving miRNAs in breast cancer metastasis: diagnosis and therapeutic implications*. Journal of Cellular Physiology, 2017.
222. Sasheva, P. and U. Grossniklaus, *Differentially Methylated Region-Representational Difference Analysis (DMR-RDA): A Powerful Method to Identify DMRs in Uncharacterized Genomes*. Plant Epigenetics: Methods and Protocols, 2017: p. 113-125.
223. Gacem, R.B., et al., *Methylation of miR-124a-1, miR-124a-2, and miR-124a-3 genes correlates with aggressive and advanced breast cancer disease*. Tumor Biology, 2014. **35**(5): p. 4047-4056.
224. Niu, J., et al., *Induction of miRNA-181a by genotoxic treatments promotes chemotherapeutic resistance and metastasis in breast cancer*. Oncogene, 2016. **35**(10): p. 1302-1313.
225. Bai, W.D., et al., *MiR - 200c suppresses TGF -  $\beta$  signaling and counteracts trastuzumab resistance and metastasis by targeting ZNF217 and ZEB1 in breast cancer*. International journal of cancer, 2014. **135**(6): p. 1356-1368.
226. Schwarzenbach, H., *Clinical relevance of circulating, cell-free and exosomal microRNAs in plasma and serum of breast cancer patients*. Oncology Research and Treatment, 2017. **40**(7-8): p. 423-429.
227. Pichler, M. and G. Calin, *MicroRNAs in cancer: from developmental genes in worms to their clinical application in patients*. British journal of cancer, 2015. **113**(4): p. 569-573.
228. Ohno, S.-i., et al., *Systemically injected exosomes targeted to EGFR deliver antitumor microRNA to breast cancer cells*. Molecular Therapy, 2013. **21**(1): p. 185-191.



229. Huang, G., et al., *Recent progress in circular RNAs in human cancers*. Cancer Letters, 2017. **404**: p. 8-18.
230. El Saghir, N.S., et al., *Effects of young age at presentation on survival in breast cancer*. BMC cancer, 2006. **6**(1): p. 194.
231. Calle, E.E. and R. Kaaks, *Overweight, obesity and cancer: epidemiological evidence and proposed mechanisms*. Nature Reviews Cancer, 2004. **4**(8): p. 579-591.
232. Deng, T., et al., *Obesity, inflammation, and cancer*. Annual Review of Pathology: Mechanisms of Disease, 2016. **11**: p. 421-449.
233. Cocquerelle, C., et al., *Mis-splicing yields circular RNA molecules*. The FASEB Journal, 1993. **7**(1): p. 155-160.
234. Nigro, J.M., et al., *Scrambled exons*. Cell, 1991. **64**(3): p. 607-613.
235. Hansen, T.B., et al., *Natural RNA circles function as efficient microRNA sponges*. Nature, 2013. **495**(7441): p. 384-388.
236. Han, L., et al., *Prognostic potential of microRNA-138 and its target mRNA PDK1 in sera for patients with non-small cell lung cancer*. Medical Oncology, 2014. **31**(9): p. 129.
237. Legnini, I., et al., *Circ-ZNF609 is a circular RNA that can be translated and functions in myogenesis*. Molecular cell, 2017. **66**(1): p. 22-37. e9.
238. Zhang, Z., T. Yang, and J. Xiao, *Circular RNAs: promising biomarkers for human diseases*. EBioMedicine, 2018. **34**: p. 267-274.
239. Briand, P., O. Petersen, and B. Van Deurs, *A new diploid nontumorigenic human breast epithelial cell line isolated and propagated in chemically defined medium*. In vitro cellular & developmental biology, 1987. **23**(3): p. 181-188.
240. Petersen, O.W., et al., *Interaction with basement membrane serves to rapidly distinguish growth and differentiation pattern of normal and malignant human breast epithelial cells*. Proceedings of the National Academy of Sciences, 1992. **89**(19): p. 9064-9068.
241. Lelièvre, S.A., et al., *Tissue phenotype depends on reciprocal interactions between the extracellular matrix and the structural organization of the nucleus*. Proceedings of the National Academy of Sciences, 1998. **95**(25): p. 14711-14716.
242. Plachot, C. and S.A. Lelièvre, *DNA methylation control of tissue polarity and cellular differentiation in the mammary epithelium*. Experimental cell research, 2004. **298**(1): p. 122-132.
243. Yue, S., et al., *Label-free analysis of breast tissue polarity by Raman imaging of lipid phase*. Biophysical journal, 2012. **102**(5): p. 1215-1223.
244. Salzman, J., et al., *Circular RNAs are the predominant transcript isoform from hundreds of human genes in diverse cell types*. PloS one, 2012. **7**(2).
245. Glažar, P., P. Papavasileiou, and N. Rajewsky, *circBase: a database for circular RNAs*. Rna, 2014. **20**(11): p. 1666-1670.
246. Enright, A.J., et al., *MicroRNA targets in Drosophila*. Genome biology, 2003. **5**(1): p. R1.

247. Pasquinelli, A.E., *MicroRNAs and their targets: recognition, regulation and an emerging reciprocal relationship*. Nature Reviews Genetics, 2012. **13**(4): p. 271-282.
248. Koutsaki, M., D.A. Spandidos, and A. Zaravinos, *Epithelial–mesenchymal transition-associated miRNAs in ovarian carcinoma, with highlight on the miR-200 family: prognostic value and prospective role in ovarian cancer therapeutics*. Cancer letters, 2014. **351**(2): p. 173-181.
249. Muramatsu, F., et al., *microRNA-125b inhibits tube formation of blood vessels through translational suppression of VE-cadherin*. Oncogene, 2013. **32**(4): p. 414-421.
250. Hu, W.-W., et al., *Periostin promotes epithelial-mesenchymal transition via the MAPK/miR-381 axis in lung cancer*. Oncotarget, 2017. **8**(37): p. 62248.
251. Zhang, J., et al., *Intermittent fasting protects against Alzheimer’s disease possible through restoring aquaporin-4 polarity*. Frontiers in molecular neuroscience, 2017. **10**: p. 395.
252. Nagy, Á., et al., *Validation of miRNA prognostic power in hepatocellular carcinoma using expression data of independent datasets*. Scientific reports, 2018. **8**(1): p. 1-9.
253. Turcatel, G., et al., *MIR-99a and MIR-99b modulate TGF- $\beta$  induced epithelial to mesenchymal plasticity in normal murine mammary gland cells*. PloS one, 2012. **7**(1).
254. Vimalraj, S., et al., *Regulation of breast cancer and bone metastasis by microRNAs*. Disease markers, 2013. **35**(5): p. 369-387.
255. Li, P., et al., *MiR-183/-96/-182 cluster is up-regulated in most breast cancers and increases cell proliferation and migration*. Breast cancer research, 2014. **16**(6): p. 473.
256. Zhang, X., et al., *MicroRNA-182 promotes proliferation and metastasis by targeting FOXF2 in triple-negative breast cancer*. Oncology letters, 2017. **14**(4): p. 4805-4811.
257. Duforestel, M., et al., *Glyphosate primes mammary cells for tumorigenesis by reprogramming the epigenome in a TET3-dependent manner*. Frontiers in genetics, 2019. **10**: p. 885.
258. Jamieson, S., et al., *Expression of gap junction proteins connexin 26 and connexin 43 in normal human breast and in breast tumours*. The Journal of Pathology: A Journal of the Pathological Society of Great Britain and Ireland, 1998. **184**(1): p. 37-43.
259. El-Saghir, J.A., et al., *Connexins: a junctional crossroad to breast cancer*. International Journal of Developmental Biology, 2011. **55**(7-8-9): p. 773-780.
260. Griffiths-Jones, S., et al., *miRBase: tools for microRNA genomics*. Nucleic acids research, 2007. **36**(suppl\_1): p. D154-D158.
261. Blaschke, R.J., et al., [25] *Cell differentiation by extracellular matrix components*, in *Methods in enzymology*. 1994, Elsevier. p. 535-556.
262. Vidi, P.-A., M.J. Bissell, and S.A. Lelièvre, *Three-dimensional culture of human breast epithelial cells: the how and the why*, in *Epithelial Cell Culture Protocols*. 2012, Springer. p. 193-219.
263. Love, M., S. Anders, and M. Huber, *Differential gene expression analysis based on the negative binomial distribution*. Genome Biol, 2014. **15**: p. 550.

264. Liu, H., *MicroRNAs in breast cancer initiation and progression*. Cellular and Molecular Life Sciences, 2012. **69**(21): p. 3587-3599.
265. Cheng, C.-W., et al., *MicroRNA-30a inhibits cell migration and invasion by downregulating vimentin expression and is a potential prognostic marker in breast cancer*. Breast cancer research and treatment, 2012. **134**(3): p. 1081-1093.
266. Li, J., et al., *MiRNA-26b inhibits proliferation by targeting PTGS2 in breast cancer*. Cancer cell international, 2013. **13**(1): p. 7.
267. Ma, L., J. Teruya-Feldstein, and R.A. Weinberg, *Tumour invasion and metastasis initiated by microRNA-10b in breast cancer*. Nature, 2007. **449**(7163): p. 682-688.
268. Wang, Y., et al., *Transforming growth factor- $\beta$  regulates the sphere-initiating stem cell-like feature in breast cancer through miRNA-181 and ATM*. Oncogene, 2011. **30**(12): p. 1470-1480.
269. Yu, X., et al., *Induction of cell proliferation and survival genes by estradiol-repressed microRNAs in breast cancer cells*. BMC cancer, 2012. **12**(1): p. 29.
270. Lu, Y.-Y., et al., *miR-183 induces cell proliferation, migration, and invasion by regulating PDCD4 expression in the SW1990 pancreatic cancer cell line*. Biomedicine & pharmacotherapy, 2015. **70**: p. 151-157.
271. Wang, Q., et al., *Downregulation of E-cadherin is an essential event in activating  $\beta$ -catenin/Tcf-dependent transcription and expression of its target genes in Pcd4 knockdown cells*. Oncogene, 2010. **29**(1): p. 128-138.
272. Shen, F., et al., *MiR-492 contributes to cell proliferation and cell cycle of human breast cancer cells by suppressing SOX7 expression*. Tumor Biology, 2015. **36**(3): p. 1913-1921.
273. Fan, R., et al., *Methylation of the CpG island near SOX7 gene promoter is correlated with the poor prognosis of patients with myelodysplastic syndrome*. The Tohoku journal of experimental medicine, 2012. **227**(2): p. 119-128.
274. Ekman, M., et al., *APC and Smad7 link TGF $\beta$  type I receptors to the microtubule system to promote cell migration*. Molecular biology of the cell, 2012. **23**(11): p. 2109-2121.